

# *Chapter - 9*

## CHAPTER - IX

### LABORATORY STUDIES

From the earlier studies (Chapter-III to VIII) it now becomes clear that the dinosaurian forms of Kutch with their associated fauna and flora continued their living during some of the eruptive phases of the Deccan volcanism and during their quiescent periods when the intertrappean sedimentary environments provided them with life supporting surroundings were existing. In this context, and before attempting a host of other laboratory studies it now becomes imperative for the author to give thoughts to the mode of eruption of the Deccan lava flows in Kutch especially during the K/T boundary time. Detail petrographic and petrochemical studies are therefore reported in the following paragraphs:

*How are these available*

(1) The Deccan lava flows form one of the important geological entity in Kutch. Their extrusive phase is restricted to mainland Kutch and extends from east near Bhachau to westernmost part of Guneri.

(2) For convenience the following sections (Fig.1) have been selected:

(3) 1. Bhachau, 2. Anjar, 3. Baladia, 4. Matanomadh, 5. Dayapar and 6. Ukra/Atda.

#### IX.1. PETROGRAPHICAL OBSERVATIONS:

##### IX.1.1. Anjar Section:

In this section the basal flow is coarse porphyritic (greenish grey in colour and fine grained in the basal part (in the basal part it is chilled and glassy), near the top pipe amygdules are present. In thin sections, this flow shows ophitic to intergranular texture with plagioclase, feldspar (mainly labradorite and bytownite), titan-augite and microlites in equal quantities. The augite poikilitically encloses plagioclase feldspar and opaques. Pyroxenes are moderate to strongly pleochroic. Olivine occurs as small grains. Glass is patchy, altered to palagonite and encloses olivine, iron oxide, feldspars and augite. Opaques (Ti) are extremely high. The rock contains extremely high opaques as well as normative olivine (6.44%) and nepheline (2.0%).

*19*  
*- of lab*

*what % ?*

The upper part is vesicular and amygdaloidal in nature with the development of calcite in amygdules and geodes. The second flow is separated from the first flow by an intertrappean tuffaceous clayey sandstone. It is a coarse grained basalt with dominant feldspar and pyroxene phenocrysts. It shows porphyritic texture with abundance of labradorite bytownite titan augite and opaques. Pyroxene is strongly pleochroic. Few small grains of olivine are seen. It is also nepheline normative.

The third flow is greenish grey, coarse, porphyritic with phenocrysts of feldspars and pyroxenes. Texture is largely intersertal with subordinate intergranular. It is composed mainly of zoned feldspars mostly labradorite and colourless augite, subhedral to euhedral

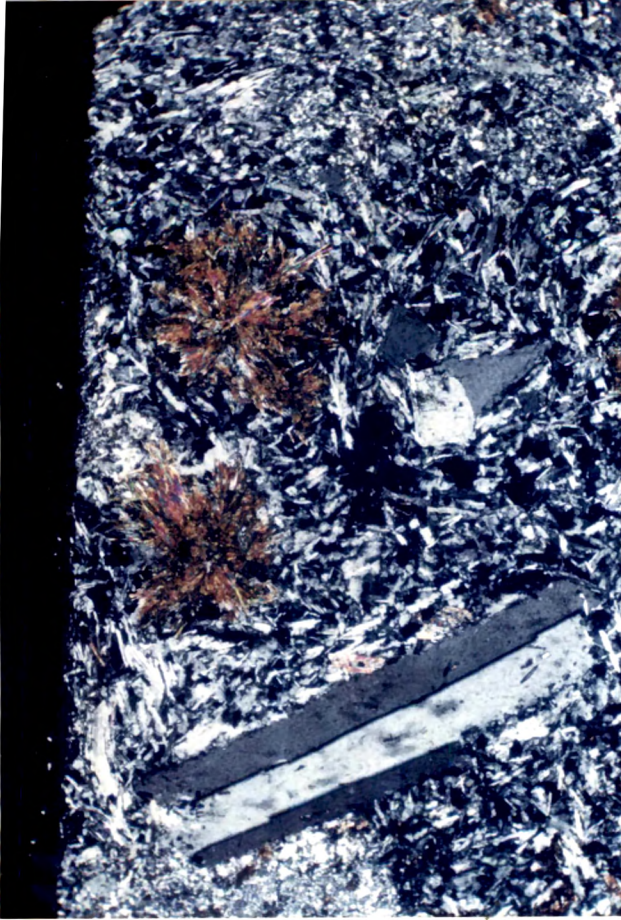


Plate XII/2 Microsection showing Olivine granules forming groundmass in lava flow at Bhaichau.



Plate XII/4 Abundant variolitic growth in microsection of Anjar flows.

7

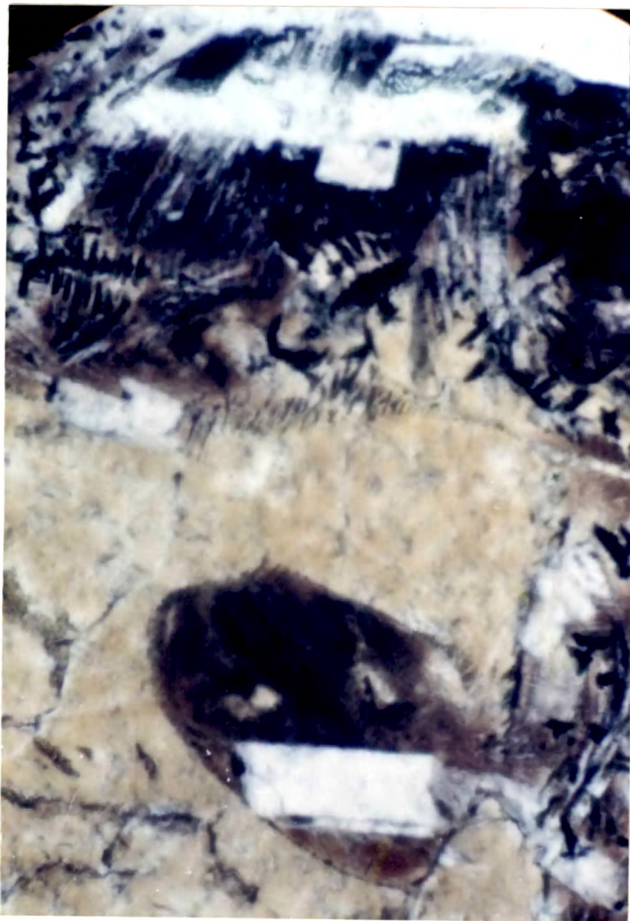


Plate XII/1 Opaque globules showing different growth patterns in microsections.



Plate XII/3 Microsections showing olivine granules forming groundmass in lava flow at Anjar.

iron oxides. Interstitial glass has altered to palagonite and patchy biotite. Glass encloses feldspar (labradorite), Fe-oxides and pyroxenes. Olivine is enclosed within pyroxenes. A fossiliferous intertrappean bed separates this one from the second flow.

The fourth flow overlying third flow with an intervening fossiliferous intertrappean at the base. It is greenish grey in colour and shows variation in granularity. It is fine grained in the basal part whereas the middle and upper portions are very coarse, porphyritic with large phenocrysts of feldspars and clinopyroxenes. Extensive vesicular cavities and amygdules are seen at the top. Few phenocrysts of zoned labradorite are seen in basal fine grained portion. Phenocrysts of augite (at times zoned) and grains of olivine are enclosed in glass which is altered into palagonite. The rock is rich in Fe-oxides (opaques). In the upper part Ti-augite encloses opaques and olivine. The pyroxenes are zoned and corroded. Phenocrysts are normal zoned feldspars (labradorite and bytownite). Glass occurs as large patches and encloses opaques and microlites of plagioclase feldspars. Opaques also enclose olivine and plagioclase. A carbonate occurs as secondary mineral and replaces glass at times.

The fifth flow overlies the fourth flow with a thin intervening patchy intertrappean. It is dark greenish grey, coarse porphyritic with distinct altered base and top with the development of amygdaloidal zone at the upper most. It is porphyritic with phenocrysts of plagioclase (labradorite and bytownite) at times zoned. West of Anjar towards Chandia and Khedoi it is seen to pass laterally into (basaltic agglomerate). Pyroxenes poikilitically enclose olivine and opaques. This flow shows olivine and nepheline normative nature.

The sixth flow is a dark green-grey in colour, compact with crude banded structure. It is highly vesicular at top surface and contains pipe amygdules at base with siliceous geodes at apex. Banding is prominent and visible only on the weathered surface. In microsection the rocks of this flow shows porphyritic texture with flow plagioclase. (Labradorite) occurs as laths and microlites. Banding/zoning is common in some feldspar grains. Augite occurs as subhedral grains and iron oxide as smaller grains. Occasional subophitic growth of clinopyroxenes is noted. The main brownish glass is largely unaltered.

The seventh and final flows are of composite sequence with alternating thin greenish grey and pinkish thin coarse porphyritic flowlets, with distinct zones of pipe amygdules and vesicular top surfaces with occasional siliceous and calcite geodes at the top. This surface is exposed along the river near south of Chandroda village.

#### **IX.1.2. Bhachau Section:**

In the Bhachau section the basal flow is porphyritic, olivine basaltic in composition, which is overlain by an Intertrappean bed of 2 to 2.5 m thickness, comprising of reddish, sandy and sticky clay, silts, marls and ash beds with numerous ferruginous partings. The second and third flows are also olivine basaltic in composition and are separated by about one meter thick ash bed. The younger flows (fourth and fifth flows are dark grey to black fine to medium grained porphyritic olivine basaltic in composition, and are separated from

third flow by intervening intertrappean bed composed of finely laminated ash and sandy clay. The fourth and fifth flows are separated by one meter thick intertrappean bed comprising sandy clay and red bole bed. Fifth flow is overlain by laterite. The total thickness of volcanosedimentary sequence is about 102 m

#### **IX.1.3. Baladia section:**

It is located in the Central Kachchh. The basal part of the section is coarse grained. The upper lava flows (F2-F6) are very coarse grained whereas 5th flow is a giant phenocryst basalt with feldspar and pyroxene phenocrysts often measuring 1 - 1.5 cm long and 1 cm across. Intertrappean beds are common in the basal sequence. The upper flows are compound type with intervening red bole beds. Alternating sequence of reddish and greenish porphyritic sheets are common. The silica geodes and pipe amygdules are common at the interflow contacts. The rock shows porphyritic texture with dominant phenocrysts of plagioclase feldspar (labradorite and bytownite), augite, titanite, iron oxides, glass and olivine in some cases. The feldspars exhibit zoning varying in composition from andesine to labradorite. Some grains show resorption along the margin and mild spilitisation (Plate-XV/2). Pyroxene displays corroded margins as well as some times pyroxenes enclose opaues and olivine. Plagioclase feldspar shows marginal zeolitisation and crude flow banding is seen at times due to subparallelism of feldspar needles. Fe-oxide globules are formed within glass due to release of iron. Chemically they contain higher silica, higher amount of total Fe, low  $K_2O$  and  $P_2O_5$ ,  $Al_2O_3$  and  $K_2O$  and high in CaO. Some of the flows have normative quartz and ortho-pyroxenes and hypersthene.

#### **IX.1.4. Matanomadh Section:**

In Matanomadh section the volcanosedimentaries comprise of nine basaltic flows with four intertrappean beds and two red bole beds, forming about 170 m thick section. The first two flows are about 25 m each thick separated by intervening two meter thick intertrappean bed comprising black carbonaceous shale, sandstone and clays. The third intertrappean bed is about 3 m thick comprising sandy clay and sandstone in basal part and shale and clay in the upper part. The third intertrappean bed is about 2.5 to 3 m thick comprising sandy clay and sandstone. The third flow is coarse porphyritic greenish grey in colour and contains pillow lava structure in the basal part. The fourth flow is coarse, porphyritic in the basal and upper part and shows quick alternations of green and purple basaltic flowlets in the central parts. The fifth flow onwards the flows are compound in nature and are separated by thin red bole beds or sandy clays.

#### **IX.1.5. Dayapar Section:**

In this section the lava flows are largely simple type, coarse porphyritic with intervening intertrappean beds. The basal flow is comparatively thinner porphyritic light greenish in colour. It shows porphyritic, intersertal texture with phenocrysts of normally zoned feldspars (labradorite and bytownite). The second to fifth flows are separated by

12

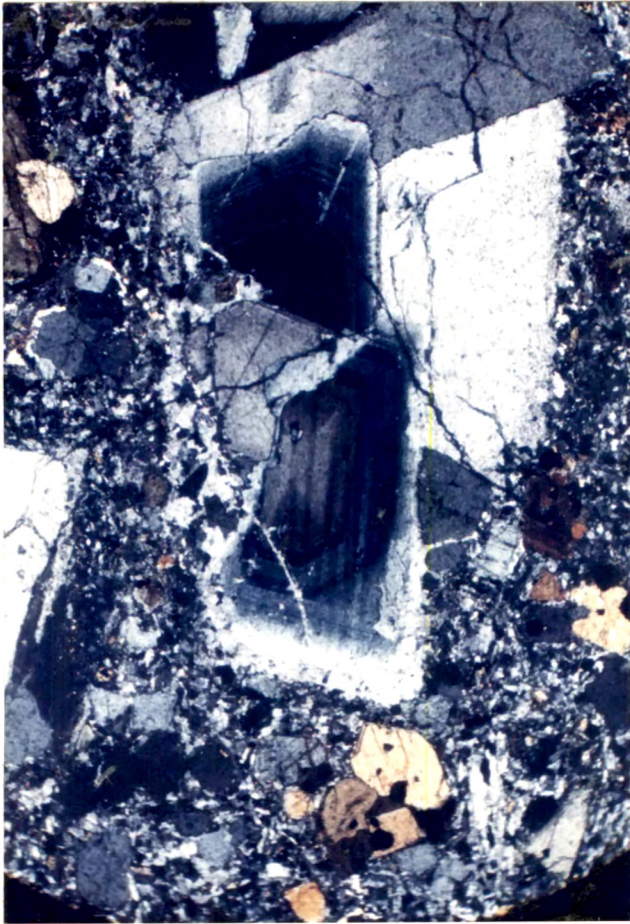


Plate XV/2 Reaction rim (and spilitisation) in the feldspars in Baladja section.

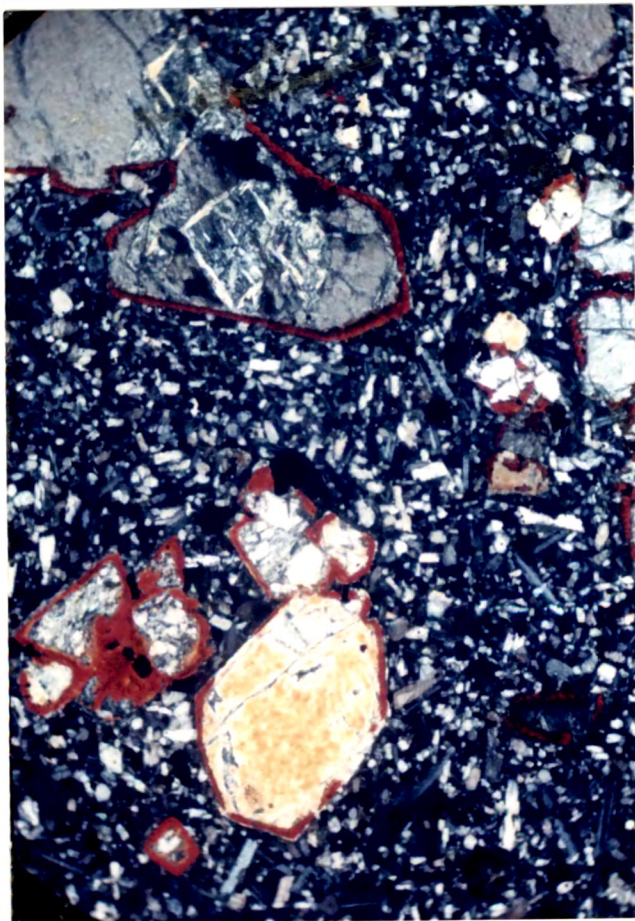


Plate XV/1 Reaction rims surrounding the olivine and pyroxene phenocrysts in flow at Dayapar.

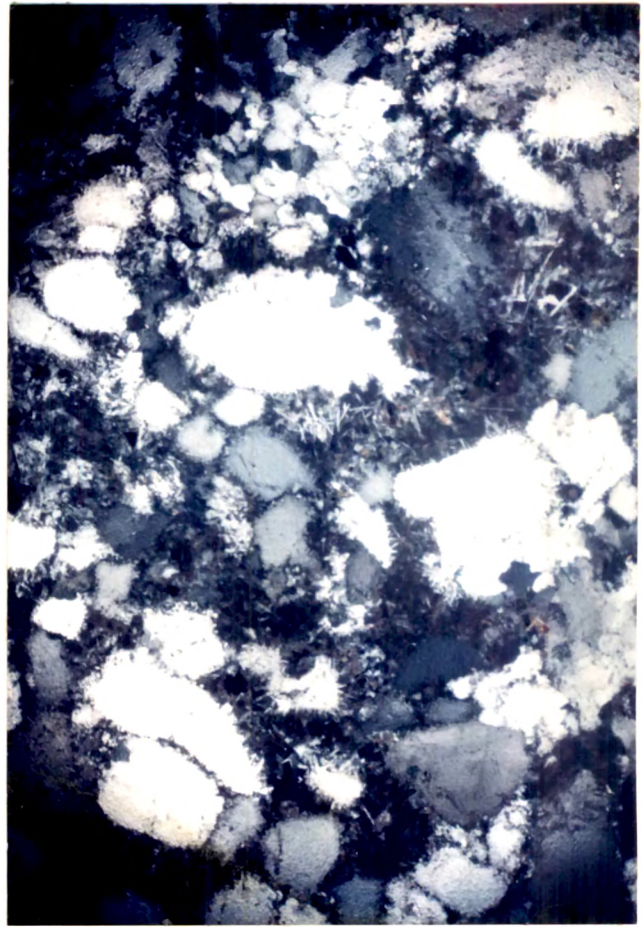


Plate XV/4 Reaction rims of magmatic material around quartz grains in host rock near dykes (due to assimilation).



Plate XV/3 Reaction rims of magmatic material around quartz grains in a dyke rock.

intervening clayey or sandy clay intertrappean beds. These flows are porphyritic with phenocrysts of labradorite, bytownite, zoned titan-augite., augite, altered olivine, opaques, glass and amygdules in some cases. Pyroxenes and olivine show embayment structures and have a reddish-brownish reaction rims (Plate-XV/1) with undisturbed continuous corroded segment of phenocrysts. Such rims are common around pyroxenes. Olivine also shows alteration. The rock is olivine tholeiite. These have high alumina, low total alkalis,  $\text{TiO}_2$  and ( $\text{K}_2\text{O}$  content). The basal flow is orthopyroxene and olivine normative whereas the 2nd and 3rd flows are nepheline normative only.

#### **IX.1.6. Ukra-Atda section:**

The rock is tholeiitic basalt. It is porphyritic with phenocrysts of plagioclase with titan augite, opaques and glass. It is ortho- and clinopyroxene normative rock. It has higher total Fe, total alkalis,  $\text{TiO}_2$  and low  $\text{MgO}$  content (Atda section) as compared to the adjacent Dayapar section.

#### **IX.1.7. General Observations:**

1. Compound lava flows show various volcanic structures like ropy lava, flow fronts bent pipe amygdules, lava tunnels, crude flowage structure, microcross ripple laminations, stretched amygdules, feeder dykelets, flow stratification, flow channels, migrating channels, etc,. Small eruptive centres are associated with pyroclastic surge deposits, lapilli (Plate-XI/2), scoriaceous tuff (volcanic debris) and volcanic vents in the mesozoic country.
2. -Comparision of logs of different sections (Fig. 1B) shows that there is a cyclicity in the granularity of the lava flows in Baladia, Anjar and Bhachau sections where micro-, coarse- and megaphenocryst flows occur in repetitive cycles.
3. The porphyritic and megaphenocryst flows also exhibit a sort of layering in Anjar and Baladia sections in which light and dark bands are seen. This banding and layering is conspicuous on the weathered surface. Thin section studies indicates that they are related to compositional features in the rocks. The layering (flow banding) is imparted to the rock due to arrangement of plagioclase phenocrysts and mafics (pyroxene, olivine and opaques) in the ground mass. The feldspar phenocrysts also show preferred orientation along these bands.
4. In the compound flows alternatively coarse purple reddish porphyritic bands and greenish grey megaphenocryst bands are seen. These form repetitive quickly alternating sequence. Each band contains bent pipe amygdules, vesicular and amygdaloidal surface and silica geodes at the top, at times ropy lava and channel structures are also seen. About 5 to 6 repetitive bands are noticed within each flow.

#### **IX.2. PETROCHEMISTRY:**

The Average chemical composition for each flow for different sections is given in Table-V. Corresponding normative composition of the flows is given in Table-VI. The felsic index (FI), mafic index (MI), Solidification Index (SI) and D Differentiation index

TABLE-V  
Chemical Analyses of the Samples\*

S.No.	SiO <sub>2</sub>	Al <sub>2</sub> O <sub>3</sub>	Fe <sub>2</sub> O <sub>3</sub>	FeO	MgO	CaO	Na <sub>2</sub> O	K <sub>2</sub> O	TiO <sub>2</sub>	P <sub>2</sub> O <sub>5</sub>	MnO	Total
BH-3	42.42	15.51	1.66	11.40	5.61	11.40	3.75	1.55	3.60	0.75	0.22	100.36
BH-2	46.00	16.29	1.93	9.75	3.91	9.60	3.70	2.05	3.10	0.28	0.20	100.22
BH-1	41.99	15.28	1.12	11.26	5.43	11.45	3.70	1.60	3.30	0.35	0.21	99.60
BH-1/1	42.29	16.02	1.73	11.07	5.52	11.11	3.85	1.65	3.50	0.63	0.21	99.68
Av.	43.17	15.77	1.61	10.87	5.18	10.89	3.75	1.71	3.37	0.50	0.21	
AJ-6	50.81	15.24	3.30	9.31	1.44	9.65	3.65	1.45	1.80	0.20	0.16	98.43
AJ-5	47.59	14.90	3.29	10.96	2.84	9.25	3.55	1.50	3.70	0.18	0.20	99.71
AJ-4	46.74	15.02	3.94	10.19	3.34	9.35	3.40	1.50	3.80	0.27	0.20	99.47
AJ-2/11	46.70	14.90	5.00	8.31	3.58	8.75	3.70	1.40	3.50	0.20	0.16	99.12
AJ-1/1	45.75	13.50	5.20	10.73	4.99	8.47	3.60	1.70	3.70	0.25	0.17	100.37
AJ-1	45.50	15.15	5.20	8.69	4.16	8.00	3.70	1.75	3.70	0.17	0.17	98.80
Av.	47.18	14.78	4.32	9.67	3.39	8.91	3.60	1.55	3.37	0.21	0.18	
B-9	50.76	13.87	3.20	7.56	3.97	11.80	2.90	0.60	1.70	0.07	0.13	99.48
B-7	49.56	13.79	3.10	7.10	6.26	11.55	3.10	0.80	1.60	0.05	0.15	99.44
B-6	47.65	17.51	2.80	6.59	4.22	10.45	2.46	0.95	1.30	0.04	0.12	99.55
B-5	50.00	12.57	3.04	10.45	5.99	8.50	3.55	1.30	3.00	0.12	0.17	100.33
B-4	51.00	14.89	2.10	10.37	2.17	9.30	3.35	1.05	2.80	0.20	0.16	99.41
B-2	49.29	12.36	4.30	9.88	4.88	9.32	3.55	0.90	2.80	0.17	0.18	99.73
B-2/1	51.17	15.07	1.38	10.49	4.04	8.10	3.30	1.25	2.85	0.07	0.19	100.01
B-1	49.96	14.63	2.71	7.39	3.62	11.20	2.90	1.05	2.80	0.11	0.12	99.49
Av.	49.92	14.34	2.83	8.73	4.39	10.03	3.14	0.99	2.36	0.10	0.15	
M-4	47.66	15.43	2.80	9.22	5.31	11.33	2.90	0.23	1.30	0.04	0.14	99.82
M-1	50.45	16.85	2.90	6.70	5.16	8.18	2.85	0.40	1.40	0.03	0.13	99.41
D-3	41.72	17.14	3.70	9.65	7.93	9.50	2.40	0.60	2.20	0.05	0.17	99.86
D-2	47.13	15.95	2.60	10.30	4.16	12.90	2.95	0.04	1.10	0.10	0.18	99.34
D-1	48.50	16.86	2.40	9.56	4.66	11.25	2.65	0.24	0.90	0.04	0.16	98.80
U-3	47.52	16.09	4.30	9.11	4.23	9.53	2.85	0.70	2.80	0.04	0.19	100.18
U-2	47.58	16.14	4.35	9.49	5.70	6.85	2.65	0.22	2.85	0.10	0.17	99.37
U-1	46.42	13.61	3.90	10.23	5.03	11.15	3.08	0.50	3.00	0.12	0.18	99.53
AT-2	48.31	15.64	4.20	10.03	3.74	9.08	3.00	0.80	2.70	0.04	0.13	99.57
AT-10	51.80	14.88	2.97	10.31	3.46	7.65	3.45	1.00	1.60	0.06	0.18	99.76
R-1	48.37	21.22	1.31	6.93	3.62	11.88	2.95	0.21	0.85	0.02	0.15	99.74

TABLE-VI  
Normative Mineral composition of the samples

S.No.	Quartz	Orthoclase	Albite	Anorthite	Diopside	Hypersthene	Olivine	Nepheline	Ilmenite	Magnetite	Apatite	Total
BH-3	-	9.45	5.76	21.13	26.90	-	11.13	14.48	6.99	2.55	1.68	100.09
BH-2	-	12.23	18.86	22.52	20.82	-	8.61	7.38	6.08	2.78	0.67	99.96
BH-1	-	10.01	3.14	21.41	29.29	-	11.06	15.90	6.54	1.62	1.01	99.98
BH-1/1	-	10.01	5.24	21.96	25.04	-	11.38	15.34	6.84	2.55	1.68	100.04
AJ-6	1.80	8.90	31.96	21.41	23.16	3.80	-	-	3.50	4.87	0.34	99.73
AJ-5	-	8.90	29.87	20.85	21.04	-	6.42	0.28	7.14	4.87	0.34	99.71
AJ-4	-	8.90	28.82	21.96	19.86	-	6.20	0.28	7.45	5.80	0.67	99.94
AJ-2/11	-	8.34	32.49	20.85	19.00	0.56	3.67	-	6.99	7.66	0.34	99.90
AJ-1/1	-	10.01	26.20	16.12	20.50	-	9.01	-	7.14	7.66	0.67	99.87
AJ-1	-	10.56	28.82	20.29	16.25	-	6.44	1.99	7.30	7.89	0.34	99.88
B-9	4.44	3.89	25.15	23.91	29.52	4.61	-	-	3.34	4.87	0.34	100.08
B-7	-	5.00	27.25	21.68	30.16	3.39	4.57	-	3.19	4.64	-	99.89
B-6	1.44	6.12	22.01	35.86	15.70	11.72	-	-	2.58	4.41	-	99.84
B-5	-	7.78	30.39	14.73	22.35	8.20	5.90	-	5.78	4.41	0.34	99.88
B-4	4.14	6.12	28.82	23.35	19.66	8.67	-	-	5.47	3.25	0.34	99.81
B-2	-	5.56	30.92	15.29	25.60	10.35	-	-	5.47	6.50	0.34	100.02
B-2/1	1.56	7.78	28.30	23.07	14.17	17.23	-	-	5.47	2.09	0.34	100.01
B-1	3.60	6.12	25.15	24.46	25.75	3.68	-	-	5.47	3.94	0.34	98.52
M-4	-	1.67	25.68	29.19	24.09	5.67	6.86	-	2.58	4.18	-	99.91
M-1	5.88	2.22	25.15	33.92	7.02	18.40	-	-	2.74	4.41	-	99.73
D-3	-	3.89	16.24	35.86	11.06	-	19.86	2.84	4.41	5.57	-	99.74
D-2	-	-	24.63	30.86	27.94	-	8.97	0.28	2.13	3.94	0.34	99.08
D-1	-	1.67	23.06	34.19	19.21	14.32	2.06	-	1.82	3.48	-	99.81
U-3	1.44	4.45	24.63	29.75	15.30	12.38	-	-	5.47	6.50	-	99.91
U-2	5.04	1.11	23.06	33.08	1.14	23.90	-	-	5.62	6.50	0.34	99.79
U-1	-	2.78	26.72	22.52	27.46	2.16	6.11	-	5.93	5.80	0.34	99.81
AT-2	1.62	5.00	26.20	27.24	15.71	12.63	-	-	5.32	6.26	-	100.00
AT-10	3.42	6.12	29.87	22.80	13.55	16.50	-	-	3.19	4.41	-	99.85
R-1	-	1.11	25.68	45.04	12.71	5.87	5.78	-	1.67	1.86	-	99.72

TABLE-VII

S.No.	Solidification Index	Differentiation Index	Mafic Index	Felsic Index
BH-3	21.56	29.69	69.95	31.74
BH-2	17.46	38.47	74.92	31.74
BH-1	21.89	29.05	69.51	31.64
BH-1/1	21.50	30.59	69.87	33.11
AJ-6	7.38	42.66	89.75	34.58
AJ-5	11.67	39.05	83.38	35.31
AJ-4	13.54	38.00	80.88	34.39
AJ-2/11	14.86	40.83	78.80	36.82
AJ-1/1	17.68	38.77	76.15	38.55
AJ-1	16.35	41.37	76.95	40.52
B-9	20.54	33.48	73.05	22.88
B-7	29.58	32.25	61.97	25.24
B-6	24.29	29.57	68.99	24.60
B-5	23.01	38.17	69.25	36.33
B-4	10.44	39.08	85.18	32.12
B-2	19.21	36.48	74.40	32.32
B-2/1	18.31	37.64	74.61	35.97
B-1	18.64	34.87	73.62	26.07
M-4	24.66	27.35	69.36	21.65
M-1	27.14	33.25	65.04	28.43
D-3	30.64	22.97	62.73	24.00
D-2	19.71	24.91	75.62	18.82
D-1	23.10	24.73	71.96	20.44
U-3	18.16	30.52	76.02	27.14
U-2	22.76	29.21	70.83	29.53
U-1	19.93	29.58	73.75	24.30
AT-2	15.80	32.82	79.19	29.50
AT-10	15.88	39.41	79.33	36.78
R-1	23.12	26.79	69.48	21.01

TABLE-~~VIII~~ III  
DISCRIMINANT FUNCTIONS OF PEARCE, 1974

S.No.	F-1	F-2	F-3
BH-3	0.1062	-1.4613	-2.4287
BH-2	0.2041	-1.3639	-2.4231
BH-1	0.1195	-1.4285	-2.3879
BH-1/1	0.1189	-1.4498	-2.4378
AJ-6	0.3463	-1.3669	-2.3278
AJ-5	0.1831	-1.4033	-2.3773
AJ-4	0.1679	-1.4030	-2.3766
AJ-2/11	0.1870	-1.3995	-2.3626
AJ-1/1	0.1693	-1.4175	-2.3450
AJ-1	0.1767	-1.3754	-2.3670
B-9	0.3046	-1.4666	-2.3278
B-7	0.2938	-1.4996	-2.3753
B-6	0.3620	-1.3816	-2.3259
B-5	0.2354	-1.4752	-2.3822
B-4	0.2755	-1.4120	-2.3569
B-2	0.2366	-1.4792	-2.3226
B-2/1	0.2861	-1.4253	-2.4012
B-1	0.2250	-1.4232	-2.3830
M-4	0.3375	-1.5135	-2.3161
M-1	0.3987	-1.4540	-2.3530
D-3	0.2704	-1.4823	-2.3143
D-2	0.3380	-1.5346	-2.3116
D-1	0.3964	-1.5013	-2.3279
U-3	0.2631	-1.4594	-2.3530
U-2	0.3023	-1.4816	-2.3154
U-1	0.1897	-1.5094	-2.3225
AT-2	0.2836	-1.4493	-2.3364
AT-10	0.4000	-1.4232	-2.3171
R-1	0.4079	-1.5048	-2.4742

Table X Concentrations of siderophile elements in Anjar III, intertrappean section, Kutch

Sample No.	Depth <sup>1</sup> (cm)	Ir pg/g	Os pg/g	Cr μg/g	Co μg/g	Fe %	Mn μg/g	Ni μg/g	Os/Ir
#21	2			25.76	20.86	5.24			
#22	52			1.82	4.20	1.08			
#23-A	62			2.47	5.09	0.62			
#23-B	63			1.15	4.34	0.70			
#25	70			10.94	17.30	4.71			
#29	73			12.16	27.40	4.50			
#28	75	95	299±76	8.40	13.60	2.73	594	23.8	3.1±1
#24-A	80	186	<171	5.54	14.50	3.11	-	-	<0.91
#24-B	81	168	400±131	8.54	23.09	4.83	-	-	2.4±0.8
#27-A	82	733✓	1123±155✓	4.19-	61.00✓	31.42✓	330-	73.5✓	1.53±0.2✓
#27-B	83	1271✓	1414±125✓	4.97-	121.2✓	37.43✓	427-	99.8✓	1.11±0.1✓
#26	103	78	<80	5.15	17.2	2.38	473	41.6	<1
F-III-32	150	<10	-	8.57	45.7	9.10	1643	54	
% Errors (1σ)		10	-	4	0.2	1	5	5	
EF <sup>2</sup>		>127	-	0.58	2.65	4.11	0.26	1.85	

1. The depth is measured from the base of F IV
2. EF is enhancement factor of sample 27B with respect to basalt FIII.

17A

Table 1. Concentration of some siderophile elements in Anjar flows

	Fe (%)	Co (µg/g)	Cr (µg/g)
F1	10.96	49.91	40.9
F1	9.07	49.10	32.73
E2	12.46	59.83	79.28
F3-32	9.1	45.7	8.57
F3	11.22	51.13	1.67
F3	10.93	50.81	1.60
F4	10.80	51.67	<del>114.5</del> 45.07
F4	10.19	43.31	<del>120.5</del> 114.5
F4A	9.15	34.13	24.91
F5	8.81	32.5	21.8
F5	11.13	49.1	93.72
F6	7.75	31.3	27.14
F7	9.87	53.1	120.19
Typical Errors (1σ)	<1%	<1%	<2%

Table X. Concentration of lithophile and chalcophile elements in Anjar III intertrappean section, Kutch'

Sample No.	Ca %	Ba (µg/g)	Na %	Sb	Zn	Sc	Hf µg/g	Th %	Se	Ag (ng/g)	Cu (µg/g)	As (µg/g)	Al %	Mg %	K %	
#21		134.7	1.13	0.13	43.5	12.74	2.96	3.10	1.97	17		<2				
#22	40.6	43.9	0.28	0.04	6.45	2.51	0.62	0.60	0.42	5.3		BDL				
#23-A		53.7	0.25	0.06	13.51	2.46	0.46	0.52	0.45	107.7						
#23-B		59.2	0.33	0.12	7.02	3.91	0.44	0.44	0.01	386						
#25		95.5	0.70	0.86	39.09	9.94	2.67	2.55	1.78	39.5						
#29		86.3	0.63	0.40	23.53	9.06	2.58	2.39	1.51	40.6						
#28	6.26	86.7	0.42	0.27	18.30	9.19	2.32	2.44	1.24		64.9		2.97	4.22	0.34	
#24-A	3.4	122.7	0.30	2.14	89.75	4.18	1.35	1.29	1.25	304						
#24-B		118.0	0.34	2.75	75.61	6.01	1.71	2.12	1.11	26.2						
#27-A	1.2	240.3	0.23	17.3	133.7	3.77	0.48	0.51	7.78	4300		494	0.38	0.27	0.029	
#27-B	0.43	166.7	0.13	15.9	112.4	2.39	0.35	0.43	37.17	38.2		750	0.32	0.52	0.024	
#26	20.3	40.9	0.37	0.25	9.70	5.17	1.35	1.34	1.00		34.6		1.63	2.36	0.17	
F-III-32	6.7	296.0	1.07	0.02	59.8	23.90	3.76	2.72	2.56	72.4	151.3	BDL	7.29	3.03	0.83	
% Errors	5	11	1	13	5	0.1	8	9	18	3	5	3	5	5	5	5
(1σ)																
EF <sup>2</sup>	0.06	0.56	0.12	795	1.88	0.1	0.09	0.16	14.5	59.4	1.79		0.444	0.17	0.02	

1. BDL = Below Detection Limit

2. EF for Ag is for sample 27A

*Handwritten signature/initials*

Table 1 Concentration of some lithophile and chalcophile elements in Anjar flows

Flow	Ca (%)	Ba	Na (%)	K (%)	Zn	Sc	Hf	Th	Ta	Na <sub>2</sub> O (%)
F1	5.22	410	2.12		147	22.57	6.48	6.43	4.56	
E1	5.44	301	2.11		?	20.97	2.34	5.24	3.14	
F2	6.53	450	2.56		178	26.90	7.22	7.34	5.23	
F3-32	6.7	296	1.07	0.83	84.7	23.9	3.76	2.72	2.81	
F3	6.39	309	1.95		111	27.68	4.43	3.71	2.81	
F3	5.98	319	1.99		116.9	28.21	4.57	3.71	2.88	
F4	4.68	386	2.02	1.03	99.5	27.05	6.55	6.33	4.13	
F4	5.78	272	2.01		114.5	31.12	5.29	5.66	1.63	
F4A		266	6.65?	4.35	-	30.3	6.12	8.29	2.35	
F5	4.59	391	2.28		99.1	31.36	6.32	10.09	2.86	
F5	6.32	476	2.07		140.2	31.21	6.72	6.48	4.72	
F6	5.61	692	2.29		92.0	29.98	6.99	7.68	2.57	
F7	8.93	52	1.49		65	41.55	2.29	1.32	2.57	
Typical Errors (1σ)	2	4	1	1	2	<1	1	1	3	

Table X<sup>1</sup> Concentration of Rare Earth Elements ( $\mu\text{g/g}$ ) in Anjar III intertrappean section, Kutch

Sample No.	Details	La	Ce	Nd	Sm	Eu	Gd	Tb	Yb	Lu	Ce anomaly <sup>1</sup>
#21	Black clay	20.4	38.30	23.11	3.81	1.18	2.67	0.50	1.33	0.24	0.40
#22	L.S.	7.02	11.30	5.10	1.01	0.32	0.98	0.14	0.73	0.13	0.39
#23-A	White chert	7.77	9.20	4.90	1.29	0.29	0.92	0.15	0.75	0.12	0.29
#23-B	Black chert	1.84	2.90	1.60	0.40	0.14	0.45	0.06	0.44	0.07	0.36
#25	Black mud	12.97	26.70	14.30	2.25	0.82	1.55	0.27	0.70	0.14	0.44
#29	Brownish shale	11.00	29.40	14.80	2.04	0.70	1.36	0.24	0.52	0.12	0.53
#28	Blackish shale	11.38	26.70	13.80	2.33	0.72	1.53	0.26	0.66	0.13	0.48
#24-A	Chocolate white shale	9.04	15.80	9.20	2.05	0.49	1.47	0.23	0.79	0.13	0.38
#24-B	Brown shale	9.32	23.50	8.80	1.91	0.58	2.06	0.27	0.49	0.12	0.56
#27-A	Brown grey shale	5.44	14.63	7.80	1.39	0.32	0.33	0.15	1.88	0.29	0.52
#27-B	Brown hard pieces	5.25	17.14	9.60	1.12	0.32	0.39	0.15	0.79	0.17	0.57
#26	White shale	10.55	16.95	9.20	1.93	0.52	1.71	0.25	0.68	0.12	0.37
F-III-32	Black hard basalt	23.30	47.40	33.50	4.90	1.99	3.47	0.78	1.26	0.35	0.39
% Error (1 $\sigma$ ), EF		2	0.8	8	2	2	13	7	4	4	-
		0.22	0.36	0.29	0.23	0.16	0.11	0.19	0.62	0.48	-

1.  $\text{Ce/La} = [\text{Ce}/(1.44\text{La} + 0.66\text{Nd})]_{\text{mass}}$

Handwritten signature/initials

Table XI: Concentration of Rare Earth Elements in Anjar flows

Flow	Site/ Sample	La	Ce	Nd	Sm	Eu	Gd	Tb	Yb	Lu	Ce anomaly	mag polarity
F1	11-13	49.31	96.96	39.4	9.01	2.76	6.2	1.26	2.91	0.5	0.46	N
F1	11-8	47.22	67.11	37.6	8.73	2.19	4.9	1.0	2.95	0.46	0.33	N
F2	1-10	55.89	110.68	51.4	10.30	3.15	6.9	1.44	3.55	0.56	0.45	N
F3-32	H.S.	23.3	47.4	33.5	4.9	1.99	3.47	0.78	1.71	0.35	0.39	-
F3	2-14	30.68	61.28	32.9	6.83	2.28	5.13	1.04	2.72	0.38	0.43	N
F3	3-10	31.08	62.58	29.2	6.86	2.32	5.28	1.08	2.73	0.43	0.45	N
F4 (Fine)	10-13	47.4	90.09	40.1	9.11	2.63	4.48	1.31	3.68	0.57	0.44	N
F4 (Porphy)	4-5	29.5	60.17	29.3	7.45	2.25	5.92	1.22	3.84	0.56	0.45	R
F4A	H.S.	56.89	73.4	49.76	12.1	2.47	6.7	1.31	3.26	0.59	0.29	-
F5	8-04	41.96	82.35	37.2	8.62	2.51	7.02	1.45	4.87	0.75	0.45	R
F5	9-2	46.34	93.52	73.3	9.13	2.81	7.0	1.30	3.73	0.77	0.47	R
F6	H.S.	42.80	67.24	52.0	8.94	2.37	7.6	1.31	4.90	0.92	0.35	-
F7	6-8	7.69	14.77	23.8	3.53	1.27	4.2	0.74	2.30	0.54	0.34	R
Typical Errors (1σ) %		<1	<1	<8	<1	<1	5	<5	<7	<3	-	

H.S. : Hayd Specimen

Table 4.1 Concentration of volatile elements ( $\mu\text{g/g}$ ) in Anjar III intertrappeans section, Kutch

Sample	Details	Depth	Ta	Cs	Zr	Rb
#21	Black clay	2	1.79	1.33	86.0	-Rf
#22	L.S.	52	0.29	0.46	42.8	26.08
#23-A	White chert	62	0.25	0.39	44.1	16.4
#23-B	Black chert	<del>72</del> 63	0.21	0.11	33.9	3.8
#25	Black mud	<del>72</del> 70	0.61	1.28	85.7	-
#29	Brown white shale sample	73	1.23	1.35	67.5	-
#28	Black white shale	75	1.25	1.03	39.9	-
#24-A	Chocolate white shale	80	0.46	0.86	105.6	27.5
#24-B	Brown shale	<del>83</del> 81	0.69	1.42	86.7	-F
#27-A	Brown grey shale	<del>83</del> 82	0.11	0.42	140.8	-
#27-B	Brown hard pieces	83	0.13	0.09	113.4	-
#26	White shale	103	0.73	0.79	81.09	40.5
F-III-32	Black hard basalt	153	2.37	0.09	93.6	-
S-5	STANDARD		0.88	57.31	223.7	117.9
% Errors (1 $\sigma$ ) EF			7	13	11	7
			0.05	1	1.21	-

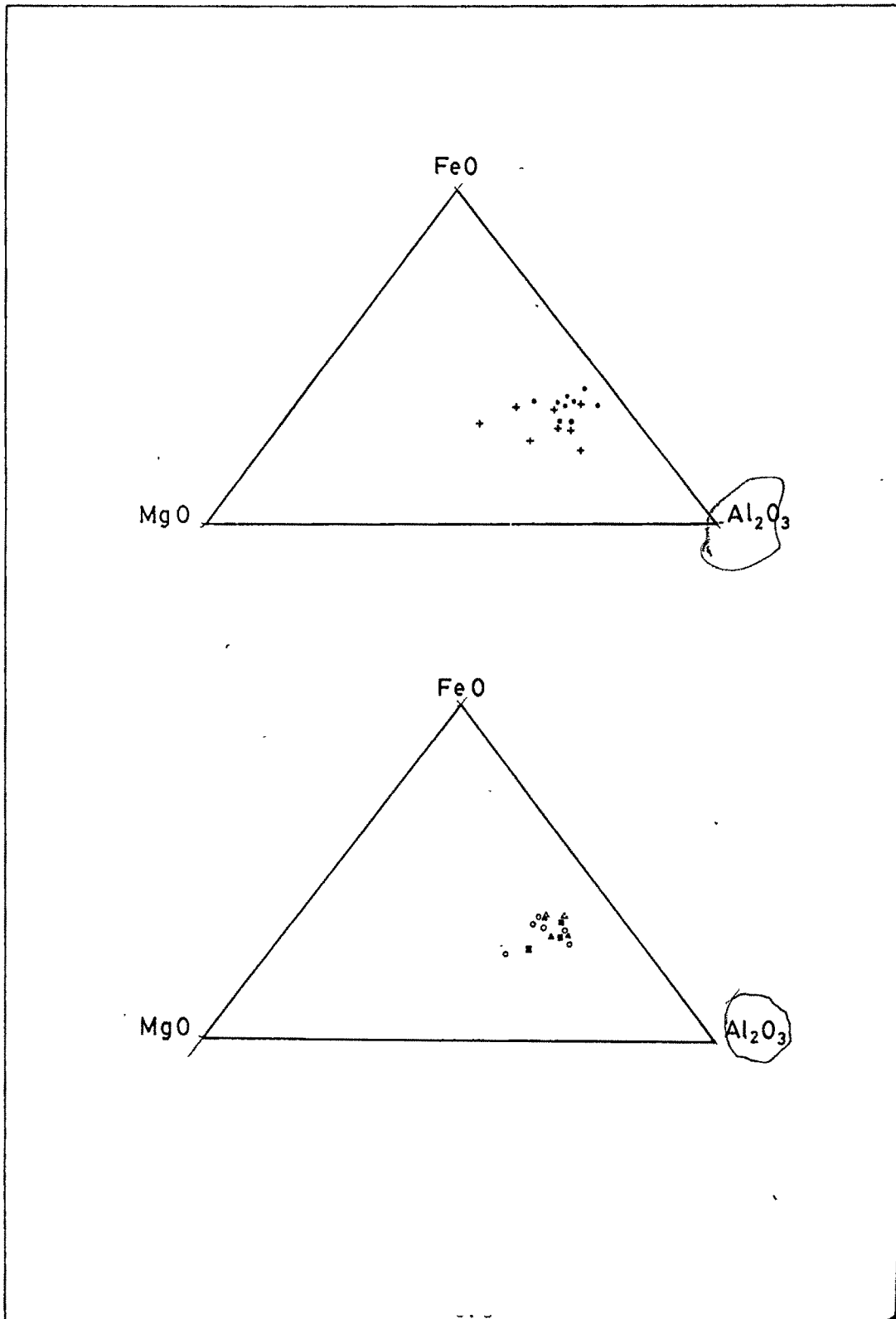


Fig. 78 A.F.M. diagram of Kutch volcanic

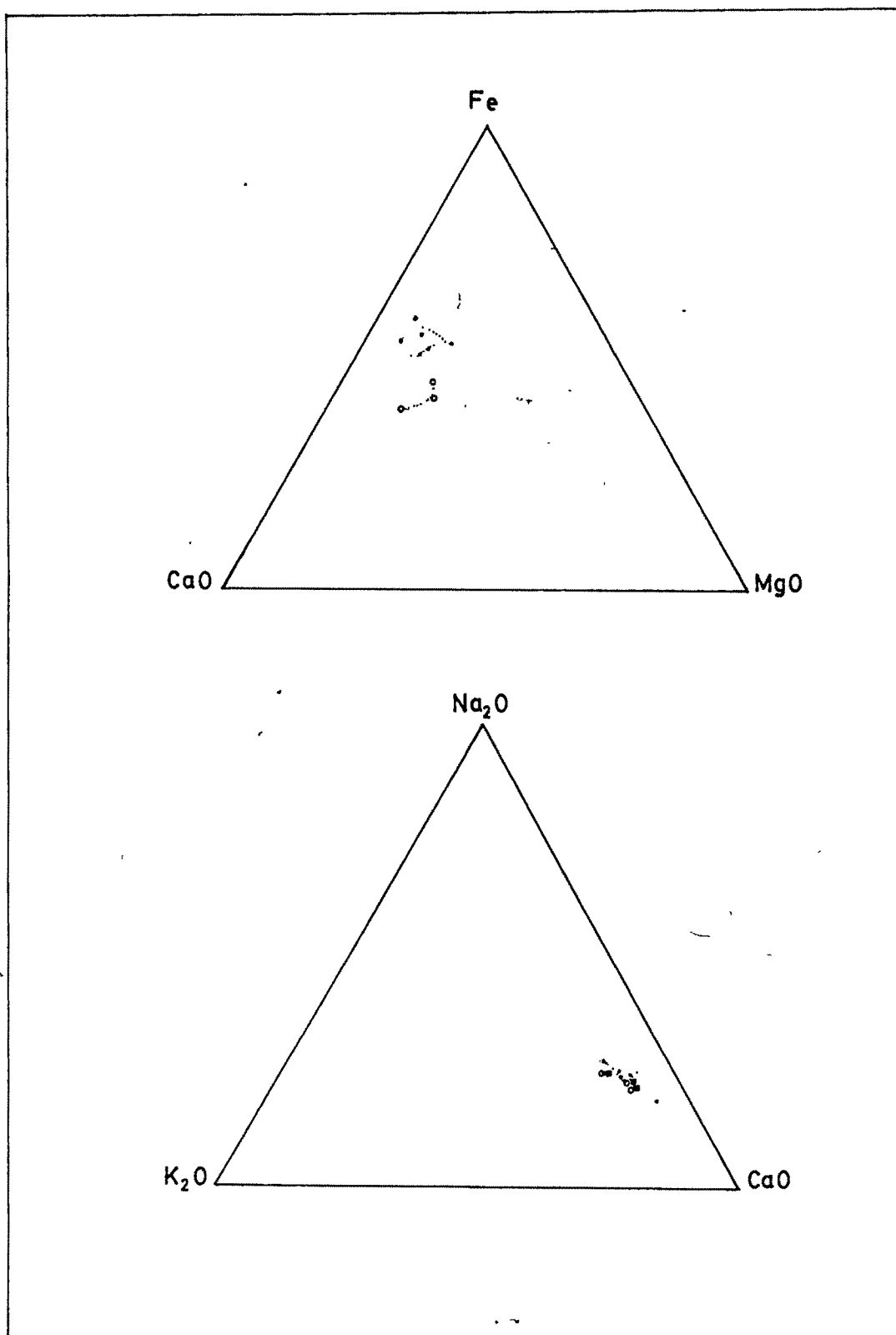


Fig. 19. FeO(T)-MgO-CaO plot of Volcanic of Kutulu, after Nichols and Allen, 1960.

Handwritten annotations: a vertical line on the left, a horizontal line in the middle, and a vertical line on the right.

12

11

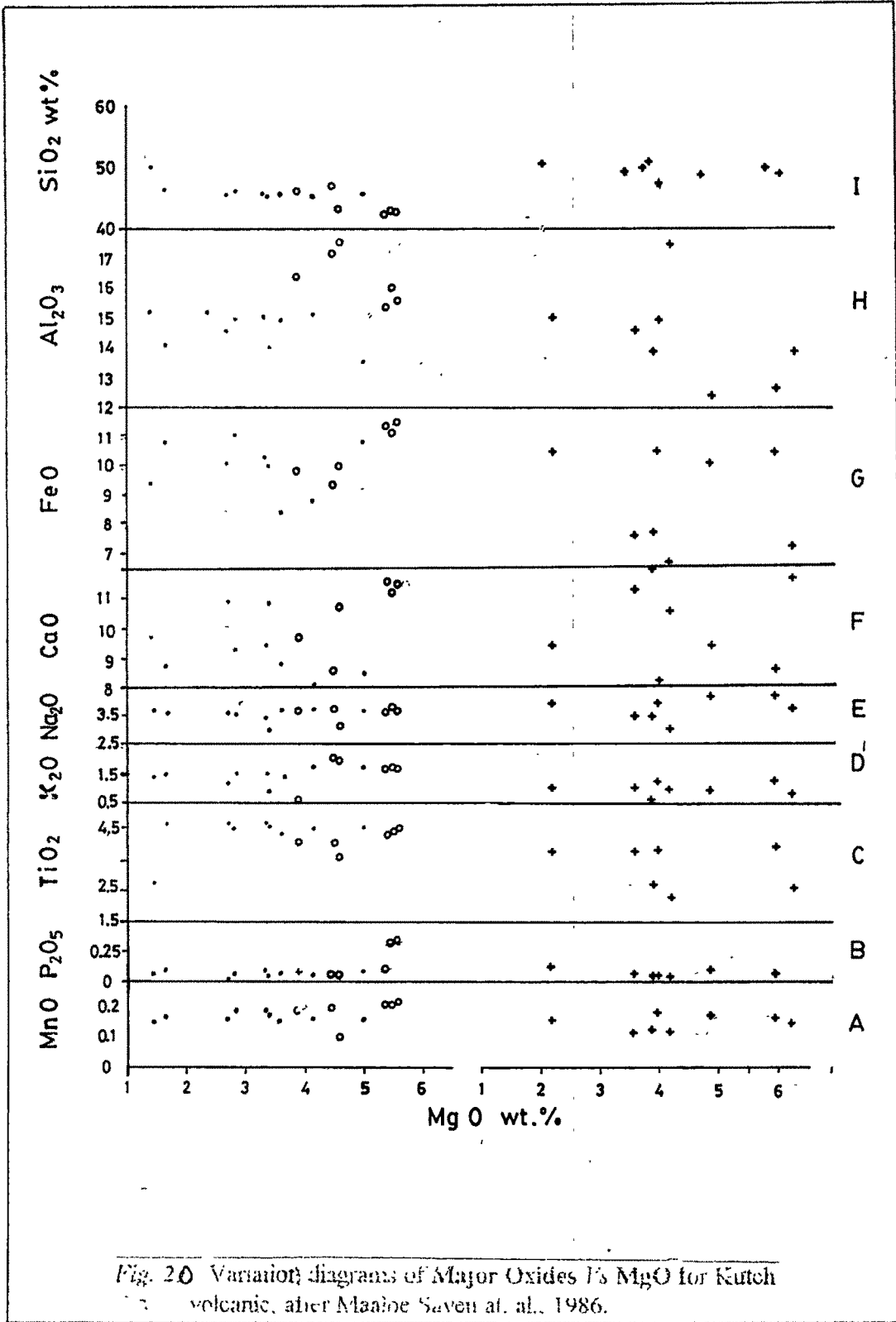


Fig. 20 Variation diagrams of Major Oxides Vs MgO for Kutch volcanic, after Maahne Saven et. al., 1986.

5/7 (1-9)

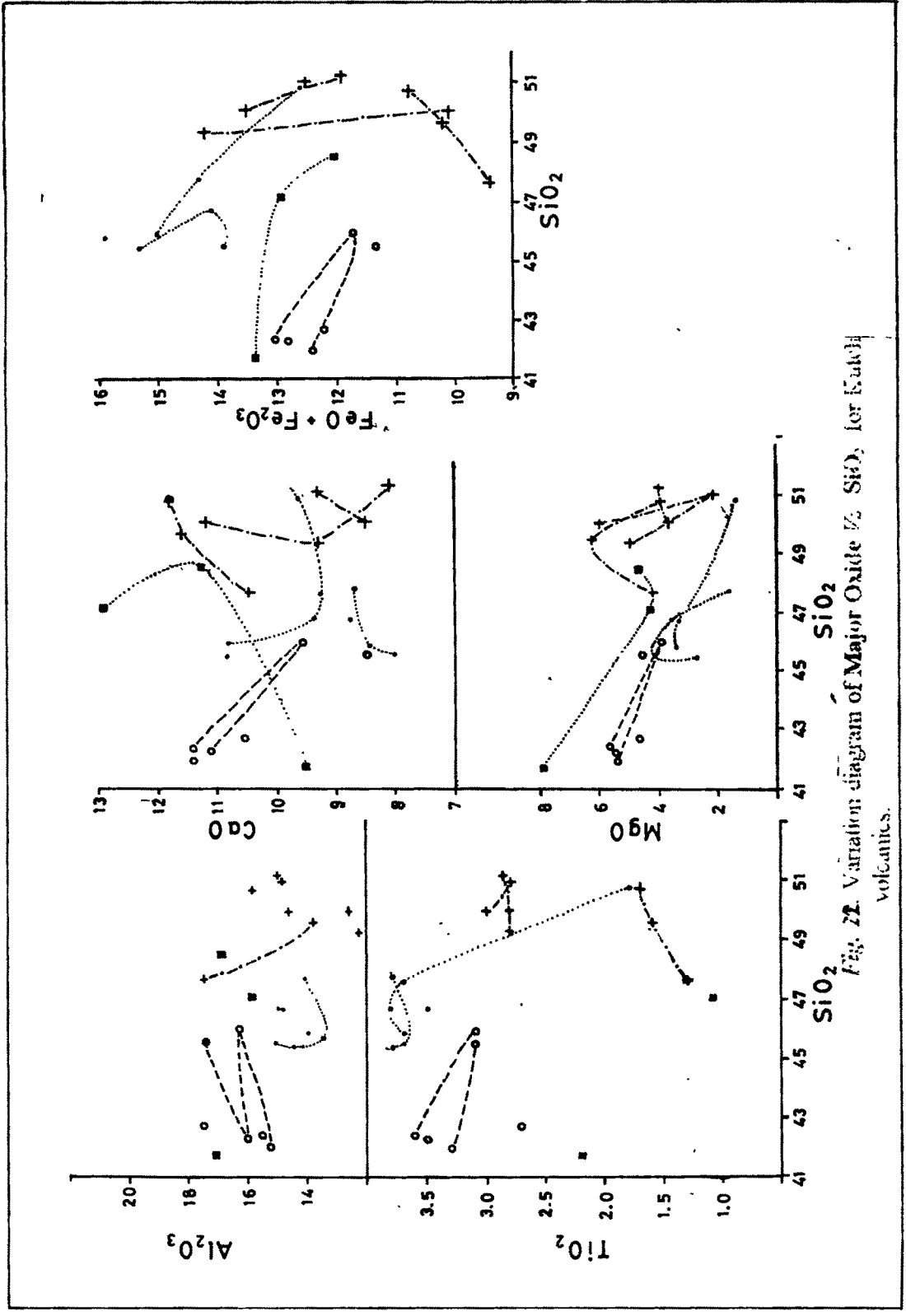


Fig. 22. Variation diagram of Major Oxide vs.  $\text{SiO}_2$  for Kaibab volcanics.

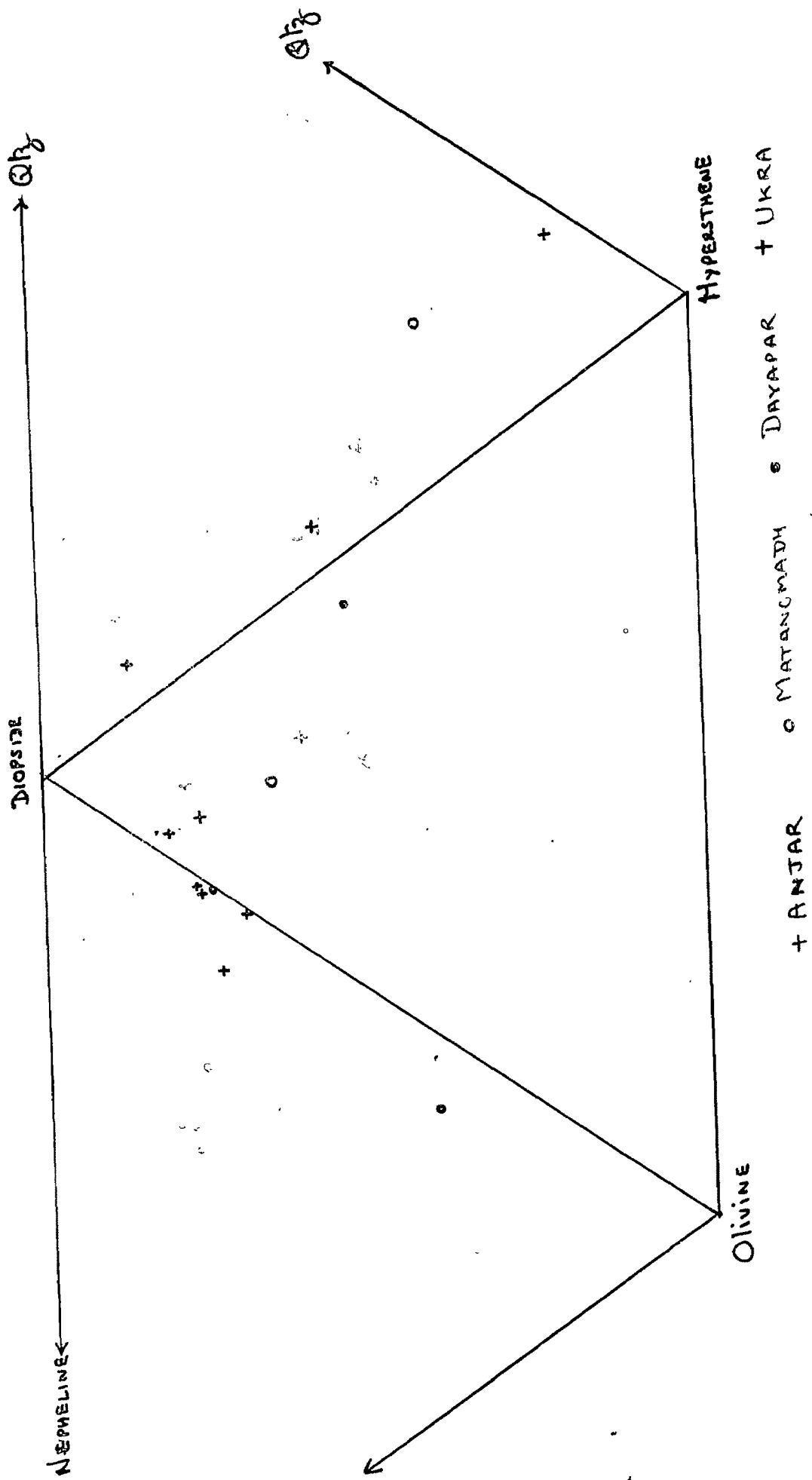
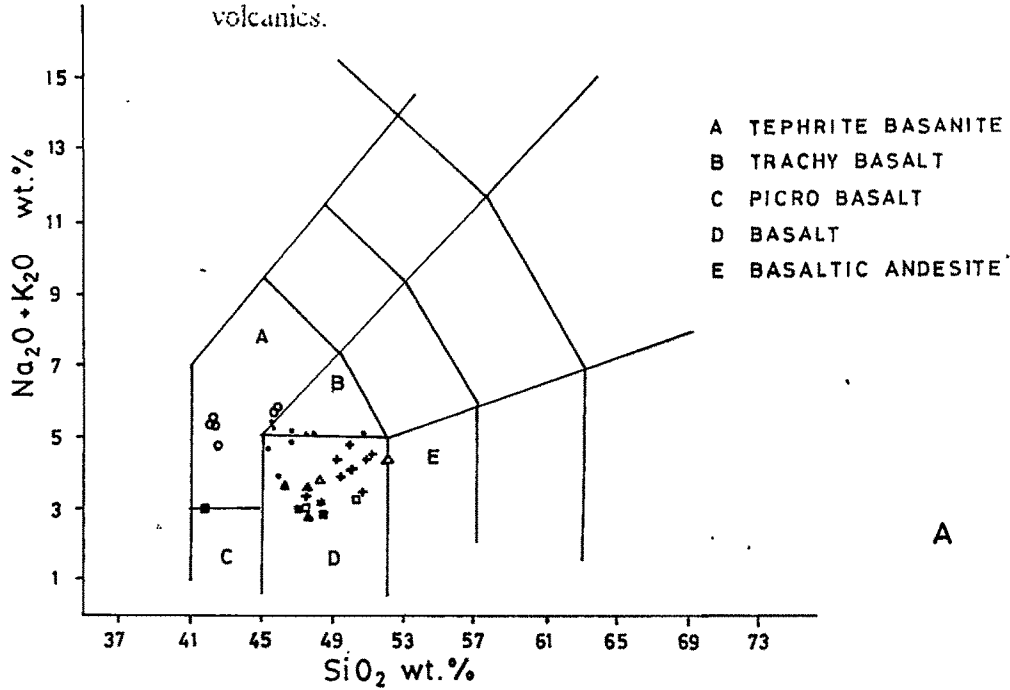
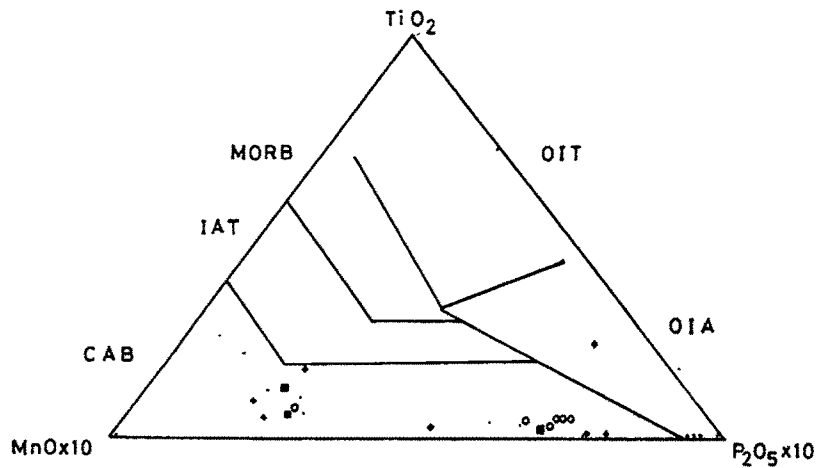


Fig. 22 Plot of normative Na-Ol-Di-Hy-Q for Kutuh volcanics to show regional variation from east to west.

Fig 23 Plot of T.A.S. diagram of LeBas, 1986, for Kutch volcanics.



(TAS DIAGRAM AFTER LE BAS, 1986)



AFTER MULLEN, 1983

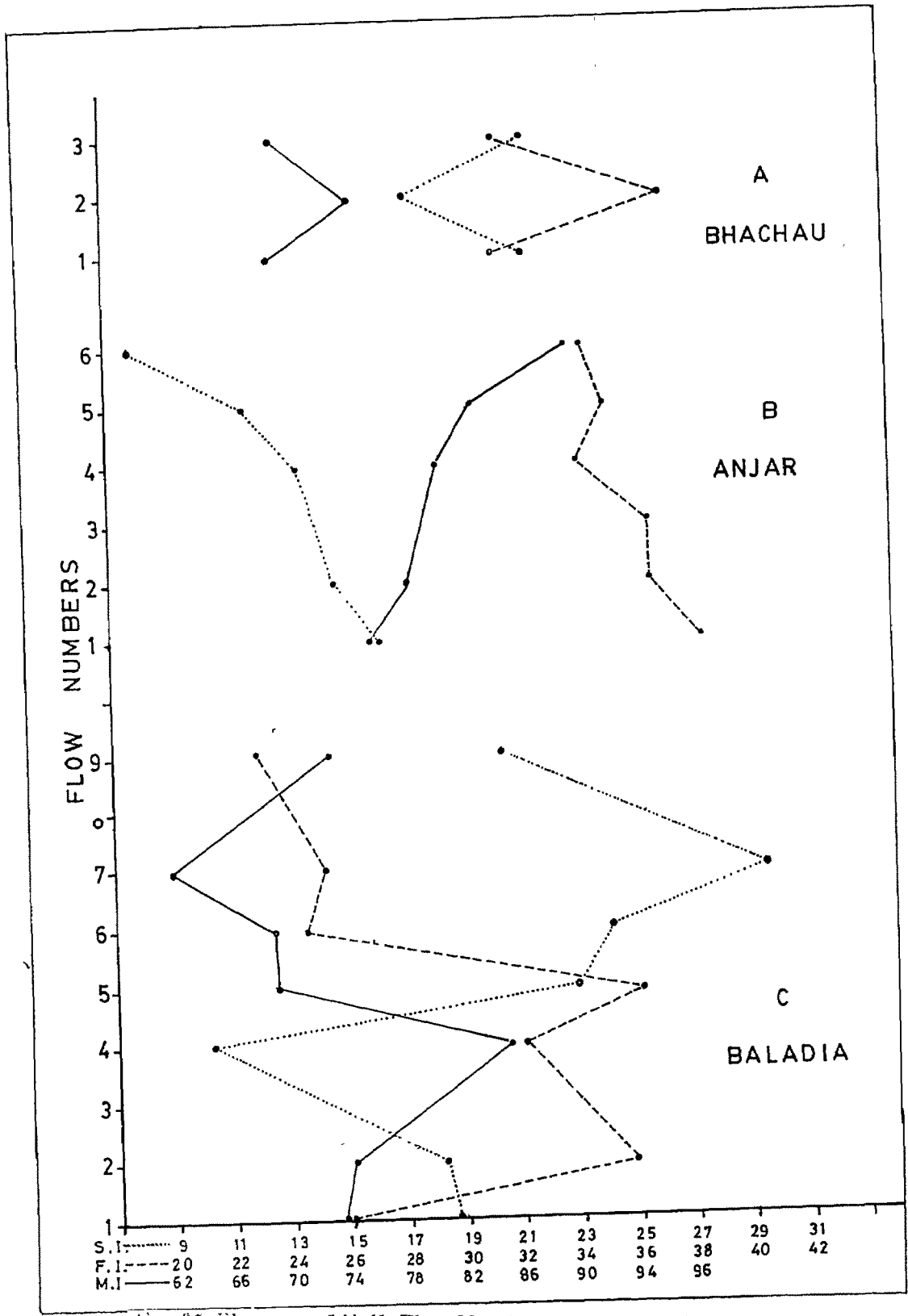


Fig. 26. Plot of SI, MI Vs Flow Numbers for Kutch volcanics.

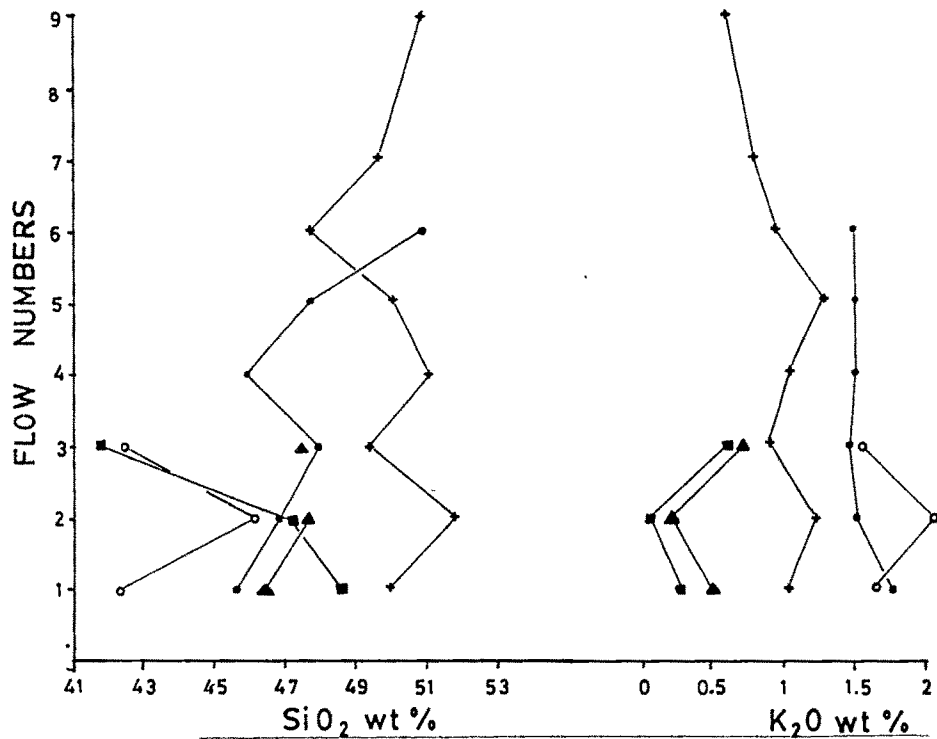
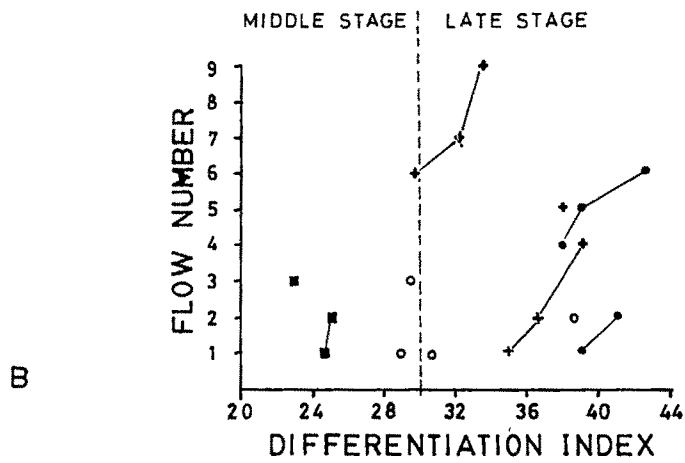
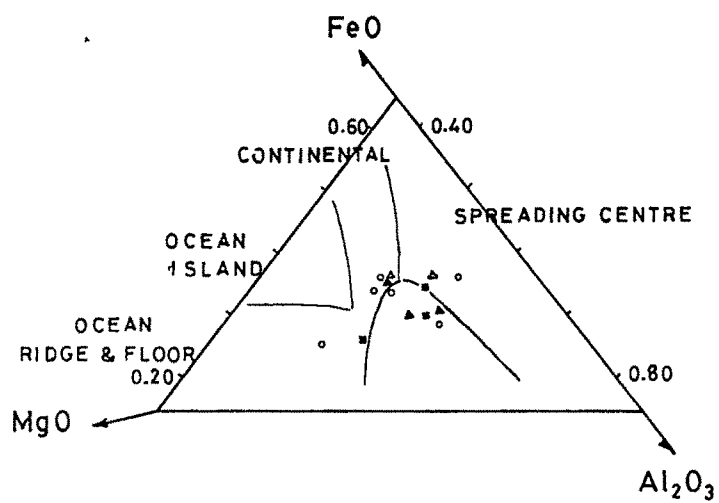
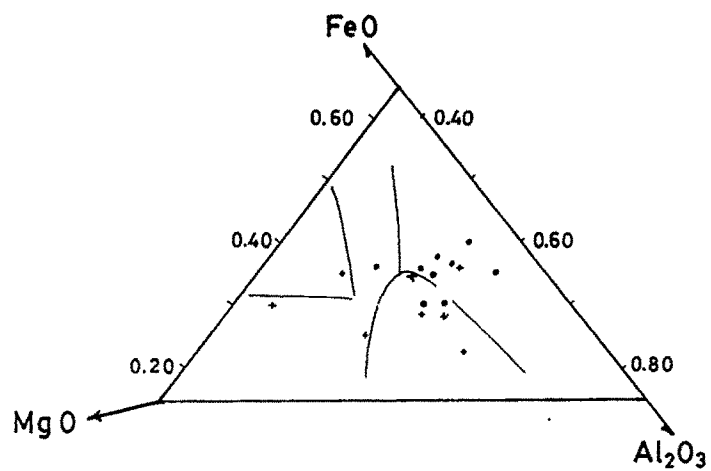


Fig. 25 Plot of SiO<sub>2</sub> and K<sub>2</sub>O vs Flow Numbers for Kutch volcanics.





AFTER PEARCE, 1977

Fig. 27 Ternary plot of MgO, FeO, Al<sub>2</sub>O<sub>3</sub> after Pearce et al., 1977. a part of field near FeO, Al<sub>2</sub>O<sub>3</sub> base is enlarged and shown.

(DI) for Kutch volcanics in different sections are shown in Table-VII. Discriminant functions of Pearce (1976) have been computed and summarised for each flow in Table-VIII.

### IX.2.1. Anjar Section:

The AFM plots indicate that the flows from Bhachau and Anjar fall close to FeO apex within the field of  $\text{Na}_2\text{O} + \text{K}_2\text{O} > 20\%$ . This flow shows enrichment in alkalis and FeO and depletion in MgO. The FeO enrichment is seen with increase in flow number, at the same time the  $\text{P}_2\text{O}_5$  V/s MgO and  $\text{TiO}_2$  plots show a gradual declining trend with respect to increase the flow numbers. The kinks in the curves represent change in the MgO content when olivine started crystallising. Fresh/additional influx of fluid increased the relative proportion of  $\text{P}_2\text{O}_5$ ,  $\text{TiO}_2$  and alkalis (Fig. 20), whereas MnO,  $\text{P}_2\text{O}_5$  and  $\text{K}_2\text{O}$  also show almost identical pattern in relation to increase in MgO content.  $\text{TiO}_2$  and FeO also show closely similar pattern in relation to rise in MgO content. The plot of major oxides vs  $\text{SiO}_2$  (Fig.21) indicates two distinct trends for each oxide. The first three flows show similar trends of  $\text{Al}_2\text{O}_3$ , CaO and  $\text{TiO}_2$  in relation to increase in  $\text{SiO}_2$ . The younger higher flows also show similar reverse pattern for total iron,  $\text{TiO}_2$ , MgO,  $\text{Al}_2\text{O}_3$  and CaO. In the An-Ab-Or plots the Anjar flows occupy a distinct field. There is a distinct trend towards increase in the normative anorthite content in the earlier lower group of Anjar flows. The Anjar volcanics occupy alkali basalt field in the AFM diagram (Fig.18) of Poldervaart & Sukeshwala (1958). In FeO-MgO- $\text{Al}_2\text{O}_3$  plot (Fig.27) the Anjar volcanics occupy a separate field close to Bhachau field and show three separate distinct trends in FeO (T)-CaO-MgO (Fig.19) plot.

### IX.2.2. Bhachau section:

Here the  $\text{SiO}_2$  and  $\text{Al}_2\text{O}_3$  show similar trends in relation to MgO (enhancement) in the initial stages and subsequently silica shows a very slow and gradual decrease. MnO,  $\text{TiO}_2$  and to some extent  $\text{Na}_2\text{O}$  show similar patterns and occupy identical fields. A sharp decline in the above can be seen at MgO content 4.3% and show subsequent normal rise in trend.  $\text{K}_2\text{O}$  shows initial rise and subsequent gradual decline. CaO and FeO show initial rise and subsequent gradual decline. CaO and FeO show initial decrease and subsequent gradual rise. The overall pattern of Bhachau indicates critical values of MgO around 4.3 - 4.35% and 5 - 5.5% where either increase or decrease is noted in values of major oxides. In the plots of various oxides vs silica (Fig.21) the Bhachau volcanics occupy a distinctly separate field. A similar reverse (mirror image) trend for  $\text{TiO}_2$ , MgO, FeO(T) and CaO is seen whereas the alumina shows an opposite trend compared to the (others). Bhachau flows occupy a distinctly separate field close to Anjar field in AFM diagram (Fig.18) and show enrichment in alkalis and depletion in MgO and also in the FeO(T)-MgO- $\text{Al}_2\text{O}_3$  plots (Fig.27) There is a distinct trend towards enrichment of FeO in Bhachau volcanics and they occupy a separate field close to the Anjar volcanics. In the An-Ab-Or

diagram Bhachau volcanics are close to Or-An line (two feldspar field) whereas the Anjar volcanics are close to Ab-An base and (two feldspar field).

### **IX.2.3. Baladia section:**

In the volcanics of Baladia section the major oxides vs. MgO plots (Fig.20) the oxide values show sharp changes between 3.5 - 4.2, 4.8 - 5 and between 5.8 - 6%. These kinks represent the separation of MgO from liquid, in the form of olivine, thereby modifying the relative composition of fluid with respect to oxides. The  $\text{SiO}_2$ ,  $\text{Al}_2\text{O}_3$  and FeO show similar closely comparable trends in the initial stage but deviate in the later part. The MnO,  $\text{TiO}_2$ ,  $\text{Na}_2\text{O}$  and  $\text{K}_2\text{O}$  show closely comparable trends. CaO shows different pattern in the beginning but in the later part is closely comparable to the  $\text{Al}_2\text{O}_3$  pattern. The Anjar and Baladia sections show different patterns which are comparable to some extent for very few oxides. Cyclicity of the events is clearly reflected in all three sections.

The variation of different oxides indicate identically opposite (mirror image) pattern for  $\text{Al}_2\text{O}_3$  and MgO. Similarly CaO and FeO (T) show two separate but opposite trends. Each segment represents separate pattern.

In the AFM diagram (Fig.18) volcanics of Baladia section occupy a separate field besides the Dayapar-Bhachau field. Similarly ternary plot of Feo-MgO- $\text{Al}_2\text{O}_3$  fall in separate tholeiitic basalt field away from the FeO- $\text{Al}_2\text{O}_3$  base and distinctly separate from the Bhachau and Anjar fields in the enlarged part of the diagram (Fig. 27). In the normative ternary plots (Fig-22) the Baladia volcanics show trend towards enrichment of An content and occupy separate field close to those from Dayapar.

### **IX.2.4. Dayapar, Matanomadh and Ukra sections:**

The variation pattern of the major oxides in relation to  $\text{SiO}_2$  for Dayapar section indicates close similarity for  $\text{Al}_2\text{O}_3$  and CaO,  $\text{TiO}_2$  and MgO show identical patterns, whereas FeO(T) shows similar but mirror image of the above pattern. In the AFM diagram Dayapar volcanics occupy separate field and show a clear trend of iron enrichment similar to that from Baladia. The volcanics from Matanomadh and Ukra also occupy a position closer to FeO (T). With higher proportion of FeO(T), MgO and alkalis and in the FeO (T)-MgO- $\text{Al}_2\text{O}_3$  plots (Fig. 19, 27) they have distinct separate field near the flows of the Baladia section.

## **IX.3. CHEMICAL VARIATIONS AND PETROCHEMISTRY OF THE SECTION:**

From the chemical data (Table-V) normative mineral composition (Table-VI), Plots of variation diagrams of different sections (Fig.20) including MgO vs oxides and oxides vs.  $\text{SiO}_2$  it is clearly seen that:

The  $\text{TiO}_2$  value can be used as a chemical criteria for grouping the lava flows into: (1) Lower group of flows with higher  $\text{TiO}_2$  content ( $\text{TiO}_2 < 2.0\%$ ) and low  $\text{P}_2\text{O}_5$  (0.04 - 0.07%) and MnO (.12 - .13%). Bhachau volcanics, Anjar flows F1 to F6, Baladia flows F1-F5 and Ukra flows are grouped under this category. The lava flows from Dayapar

(basal 2 flows) and Atda flows. F6-F9 of Baladia and F7 of Anjar region can be grouped in this category and occupy higher stratigraphic position in the Anjar-Baladia region; whereas the flows from lower group in the Dayapar-Matanomadh-Ukra show similar values.

Bhachau and Anjar volcanics show normal variation trends for  $\text{SiO}_2$ ,  $\text{Al}_2\text{O}_3$ ,  $\text{CaO}$ ,  $\text{FeO}$ ,  $\text{K}_2\text{O}$ ,  $\text{Na}_2\text{O}$  and  $\text{P}_2\text{O}_5$ , whereas in Baladia these trends are seen to be reverse for all major oxides and all incompatible oxides. In the Dayapar-Ukra sections all the major oxides and incompatibles show normal trends.

Details of other laboratory studies by the author include the following:-

- (I) Petrographic studies,
- (II) Palaeontological studies,
- (III) Geochemical studies,
- (IV) Palaeomagnetic studies,
- (V) Geochronological studies.

A detail account of each of the study is given below:-

The chemical data overall indicates that the Anjar and Bhachau sections and to some extent Baladia section (basal part) contain high  $\text{TiO}_2$ ,  $\text{Na}_2\text{O}$ ,  $\text{K}_2\text{O}$  and  $\text{MnO}$  flows. These values are maximum for Bhachau, whereas the upper part of the section at Baladia (flow 5, 6, and 7) and some flows in the top part of Anjar. Dayapar volcanics can also be grouped on the basis of flow  $\text{TiO}_2$  (Upper group). Baladia section encompasses both the group of flows.

Such flows form the lower group in the Dayapar, Matanomadh and Ukra area. Overall concentration of the incompatible and major element oxides e.g.  $\text{TiO}_2$ ,  $\text{P}_2\text{O}_5$  and  $\text{MnO}$ ,  $\text{FeO}$ ,  $\text{K}_2\text{O}$  are low in flows of these sections as compared to those of Bhachau and Anjar sections. Baladia section encompasses both type of lava flows.

In the variation diagrams of  $\text{MgO}$  vs major oxides (Fig. 20 except  $\text{FeO}$ ) and  $\text{SiO}_2$  vs major oxides it is seen that Anjar and Bhachau flows have normal variation trend in relation to  $\text{SiO}_2$  whereas  $\text{MnO}$ ,  $\text{TiO}_2$ ,  $\text{P}_2\text{O}_5$ ,  $\text{FeO}$ ,  $\text{Na}_2\text{O}$  and  $\text{K}_2\text{O}$  show reverse trends in the Anjar section. In Baladia section  $\text{SiO}_2$ ,  $\text{Al}_2\text{O}_3$ ,  $\text{CaO}$  and  $\text{TiO}_2$  show normal trends whereas rest of oxides and incompatibles show reverse trends in relation to  $\text{MgO}$  vs oxides. In the variation diagrams in relation to  $\text{SiO}_2$  (Fig.21) the Baladia flows have reverse pattern. In the Anjar and Baladia a scattering and divergence is observed in some cases. The gradient of the curves for  $\text{CaO}$ ,  $\text{FeO}$ ,  $\text{MgO}$  and  $\text{TiO}_2$  suggest a crystal separation and early fractionation and all the three phases were operating simultaneously.  $\text{TiO}_2$  was involved in early separation with Fe in titan-augite. Under the microscopic study evidences of early separation of olivine, plagioclase and pyroxene are observed for various sections. In Baladia section and Anjar section two separate batches of magma are suggested. The flow wise variation of major (type) oxides in vertical sequence in various sections when

examined in detail show a cyclicity of the higher to lower values of all major oxides. Each of such repetitions were grouped as a single continuous event. Accordingly there are two cycles in Bhachau section. Table-VII show different values of DI., SI, FI and MI for all the sections. These values were used for classifying the flows into different groups as early stage basalts and middle stage basalt differentiates in different sections. According to this groupings (Fig.25 and 26) the flows from Bhachau section are of middle stage basaltic differentiates. Anjar and partly Bhachau volcanics are late stage basalts.

### **IX.3.1. Overall Variation:**

In TAS diagram (Fig.23) of Le Bas (1986) Bhachau flows fall in alkaline field (tephrite/basanite field), Anjar volcanics plot in the trachybasaltic and micro-basaltic field while the Baladia, Dayapar and Ukra-volcanics fall in the basaltic field. The Kutch volcanics were plotted on discriminant function diagram of Pearce (1976) based on various functions (Fig.1, likewise F2 and F3). Majority of the plots for chemical data of Bhachau, Anjar and Baladia fall within plate Basalt (WPB) field (continental Group) with a few samples from Dayapar and Matanomadh falling in Low Potassic Tholeiite (LKT) field (Fig. 27). The plotting of the volcanics on Pearce (1976) diagram based on F1 and F3 indicate a scattered nature in LKT and CAB fields. Majority of the plots in the FeO-Al<sub>2</sub>O<sub>3</sub>-MgO diagram of Pearce (1977) fall in the spreading centre and continental fields with some scattering of the data (Fig.27)

### **IX.4. MODE OF ERUPTION:**

*How is this beneficial here*

The Deccan flows between Anjar and Matanomadh show frequent association of pyroclastics (Plate-XI/2), porcellanite, agglomerates, welded tuff and pyroclastics associated with intertrappeans. The porcellanite partly resembles with the three units ash, lithic and porcellanite from Chanchi (Radcliffe & Srivastava, 1984). The basaltic agglomerate and pyroclastic flows are traceable over wide areas in central Kutch. The authors have recorded close association of pyroclastic flows and composite dykes some of which are traceable for a distance of more than 60 km along strike length between Anjar and Chunadi (Fig.1A). The lithic fragments comprising of different composition of basalts (more than 95%) with variable size (from few cm to 70 cm). Largest size variation of the lithic fragments are seen near Anjar and Matanomadh. The pyroclastics show crude gradation in size. The basal part of the section is lithic as mentioned above which grades from coarse to medium size fragments, lapilli and finally into ash and fine granulose loosely welded material containing, giant size feldspar clasts embedded within the matrix along with large pieces of reddish, purple and greenish grey, amygdular (of analcite-calcite) aphanitic rocks, ash, scoriaceous and porous ropy lava. The highly vesicular and scoriaceous rock gives an appearance of pumice, association of pumice and ignimbrite is well known (Sparks et al 1990, Le Bas and Sabino, 1990, Shano, 1961, Thurston, 1980 and Hitch et al 1961). This grading is not visible everywhere. At Chandroda the pyroclastics show a crude stratification (Plate-XIII/2), micro-cross-ripple lamination on the ropy lava



Plate XIII/1 Pyroclastics near Anjar, Kutch.

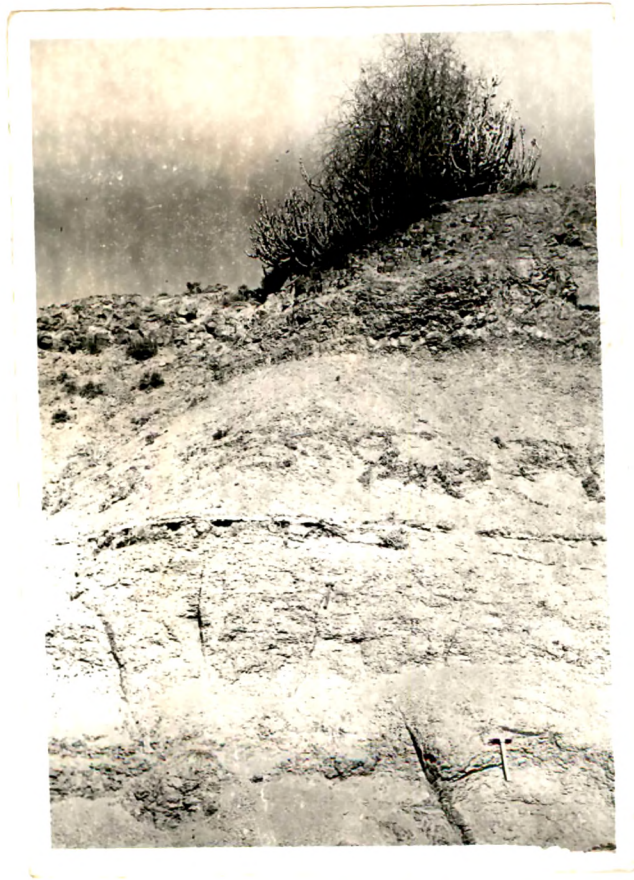


Plate XIII/2 Stratification in pyroclastic material near Chandroda, Anjar area.

surface, flow fronts, lava tunnels and similar primary volcanic structures, bent pipe amygdules and stretched amygdules in the upper part of the compound flows indicate change in the viscosity of the lava within the vertical piling. Such pyroclastic flows are associated all along the composite dykes which are connected to chain of small conical plugs (Fig. 1A) and a dykelet swarm. These dykelets originate from the composite dykes as well as from conical shield volcanoes and merge with higher flows. Generally it is seen that the margins of the small volcanic cones are associated with pyroclastic surge deposits, and crude erosional channels indicating a sort of debris flow along the slopes of the volcanoes. Along the channel margins accretionary deposit similar to those described by Cas and Landis (1987) and Schumarcke, have been recorded. The authors have noticed three such multiple dykes associated with debris breccia clasts at different stratigraphic positions in the Anjar-Baladia section. Each of the dyke a chain of small eruptive centres is considered as a separate eruptive phase from the feeder. The small shield cones tapped in lava from shallower depth forming small arches or chains, which forcefully ejected the debris and lava highly charged with gases, dust and fumaroles in an effective manner as suggested by Hatch et al (1961). At times the small cones are associated with composite ring dykes. An analysis of the directional parameters clearly indicate that these fissures and chains of volcanoes acted as a local source of lava. These feeders are associated with 3rd, 5th and 8th flows in Baladia section and with the 2nd and 4th flow in Anjar area. The plot of SI vs flow numbers (Fig-24) suggests correlation with the feeder eruptive phases. There are some isolated large plugs within the Upper Cretaceous rocks. These plugs are associated with pyroclastic surge deposits. They show tholeiite-basalt and alkaline nature. The dykes emerging from such plugs are seen connected to the basal flows in Anjar and Baladia area indicating them to be the source for the basal flow in Central Kutch. Similar plugs are also recorded in the higher part of the section and ash tephra dominated ignimbrite horizon with exceptionally high thickness (15-20 cm) is recorded near Shinugra and Viri.

combined  
account.

loss  
usage

What is  
the reason  
of these  
deposits

What  
does this  
mean?  
no support  
for this  
conclusion

?

Pyroclastic flows were ejected under high pressure highly charged with gases. Feeder dykes and chain of small volcanic produced a crude arrangement of larger boulders and blocks near the source and admixture of lapilli, granules with little ash and dust away from the source. The ash and the pyroclastics represent sub-aerial eruption. Ash appears to be the simple air-fall out indicating subsequent transportation and deposition in inland lakes or depressions.

#### **IX.5. IMPLICATIONS:**

The present study has brought out important chemical variations of the Kutch volcanics within this single large Deccan sub-province. A comparison of plots of SI, FI, MI Vs flow (Fig.24) numbers indicates three chronologically distinct spontaneous eruptive cycles with lavas of different maturity at different places. Contemporaneous eruption of different lava flows at different places suggests the possibility of small multiple sub-chamber. Differentiation to various degrees in the sub-chambers or cupola may have resulted in the

why?

lava of diverse maturity. During the first eruptive cycle flows of middle, intermediate and late stage basaltic differentiates were erupted at different places. During the second eruptive cycle, the late basaltic differentiates were erupted in Anjar and Bhachau whereas in Baladia and Dayapar late stage basaltic flows were erupted. The same differentiating source appears to have been tapped during second eruptive cycle as there is a smooth continuity and transition to higher stage in the degree of maturity in the magma (Fig. 26) during the culmination of the second eruptive cycle as shown by Anjar, Baladia and Ukra sections. The successive cycles were separated by sufficient interval of time. The 3rd eruptive cycle in Baladia comprises flows with lower maturity and indicate an inconsistency of source. During this cycle there is mixing of fluids as indicated by petrographic studies. In Anjar maturity of differentiation was maintained in the 3rd cycle. It was faster in Anjar and Baladia. Upper flows of the section show quick cyclic repetitions between aphyric and phyric flows (with middle and late stage basaltic flows). This cyclic nature could be due to squeezing of lava through a mesh of phenocrysts from partly solidifying (crystallising) flows due to front collapse or due to blisters and dykelets, due to change of viscosity and change of the aerial extent of the flows. At times there is crude banding of phenocrysts indicating differentiation by crystal settling. The alternate banding is common in the upper, part of Anjar. Baladia and Dayapar areas. The eruptions were largely within continental crust through deep fractures.

#### **IX.6. RELATIONSHIP OF LAVA ERUPTION TO K/T EVENTS:**

*only relevant aspect for the entire thesis.*

Anjar lava sequence has been dated as  $68.2 \pm 1.2$  -  $61.2 \pm 1.2$  m.y. and hence the span of volcanism extended for about 7 m.y. Iridium rich layers are recorded within the 3rd Intertrappean bed (Bhandari et al, 1995) below which dinosaurian fossils were recorded. The 3rd Intertrappean is bounded by 3rd, and 4th flows. Deccan volcanic event predates the K/T event (Venkatesan et al, in press). Third Intertrappean has yielded uppermost Maestrichtian and Danian microbiota. The 4th flow overlying the 3rd Intertrappean dated 65 m.y. indicating that the 3rd Intertrappean contains palaeontological, geochronological, geochemical and palaeomagnetically defined boundary. The initiation of deccan event predates the K/T boundary event by 3 m.y. - the main phase of the quicker widespread eruptive cycles intensified and ceased within 3.5 - 4 m.y. as shown by the dates. It is also possible that the oldest basaltic flow sequence of Deccan traps may be somewhere in the east and the youngest flows in the west.

#### **IX.7. PETROGRAPHIC STUDIES OF THE INTERTRAPPEAN BEDS:**

##### **IX.7.1. Anjar Area:**

Petrographic studies of various rock types of Intertrappean beds at Anjar and Dayapar were done for various purpose. The Intertrappean beds at Anjar consist of the following main rock types, which can be studied by preparing thin sections. Calcareous sandstone, laminated ash, limestone, banded and laminated chert, iridium rich brown layer, fossiliferous limestone, nodular marl from second and third Intertrappean bed. From the first

Intertrappean bed, the important rock types include banded chert, massive chert, laminated limestone, stratified and microcross rippled limestone, sandy limestone.

#### **IX.7.1.1. Calcareous Sandstone of Second Intertrappean Bed:**

This rock forms important horizon in the second Intertrappean bed towards west of Viri village. It is greyish white, yellow and buff coloured, coarse, concretionary, tuffaceous, calcareous sandstone. On weathered surface, it shows aggregates of small, spherical, concretions with 1.0 to 2.0 mm diameter. Under microscope, it shows coarse, granular to crystalline with angular to sub-angular grains of quartz, set in calcitic and clay matrix. The grains show coating along the margin. At times, fragments and pieces of small invertebrate and fossil wood are also seen. At times, the volcanic material dominates in the matrix to such an extent that rock can be termed as volcanoclastic sandstone.

#### **IX.7.1.2. Laminated Ash:**

This forms important part of sub-unit of second and third Intertrappean beds. The ash is brownish grey in colour and shows finely laminated nature. The laminations comprise extremely thin alternating light coloured and dark coloured bands within the light and dark coloured thin bands. There is gradation from comparatively thicker darker unit at base to gradually thinner and lighter coloured band (laminated) towards top. Each lighter coloured and darker coloured bands comprise about 15 to 26 number of bands of microlaminations within single unit. Thickness of each such unit varies from 1 to 1.2 cm. At one place, about 40 such alternating cycles of units within 40.3 cm with 210 microlaminated units were recorded. Successive laminae bands show thinning up the section, as compared to previous one. Such ash is very light in weight and is very soft.

Under microscope, each laminae comprises clasts of feldspar needles, (shards) and some biogenic objects - most of them altered. These are arranged in layer as rounded, spherical and linear structures. Such spherical bodies show thin lining of green layer with definite structure (Plate-XVI/1). Further, details of internal structure and maceration (microlayer) may help in detail identification of such bodies. They are suspected to be some organic remains. The micro feldspar clasts show characteristic twinning of plagioclase feldspars in some cases. The shards and clasts are arranged in different microlayers.

#### **IX.7.1.3. Banded Chert:**

Banded chert is found as predominant rock type in the third Intertrappean, fifth Intertrappean and to some extent in the second Intertrappean bed. These cherts are in form of regularly bedded deposit, with petrification of existing fossils and to some extent in form of replacement of earlier rocks.

#### **IX.7.1.4. Chert from Second Intertrappean Bed:**

The second Intertrappean bed contains small lensoid partings of banded chert in form of algal laminated bands and as replaced fossil wood. Under microscope, it shows

microlaminated fibrous spherulitic and largely floating type cherts and quartzine grains with length slow type character in the basal layers and in the entire replaced part of the original material with some central patches of coarsely crystalline quartz with length fast characters. Fine aggregate of the quartz and spherulitic chert also show some continuity of earlier pseudomorphs indicating a later replacement of earlier ones by silicification. Such masking effect is clear only on viewing under cross nicols and on insertion of sensitive plates. The laminations and nodular structure also contain rhizomes and show calcification.

#### **IX.7.1.5. Banded Chert and Porcellanite from Third Intertrappean Bed:**

The chert occurs as banded stratified and laminated bed and also as lensoid bodies and stringers within the fossiliferous limestone and shales. It has greyish white, brownish yellow and black colours. It also occurs as chertified fossil plants within the black and brown coloured shales.

Under microscopes, the banded cherts shows cryptocrystalline aggregates of quartz, chert, quartzine in various forms. Fine rhythmic laminations comprise of spherulitic and mesh wire structure of length slow chert and quartzine. Relict pseudomorph show continuity of shape under cross nicols and sensitive plate/quartz wedge indicating existence of earlier (now) replaced minerals/fossils by silica. Chert and quartzine veins show isotropic characters with typical rhombic cleavage, indicating a thorough replacement of the calcitic veins by length slow chert and quartzine. It shows laminated nature, concretions and calcritisation in hand specimens.

#### **IX.7.1.6. Banded Chert and Finely Laminated and Stratified White Silica of Fifth Intertrappean Bed:**

In the fifth Intertrappean bed, it occurs as white greenish and yellowish green apparently fine grained, massive unit at base, followed by a banded and finely laminated and stratified yellowish white and at times brownish silica, interstratified with white banded limestone, sandy limestone. In microsections, the massive chert shows cryptocrystalline, spherulitic and coarse (quartzine) floating and chicken wine (spheritic) aggregates of chert, with relict (in back ground) shapes of pseudomorph crystals with minute inclusions. These shapes are apparent on examination under cross nicols with the help of sensitive tint/quartz wedge. At times, oolitic chert and spherical growth of silica are seen. Greenish chert replaces long, filamentous structures, which apparent to be of green algal filaments and spores. These are composed of length slow chert. In microsections, the chert shows microlaminations and layers of opaline silica and chert followed by spherulitic growth of chert and cryptocrystalline aggregate of chert and quartzine and finally by larger interlocked quartz, chert and quartzine show length slow characters. Whereas, the interlocked quartz show fast character. Brownish patches of relief crystals are very common in such silica, which indicates that the massive and banded chert are not simple geodes or vug/vein fillings, but they occur as the replacement of earlier carbonates with some evaporite. The chert-banded/laminated limestone association indicates this fact.

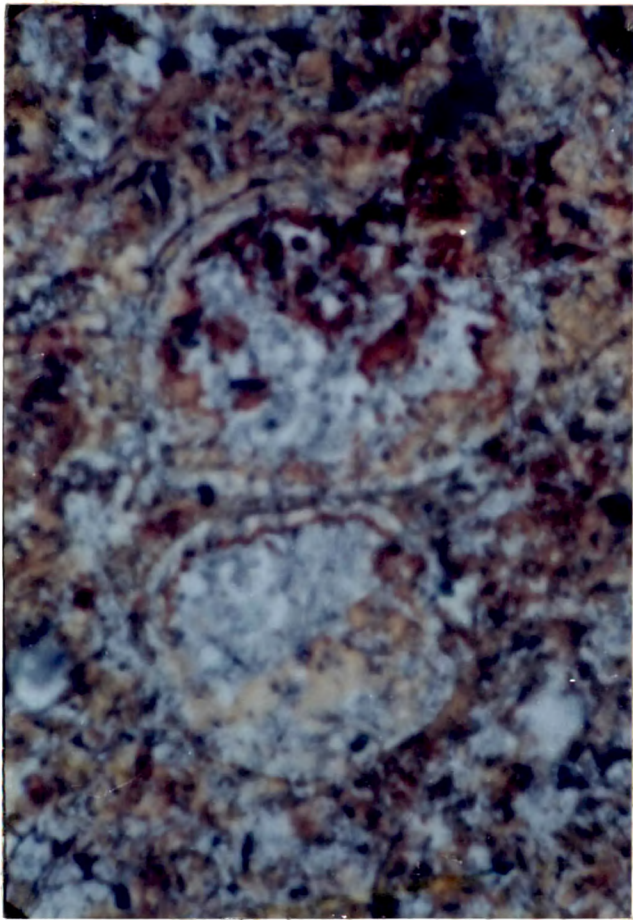


Plate XVI/1  
Microsection of Ash layer, Intertappean bed, Anjar,  
Kutch.



Plate XVI/2  
Microsection of anomalous lateritic nodular layer, rich  
in Iridium - A close up view.



Plate XVI/3  
Magnified view of Iridium rich nodule. Iridium  
spherules with calcite coatings.



Plate XVII/3 Microsection of fossiliferous sandstone. (a) Algae, (c) larger foram and (c) plant tissues are visible

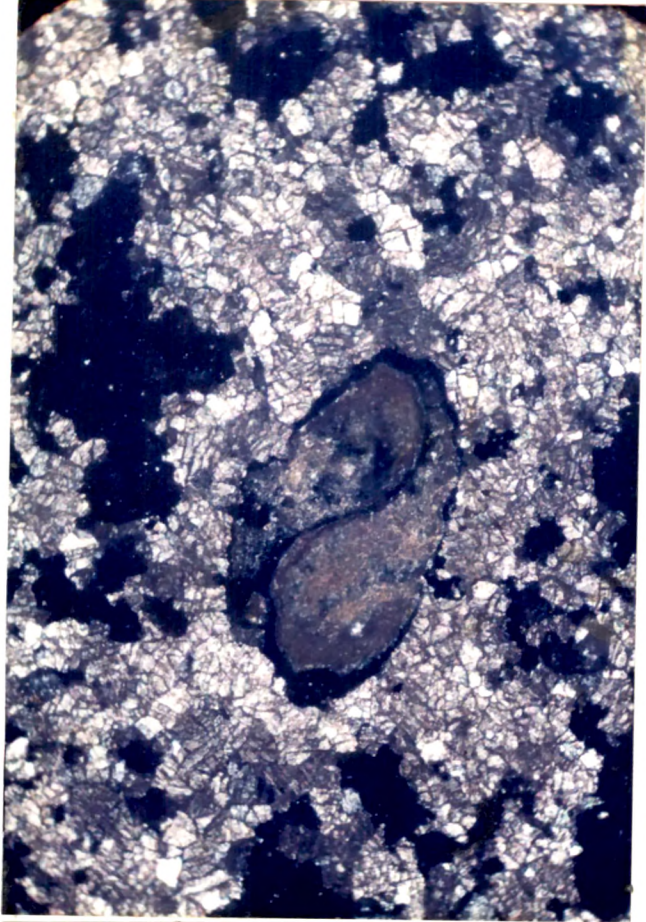


Plate XVII/2 Microsection of laminated limestone from V in rhyolite bed, Anjar.

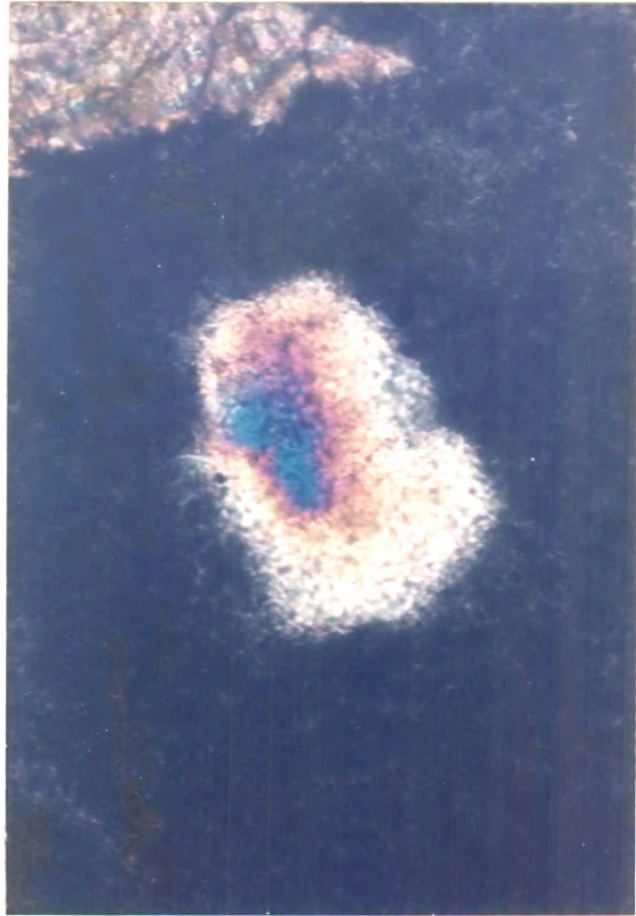


Plate XVII/1

Photomicrograph of shocked quartz showing interference colour zoning. The impact fractures are faintly visible in form of criss cross marks.



#### **IX.7.1.7. Iridium Rich Brown Layer of III Intertrappean Bed:**

In hand specimen, the iridium rich brown layer comprises ochreous nodules and fine grained material of 0.5 to 1.0 cm thickness. At times, this is associated with fine grained sand particles and calcareous matter. The brown material contains patches of white material. In microsections, this shows brown to yellowish brown patches of limonite, calcite and grains of grey quartz (Plate-XVI/2, 3). The Intervening cracks are filled by isotropic chert with rhombic cleavage. At times, relict pseudomorphs of earlier specks are visible within chert in cross nicols after the use of sensitive tint/quartz wedge indicating a replacement of earlier minerals and calcite by chert and quartz. At times, the white transparent mineral (quartz) shows zoning pattern of interference colours, which are very much similar to the shocked quartz (Plate-XVII/1, 1a) described. The ochreous (limonitic) matter and calcite are replaced by chert. The nodules from other brown layers also show similar order of replacement of calcite by chert and quartz. The Ir rich spherules show a coating of calcific matter and it appears to be the dust spray from the air over lagoon (Plate-XIX/3)

Ref

?

} on chert, 600x

#### **IX.7.1.8. Cherty Fossiliferous Limestone (of III Intertrappean):**

The white, siliceous, cherty limestone of third Intertrappean bed occurs intimately associated with chert bed and nodular bed. It contains numerous small fossils of charophytes (chara), small gasteropods and other minute forms. Their extraction is not possible as they occur as complete replacement in chert. Hence, only possible means were through microsection studies.

It comprises crystalline and clastic grains of calcite, quartz and chert with calcitic ground mass. The charophytes, coccolith and oncolithic growth of calcite is conspicuous in some cases. The oolites comprise concentric layers of calcite and silica with a nucleus of calcite crystals. Certain spherical structures with greenish wall like structure (chlorophyll wall (?)) are seen, which are suspected to be pollen-spores/seeds. The fossils shell show sharp outlines differentiating it from surrounding background and it can be demarcated easily. Studies of internal structure is not possible as they are thoroughly replaced. Foraminifera and some forms are suspected on the basis of multi-serial chamber sections. However, definite identification is possible only on morphological studies of tests after disintegration from chert. Lamellibranch and gasteropod shells are replaced and show filling.

#### **IX.7.1.9. Nodular Marl (III Intertrappean Bed):**

This is a dirty white, coarse grained calcareous, granular looking compact nodular aggregated as lensoid bed within black fossiliferous shale bed.

In microsections, it shows a granular texture with clastic grains of calcite, quartz and at times some ferruginous coated grains in clayey and calcitic matrix. Oolitic growth is not predominantly seen within them. Some charophytes can be seen in microsections.

#### **IX.7.1.10. Fossiliferous Marl (III Intertrappean Bed):**

The third Intertrappean bed contains white to dirty greyish white and yellowish profusely fossiliferous marly limestone bands with cyclically repeating grey, fossiliferous shale sequence in the higher part. In hand specimen, it shows yellowish algal bands. The bedding surface shows profuse studding of calcite, anhydrite crystals, charophytes, tiny shells of gasteropods, limonitised fossil wood. Algal and limonitic bands are seen parallel to the bedding surface.

In microsections, the marly limestone shows clastic granular texture with oolitic growth, calcite, quartz grains and fragments of shells. Blue green algal filaments are common in the yellowish and brownish bands. Charophytes with oval and spherical shapes are common. Microscopic shells of gasteropods are seen. Oolitic, oncolithic growth of green algae is commonly seen.

From the microscopic studies, it is clear that the lower nodular horizon is different from the present one.

#### **IX.7.1.11. Laminated Limestone of V Intertrappean Bed (and Yellowish Banded Fossiliferous Limestone):**

The rock shows very fine grained, finely laminated nature. The lamination comprise in form of alternate thin white and greyish bands with crystalline appearance.

In microsections, the rock shows granular texture with predominant sub-equal grains of rectangular to sub-angular calcite, minor grains of feldspars (plagioclase), quartz, limonite and chlorite. Alternations of bands with fine to medium grains of calcite and bands containing coarse grains of calcite are seen. The bands are 30 to 60 micromillimeters thick. Occasionally layer elongated grains are seen parallel to banding. The rock contains occasional microgasteropods shell with all features clearly visible (Plate XVI/2). Some times fossil wood fragments are also seen.

#### **IX.7.1.12. Stratified Limestone:**

The stratified limestone shows alternate white and dirty white bands of microcurrent laminated calcitic matter.

In microsection, it shows clastic granular texture. The grains are coarse, subequant, sub-angular to angular with distinct rhombic cleavage. Few occasional grains of quartz, feldspars (plagioclase) limonitic grains and some fossil wood fragments are also seen. Chert occurs as later replacement in some grains. The calcite grain within each band show different grain size.

#### **IX.7.1.13. Sandy Limestone:**

The rock occurs as lensoid, partings within and on the stratified limestone. It is greyish white on weathered surface and yellowish white when fresh. In microsection, it

shows equigranular, sub-angular grains of calcite with few grains of quartz, felspar (plagioclase), staurolite, magnetite, limonite and chert as replacement after pseudomorphs of evaporite and limonite, calcite. Cement comprising calcite, limonite and clay. The sandy limestone contains fragments of fossil wood, gasteropods, lamellibranchs, microscopic size shells of bryozoa, algal filaments and spores.

The rock is sandy limestone.

### **IX.7.2. Dayapar Area:**

#### **IX.7.2.1. Marly Limestone:**

In the Dayapar section, the microscopic studies of the marly limestone shows greyish, greenish, white colour and comprises calcite, quartz grains, oolitic growth of (oncolithic growth) calcite, fossil shells of gasteropods, lamellibranchs, charophytes spores, algae and some spores.

### **IX.8. PALAEOLOGICAL STUDIES:**

The palaeontological studies include studies on mega fossils, microfossils, dendrological studies on wood tissue structures, bone histological studies, and studies on egg shell structures in relation to palaeopathological condition.

A detail account of each of these studies is given below:

The major important groups in order of importance in Anjar and Dayapar sections include the following which help in identification/inference of probable important groups/families.

#### **i. Fauna**

##### **1. Vertebrate Groups:**

- a. Dinosaurian fossils
  - Bone fossils
  - Eggs
  - Teeth, dermal scuts
- b. Crocodilean/Geekoid Eggs and Chilonian Geekoid
- c. Avian elements, egg shells, bone fossils (Dayapar)
- d. Chilonian Boidian skeletal parts

##### **2. Invertebrates (megafossils):**

- a. Mega invertebrates
  - Gasteropods - *Palludina*, *Lymnea*, *Physa*.
  - Bivalves, Lamellibranch
- b. Micro invertebrates
  - Arthropoda - Ostracoda, Foraminifera, Bryozoans, Sponge (spicules).



Plate XXV/1 Mega sporophylls of Cycade (L to R) C. circularis, C. thourasii, C. revoluta and fern spikes respectively.

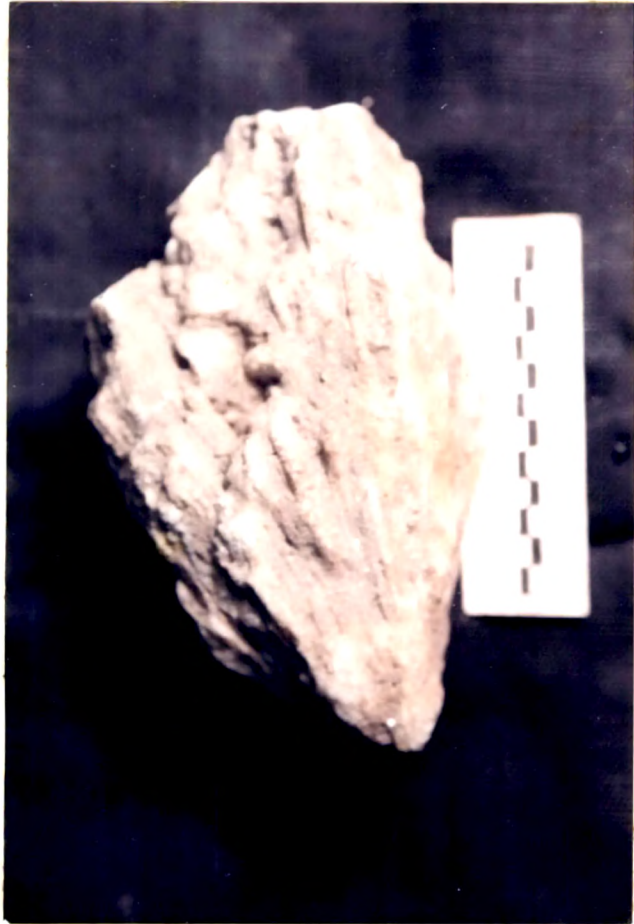


Plate XXV/2 Part of fossil crown of fern.



Plate XXV/3 Fossilised crown of fern.

**3. Worms:**

Planolite spreiten

**ii. Flora:**

Graminae-stems

a. Angiospermous woods of different types

Dicotyledonous, monocotyledonous - Palm - Irse Graminacea (Iridaceae)

b. Gymnospermous wood

Cycadales, mega sporophylls, *C. circinalis*, *C. rumphi*, *C. thourasii*,

*C. revoluta* (Plate-XXV/1).

Pteridophytes, *Schizaea rupestris*-leaves of cones-unidentified;

*Arancaria* sp.

c. Algae blue, green algae, chlorophyta

Charophylocae, *Azolla*, *Hallimeda*, *Girvanella*

**IX.8.1. Fossil Spores and Pollens of Intermediate Affinity:**

These include the spore and pollen like structures (based on microsections - definite identification of which is not possible).

The detail description of these fossils is given here on the basis of the microscopic studies. Majority of the studies include the petrographic examinations, except those of major vertebrates and invertebrate fossils.

**IX.8.2. Fauna: Vertebrates:****IX.8.2.1. Dinosaurian Fossils:****IX.8.2.1.1. A. Ichnofossils: Foot Tracks and Foot Prints at Fatehgarh:**

The dinosaurian foot prints on the top of the bedding surface of the burrowed quartzitic sandstone of the Upper Member of Bhuj Formation (Plate-IV). The foot prints comprise of different size groups. The foot prints occur as progressive in westwardly and southwesterly direction from east/northeast. These foot prints were first grouped in to different shapes and photographed. Detail sketches were prepared for different size-shape groups to show detail of morphometry and morphological features. The details of claws, muscular scars, parts and digital impressions, angle of inclination of foot prints, rear and front sides etc., were determined and marked. After analysing different shapes/size of groups, the foot prints were marked in to pes and manus, right/left and the direction of progression was determined. These were used to determine and measure type of overlapping relationship of pes and manus, types of coupling and gaits based on standard procedures and calculations (Sarjeant, 1975, Lockely et.al., 1990)

After determining the pes and manus and right and/or left foot prints, a possible reconstruction of foot tracks of different age groups were identified on the out crop,

numbered and photographed accordingly. These were then mapped with the help of the tape and compass by fixing reference lines on 0.5 m grid along north-south and east-west reference lines. Thus, a detail plan of the foot prints was prepared (Fig-15 B,D).

These measurements were used to calculate the speed of motion, hip height, possible weight and pes/manus structures of the trace maker based on the standard case histories and literature (Lockely et.al., 1990; Searjant, 1975). Further the detail plan of the foot prints was also used to study the social behavioural patterns and other important aspects related to the life cycles of the *dinosaurian* communities of different groups. The study of the *dinosaurian* foot prints at Fatehgarh has indicated that there were at least three age groups in the same herd. Some important information derived from these foot prints is used for ecological and environmental inferences.

#### **IX.8.2.1.1.1. The *Dinosaurian* Foot Prints at Tharauda and Pakhera:**

The *dinosaurian* foot prints at Tharauda occur on the top of bedding surface of the calcareous sandstone of the Katrol Formation and on the top of a backed ferruginous sandstone of Lower Member of Bhuj Formation at Pakhera (Fig-9, 10).

These foot prints were also analysed marked in to left and right, and the direction of progression was determined in the similar way like that of Fatehgarh. The foot prints at Tharauda are of bipedal tridactyl type. They are of Theropod and Ornithischian type. The traceable foot tracks length is about 60 m. The Ornithischian foot prints show progression in north-north-easterly direction (Fig-16).

The maps were further used to calculate pace, angulation, gaits, stride and speed of locomotion and body height of the animals.

Similarly, the detail study of the quadruped *dinosaurian* foot tracks at Pakhera was also carried out and the detail plan of the foot print was prepared which was used for studies of important life habits of *dinosaurian* herds (Fig-15 A, B, D).

After preparing detail plans and maps of the foot prints, the plaster casts of the foot prints were prepared from each group type based on morphology, shapes and size. For these plaster casts of different type groups, foot prints were first cleared thoroughly, then covered with tissue paper and then a paste of plaster of Paris was filled in completely in the depressions of the foot prints depending on the morphological out line. These casts were removed from the foot prints on drying and kept in the museum after coating with varnish/resins.

#### **IX.8.2.1.1.2. A. Ichnofossils of Dinosaurs from Katrol and Bhuj Formations:**

##### **Tharauda:**

Calcareous sandstone of Katrol Formation contains well preserved impressions of tridactyl dinosaurs near northeast of Tharauda village. The foot prints and foot tracks occur on the top surface of the calcareous sandstones which are intercalated with gypseous shales and siltstone beds (Fig-10). The foot prints comprises three distinct types in the

bipedal tridactyles viz.:

1. Tridactyl ornithischian type - Bipedal - 1.
2. Tridactyl ornithischian type - Bipedal - 2.
3. Tridactyl Theropod - Bipedal.

1. Bipedal Ornithischian Tridactyl type - 1:

One impression of this type was observed. The foot print is short, broad at the rear side, central digital impression is longer than the other two (about 20 cm long). The left side inner digit is moderately long (14 cm), with narrow apical end. The right digit is relatively short (about 5 to 10 cm long). This impression has not created any depression on the surface substrate. This could be the foot print impression of a westerly facing dinosaur possibly in a standing posture.

2. Bipedal Ornithischian tridactyl type -2:

This type of impression forms a foot track, which is traceable for a distance of about 50 cm. There are five such impressions (fig-3) with progression on northeast direction from southwest direction. In these foot prints, the substrate shows slightly deeply incised impression. The middle digit is about 21 cm long, tapering at apical part. Three distinct depressions are noted within the impressions of the toes, which are due to the metatarsals. Slight backward depression is created (towards southwest wards in the foot print) in the digital impression in the foot print, due to the fast motion of the animal in the northeastern direction. These impressions are associated with an impression of claw, which were common in the small Ornithischian type of dinosaurs. Such impressions could have been produced by Coelureus type of small carnivorous dinosaurs.

3. Bipedal Tridactyl Theropod Type:

In such impressions, the digital impressions are quite clear on the substrate. The bony parts have produced some depressions. Three to four such impressions are found, which show progression in the north-northeast direction (Fig-16).

**Pakhera Area:**

In the Pakhera area, the quadruped type of foot prints of different sizes are recorded in the top surface of the quartzitic ferruginous sandstone. The sandstone forms part of Lower Member of Bhuj Formation (Fig-10). The foot prints were mapped on large scale with the help of tape and compass (Fig-15). The foot prints show adult, sub-adult and juvenile. The adult and sub-adult foot prints are found towards eastern part of the out crop and show a general direction of progression towards north. Here, the foot prints belong to the same group of quadruped Sauropod type with different age groups, as there is uniformity in shape. Thus, the dinosaurs were gregarious in habit and moved in herds.

**Fatehgarh:**

The *dinosaur* foot prints are also recorded on the quartzitic sandstone of Bhuj Formation near Fatehgarh in eastern Kutch (Fig-15D).

The foot prints show various shapes and sizes indicating different type of individuals were responsible for trace making. The overall analysis of the shapes and sizes (Plate- III; Fig-14) indicate that they belong to the same group. The depth of incision of foot prints is shown in sketches (Fig-13, 14; sections), which varies from 5 to 12 cm at times up to 15 cm. The depth of incision is more on the front side of the foot prints, whereas the rear side shows a gentler sloping surface. The details of digital impression and the muscular scars are clearly visible within the impressions (Fig-13, 14). At times, the impressions of the claws are also visible. These details are reflected in the plaster casts shown in Plates-I, III and V. The foot prints when mapped on larger scale and plotted (Fig-15) show a westerly direction of progression. The stride, pace, angulation, glenoacetabular distance vary with the size of foot print. In case of adult foot prints, the distances are 1.15 m to 1.4 m; 1.04 m to 1.30 m and 1.61 to 2.0 m respectively at Pakhera and 2.60 m, 1.30 m and 1.5 m respectively at Fatehgarh. The overlapping relationship shows primary coupling at Pakhera as well as at Fatehgarh. The foot prints at Fatehgarh and Pakhera indicates that the sauropod dinosaurs moved in structured (spear headed) herd.

**IX.8.2.1.2. Thematic Description of dinosaurian fossils and associated fauna/flora:**

The *dinosaurian* fossils from Kutch are dealt under Bone fossils and Ichnofossils under the following heads:

**A. Bone fossils (Skeletal fossils):**

- a. *Dinosaurian* fossils from Patcham Island.
- b. *Dinosaurian* fossils from Anjar and Dayapar areas.
- c. Associated fauna of Anjar and Dayapar areas.
- d. Flora.
- e. Microfauna of Anjar section.

**B. Ichnofossils:**

- a. *Dinosaurian* foot prints and foot tracks from Tharauda.
- b. *Dinosaurian* foot prints from Pakhera.
- c. *Dinosaurian* foot prints and foot tracks from Fatehgarh.

**IX.8.2.1.2.1. Bone fossils:**

After excavation and exposing the fossils were wrapped with a cloth on which thick coating of plaster of Paris was applied to impart strength to the fossils during transportation. The remains of lower half of the fossils were also covered by plastering in the similar way

Table-VIII  
DATA OF FOOTPRINTS OF DIFFERENT PLACES

Area Foot Morphotype	Track Type Adult/ Sub-Adult	No. of foot prints	Footprint size		Average Stride Length $\lambda$	Pace m (m)	Hip height Alexander, 1976	Gleno- acetabular distance(m)	Average speed (v) m/sec	Direction of progression	Indica- tions
			Length (cm)	Break width (m)							
<u>Tharanda</u> Bed A Bed B	I	5	42.7	35.5	3.4		1.7		3.2	N75°E	Ornithopod Theropod Carnosaur
		4	15.35	11.4	-		0.61			N60°E	
			26.7	24.9	-		1.06			N60°E	
<u>Pakhera</u>	Sub.Adt. Juvenile Adult		32	21	0.38	0.42-0.49	1.28	0.28-0.33	5.5/2.16	Due S	
			12	10	0.48						
			41	28	1.15-1.47	1.4-1.3	1.64	1.61-2.0	0.7/2.52		
<u>Fatehgarh</u> I	Adult Juvenile Aub adult	13	50	22	2.6	1.3	2.0	1.4	3.25	260°	
		4	10	6			0.4		11.7		
		8	22	17	1.6	0.86	0.88	1.1	0.63		
II	Subadult	6	30	20			1.2		2.26	North	
III	Adult	1	34	20			1.36			West	
IV	Adult	4	45	35			1.20				
		4	30	12							
		4	33	35							

The speed estimates are based on Alexanders (1976) method.

$v = 0.25, g^{0.5}, \lambda^{-1.67}, h^{-1.17}$ ;  $v =$  speed of animal in m/sec.;  $\lambda =$  stride of animal in m;  $h =$  hip height in m (4 x l);  $g = 9.81$  m/sec.

after proper cleaning. The fossil specimen were photographed insitu after exposing and cleaning and before plastering and preparing detail plan. To prevent damage to the bone fossils and for further hardening liquid acropol was applied to weather fragile parts and cracks of the fossils.

The plastered fossils were thoroughly wrapped in paddy grass and tied properly to prevent any disintegration of parts of fossils while in transport. The dinosaurian bone fossils of Patcham Island are composed and do not require further treatment.

#### **a. Patcham Island:**

The *Dinosaurian* bone fossils show definite bone histology in microsections (plate-XXVII/1) which is comparable to the mammalian bones (plate-XXVII/1,2,3). The haversian system is of more primary spaced in case of the *Dinosaurian* bones from Patcham Island, whereas the *Dinosaurian* bones from Anjar show compact closely spaced haversian canals. The *Dinosaurian* bone fossils from Patcham Island are found from Chhapri Bet and Nirwandh. The fossils from Chhapri Bet include different types of vertebrae, femur bones, parts of ilium plate, Ischum plate (Fig-29), those from Nirwandh include ilium plate and parts of limb bones (Plate-XVII/A/1-4).

#### Vertebrae:

The vertebrae are plano-concave with a distinct neural spine and neural canal opening. One such vertebrae (Fig-29; Plate-XVII/A/3) is 14 cm in length and about 8 cm in diameter. Another such vertebra is concave-plane, broader at either ends and narrower in the centre. The vertebra is about 20 cm in length and 8 cm in diameter, at either ends and 8 cm in centre. The neural canal opening and lateral processes are developed. This shows resemblance to antarctosaurus vertebra (Matley and Von Heune, 1932) found from Jahalpur area. However, the precise identification is not possible.

#### Ilium Plates:

The ilium plate is 22 cm in length and 18 cm in width. This is oblong with a distinct pointed end at the anterior end. The posterior end is convex. The plate is tapering at one end and thick in the centre. The specimen is damaged (Fig-31) and broken from centre. The exact affinity is not known, but it shows resemblance to sauropod ilium plate (Plate-XVII/A/4).

The other ilium plate found from Nirwandh is not studied in detail.

#### Femur Bone:

The femur bone (plate-XVII/A/4) represents proximal end of a femur. It is 30 cm long broad at proximal end (also 15 cm in longer diameter and about 10 cm in shorter diameter). The distal end is broken and about 8 cm in diameter.

#### Teeth:

The *Dinosaurian* teeth are recorded from conglomerate horizon in the basal part

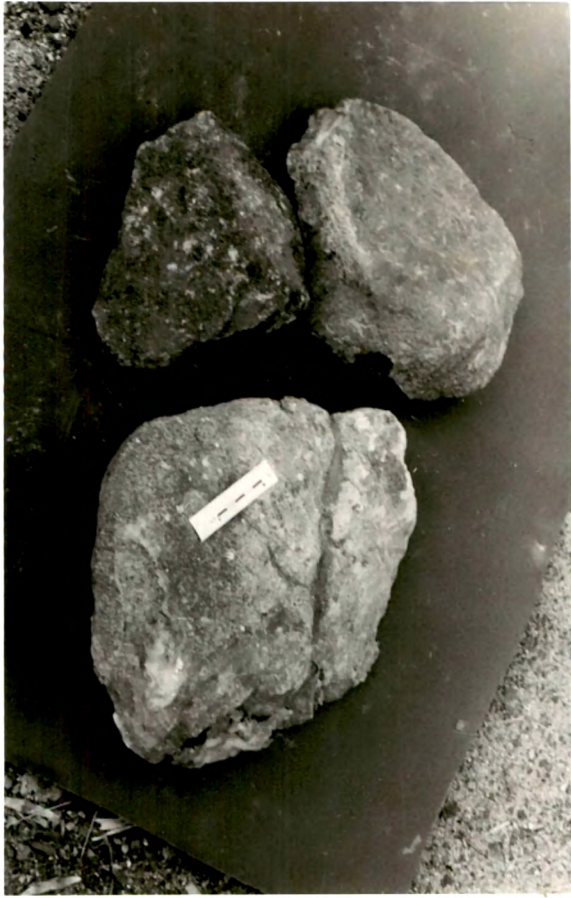


Plate XVII/A/2 Parts of Ilium plates (pelvic girdle) from Patcham Island (Up. Jurassic).



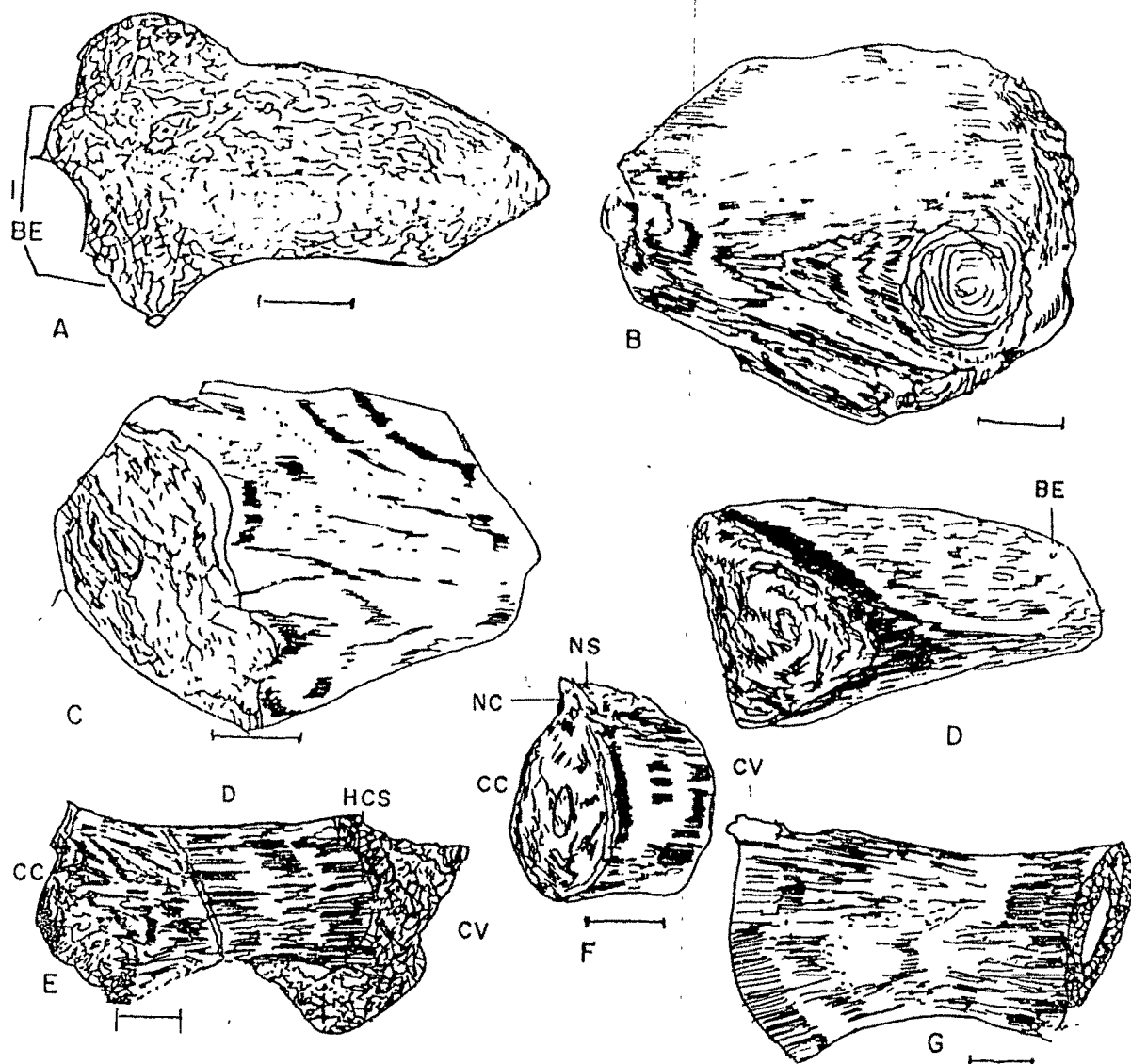
Plate XVII/A/4 Part of femur bone of dinosaur from Patcham Island. The bone was fractured during life time and subsequently healed F-F show fracture line.



Plate XVII/A/1 Dinosaurian bones from Patcham Island.



Plate XVII/A/3 Dinosaur vertebrae from Patcham Island with Neural canal and notochord preserved (N.C.)



D-DORSAL, V-VENTRAL CC-CONCAVE END, CV-CONVEX END,  
 BE-BROKEN END, NS-NEURAL SPINE, NC-NEURAL CANAL,  
 HVC-HAVERSIAN CANAL SYSTEM AFTER WEATHERING, BAR SCALE 5x5 CM. CC & CV : 5 (11)  
 A,B,E,F A,B,E,F ARE LATERAL VIEWS, G-SAME AS IN TRANSVERSE VIEWS.(g)  
 AS SEEN FROM OTHER LATERAL SIDE, C&D ANTERO-LATERAL VIEWS

SKETCH OF DINOSAUR FOSSILS FROM PATCHAM FORMATION, KACHCHH

- A. ILLIUM PLATE , Location : NIRWANDH
- B.C. ILLIUM PLATE , Location : CHHAPRI BET
- D PART OF TIBIA, Location : "
- E.G. VERTEBRA, Location: "
- F. VERTEBRA Location: "

Fig. 29. Sketches showing dinosaur bone fossil from Patcham Island, Kutch.

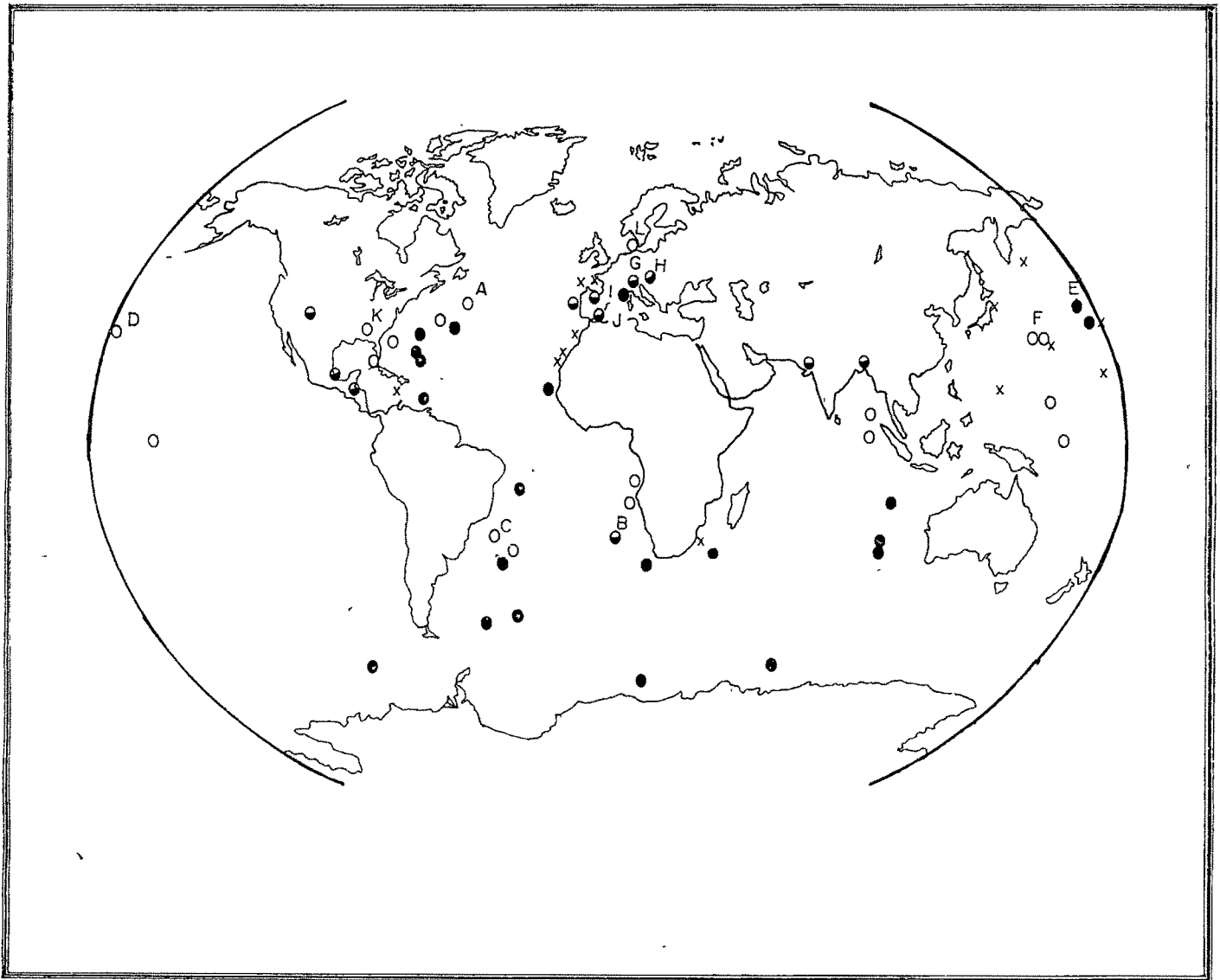


Fig. 33.A Global distribution of impact craters, flood basalt provinces, hot spots and high Ir content concentration in K/T boundary horizon based on studies by different groups

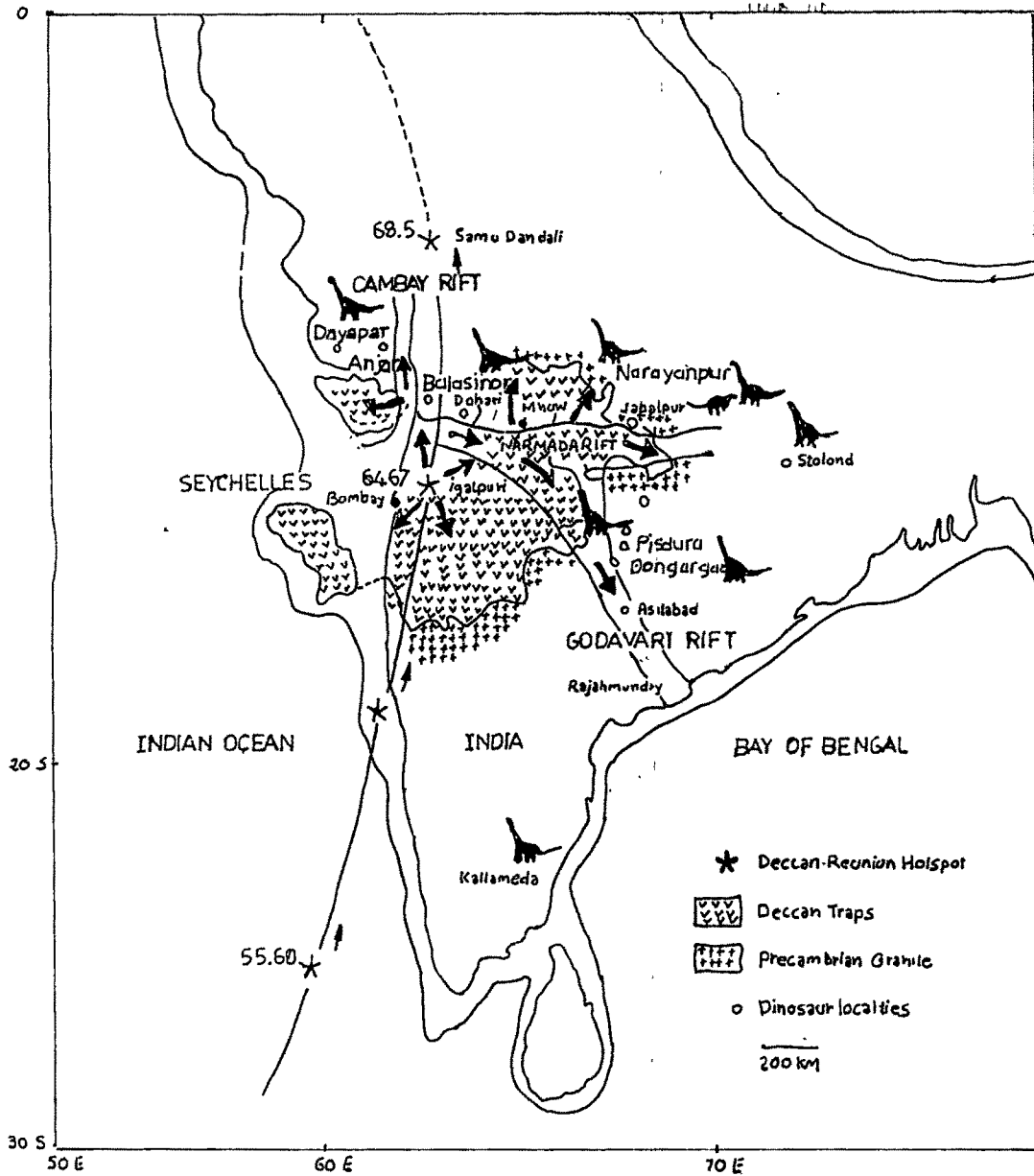


Fig. 33E. Sketch map showing the localities of Maastrian dinosaurs around the Deccan volcanic province before the final separation (Proposed Fig 34). Microcontinent Chelles was adjacent to India. The bold arrows indicate possible directions of interocean extensions of upper Cretaceous Sea and Deccan lavas along the Narmada, Godavari and Cambay basin (Ajay Chatterjee, 1996)

(Kuar Bet and Chhapri Bet) and also from the upper part of sandstone near Dhopavar in Goradungar area. The teeth structure is sharp pointed at crest, conical, incurved and resemble to those of carnivorous in structure.

#### Tail Spine:

It is about 45 cm long, conical, pointed in shape at distal end and broader 10 cm in diameter with pointed upper end. This resembles to the tail spine of Stegosaurian dinosaurs found in America and parts of Africa. Similar *Dinosaurian* fossils are found in the lower Cretaceous of South India (found from Trichinopoly area, Yadgiri et.al., 1979; Plate-XVII/A/1).

#### Associated Vertebrate fauna:

The other associated vertebrate fauna include crocodilian scuts, teeth and vertebrae, parts of limb bones from Kaladungar and also from the upper horizon. The upper horizon contain various crocodilian elements like teeth, scuts, vertebrae etc.

#### Flora:

The *Dinosaurian* fossil bearing horizon contains huge tree trunks, some of them in upright condition and suggest insitu fossilisation of the trunks. Some of them also show drifted characters. These trunks show very little replacement/petrification. The original woody material is unaltered and the bark structure is also well preserved and at times coated with gypseous matter. The wood tissue structure indicate their gymnospermous affinity, which was very prevalent during the Jurassic period.

The plant fossils (Gondwana affinity) are found near Dhorawar village. These fossils include cones and equiselaceous woody structure.

Poorly preserved leaf impressions are found in the friable sandstone horizon near Dhorawar village.

#### b. Anjar Area:

The second and third Intertrappean beds at Anjar have yielded dinosaurian fossils consisting of bones and various other elements. The bones from second Intertrappean bed include the limb bones of Titanosauridae affinity. Most of them are highly transformed by volcanic material to the extent that, they can easily be mistaken either for fossil wood fragments or a large vug filled calcareous material. On petrographic examination, the haversian canal system is very clearly seen. These haversian canals consist of central circular two oblong opening and a surrounding rings of oblong, circular or ellipsoidal shape with numerous, closely spaced rings surrounding the central opening. At times the intervening space between the canals is filled with calcareous matter.

Larger limb bones from greyish and chocolate coloured, brownish, fossiliferous shales consists of various parts of dorsal vertebrae of Titanosauridae, haemapophysis, femur bones and humeri bones and parts of pelvic girdles including a giant articulated scapula of

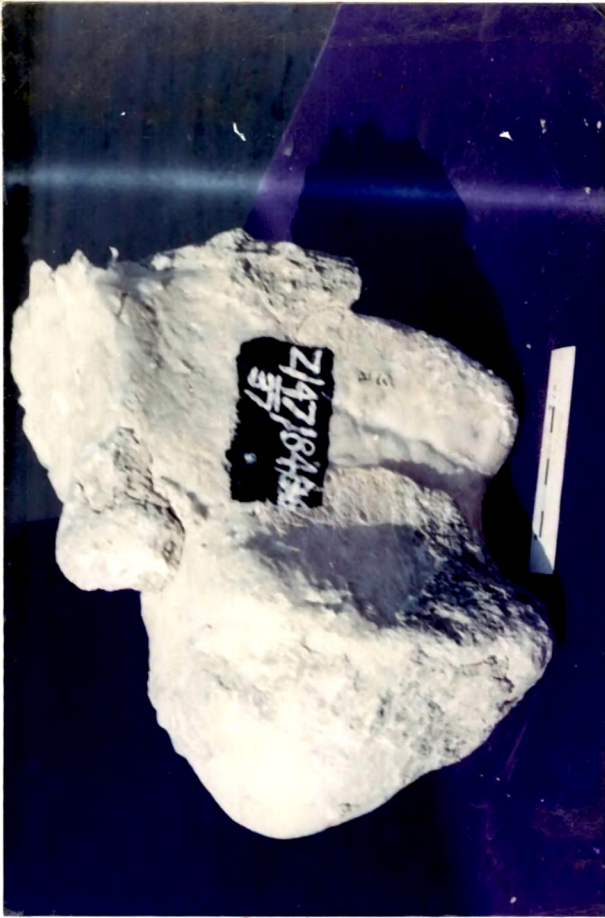


Plate XVIII/1 Dorsal vertebra of Titanosauridae from III intertrappean bed, Anjar.

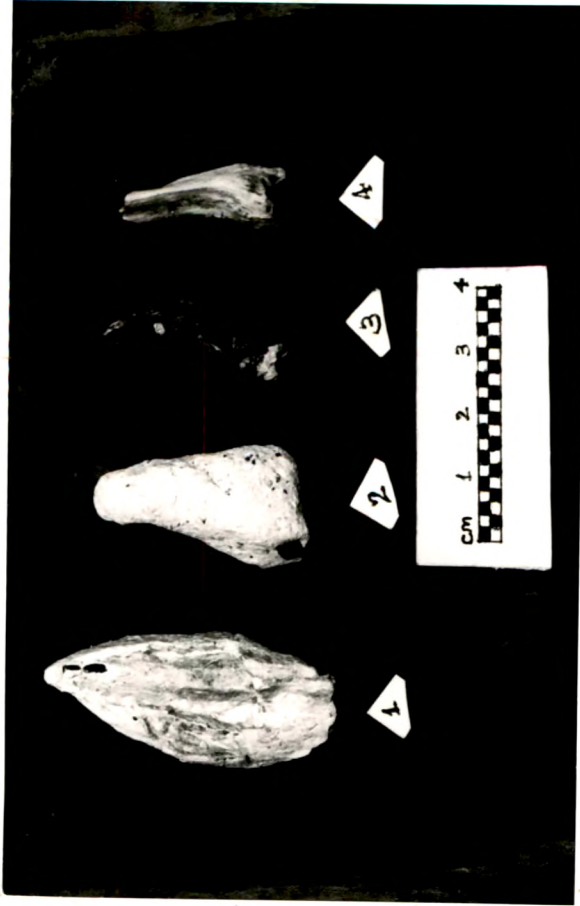


Plate XVIII/2 Allosauridae (1,3 Titanosauridae) and other related claw bones and tarsal bone (4) from III intertrappean bed, Anjar.



Plate XVIII/3 Fragmentary parts of pelvic girdle from III intertrappean bed at Anjar.



Plate XIX/2 Clutch of egg from II Intertrappean bed.

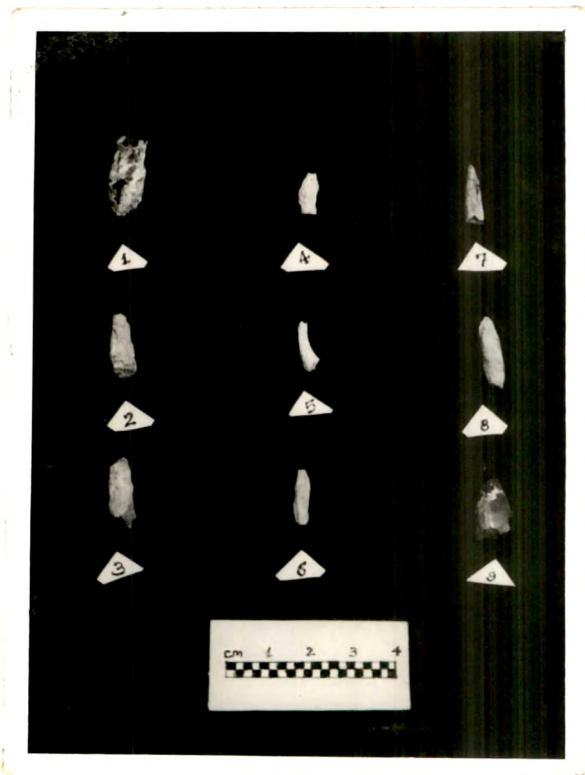


Plate XIX/1 Dinosaurian teeth from III Intertrappean bed at Anjar, Kutch, anterior view (anterolateral and labial view).

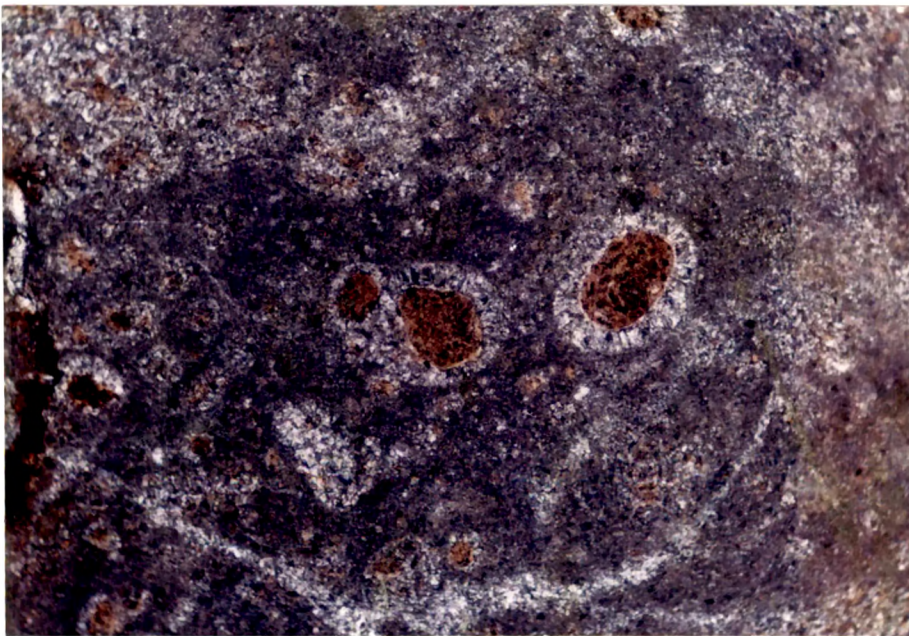
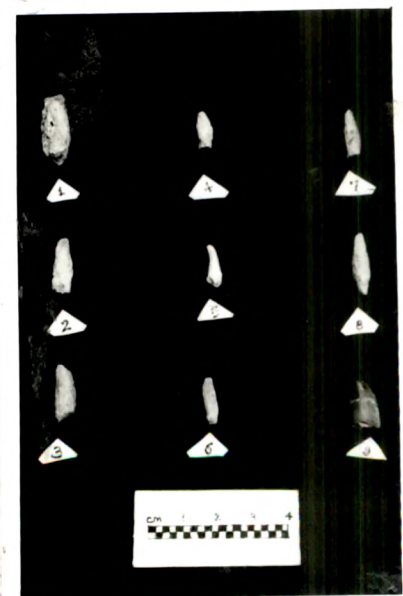


Plate XIX/3 Oolitic spherule of Iridium rich matter enclosed in calcite globule, III Intertrappean, Anjar.



### Sauropod.

The composition of dinosaurian teeth show a mixed herbivore (dominantly) and carnivore (*Megalosauridae*) of Uppermost Cretaceous affinity. The presence of dinosaurian and avian egg shells and geckoid type of egg shells also point to the fact that, the brown and grey shale below cherty limestone horizons are possibly of Uppermost Cretaceous (*Maestrichtian*).

The second and third Intertrappean beds in Anjar area contains *Dinosaurian* bones. Huge limb bones (Femur and humeri) were found (Fig-12, Plate-VI/1, X/1,2). The femur and humeri resembles those of *Titanosaurus* (collected from Central India by Matley and Von Heune, 1932). These fossils are very fragile in nature as they have not undergone replacement or petrification. These bones (from second Intertrappean bed) are lava coated and show weathered nature on surface. The lava coated nature of these bones indicate that these were trapped in the lava during active eruption.

### Third Intertrappean Bed:

The Dinosaurian fossils from third Intertrappean include sauropod as well as Theropod elements. These include parts of limb bones, ilium and ischium plates, scapularick bones, vertebrae, femur bones, teeth, egg shell fragments and associated plant fossils and invertebrate fossils. Some of them (Fig-30) were collected from surface and some were excavated during 1986 (Plate-X). These fossils do not show replacement and are very fragile in nature. A brief description of these, is given below:

#### Scapulas:

The Scapula is largest single bone fossil found at Anjar. The bone is 1.35 m long, wedge shaped, 80 cm maximum width at broader anterior end. It is curved arcuate in shape. The upper margin is convex, sharp and tapering, whereas the concave margin is about 50 cm thick (Plate-X/; Fig-12). It has a opening (glenid cavity) for attachment with humerus at the proximal end. It was articulated to the dorsal vertebra at the time of excavations (Plate-VI/1;XVIII/1). This shows close affinity in characters to the Sauropod Scapula.

#### Ilium Plates:

Two distinct ilium plates were found. The ilium plate with pubic process is found. The plate is about 45 cm long and 30 cm width and shows a convex-dorsal margin and convex inner margin. The pubic process is about 50 cm long. This ilium plate resembles to that of *Titanosaurus* morphological characters. Another fragmentary ilium plate (Fig-12) was also found from surface (Plate-XVIII/3).

#### Femur:

The femur bone is about 80 cm long with rounded at either sides and shows trochantaris for muscular attachment at the proximal end.

Haemopophysis:

This bone is a forked shaped at distal end. The two processes form together from one end. This process is about 15-20 cm long, tapering at distal end and broadening at the proximal end. This represents a jugaural bone.

Rib Bones:

Rib bones are of different sizes and shapes. Some of them are Cervical and some are dorsal ribs. The Cervical ribs are straight tapering at distal end and broken at proximal ends.

Vertebrae:

These are concavo-convex in shape. The neural processes is seen in some vertebrae. The neural canal opening and lateral processes are not seen in some of them. Some of them show similarity to the Titanosaurus vertebrae in shape. Various characters described from Central India by Motley and Vonthem (1932). The larger one is about 25 cm long and 18 cm wide (Plate-XVIII/1 , dorsal vertebrae of Titanosauridae).

Teeth:

The teeth show all varieties (Plate-XIX/1). Teeth of herbivore, Theropod and some with common characters are found. The Theropod teeth show sharp centred margin, sharp apical portions (Plate-XIX/1), and slightly incurved nature. A small apical portion of carnivorous teeth fragment shows sharp incurved apical end, with serrated margin and longitudinal striations on surface may belong to Magalosauridae (Fig-30d). The carnivorous teeth may belong to either Theropod group or to small Ornithischian groups. The herbivorous type teeth show rounded apical ends (Fig-30a) circular section outline with longitudinal sections from base to the apical end (Fig-30 a & b). The cross sectional view (transverse section) shows radiating structure from centre (Fig-30c). Such herbivorous type of teeth may belong to some sauropod *Dinosaurs*.

Pubis:

This is a fragmentary bone with partial characters (Fig-30/2a,b). The bone specimen is about 20 cm long broader, slightly flat at proximal end, curved in inner side, triangular in sectional view at distal end.

Radius:

This is a fragmentary partly preserved bone (Fig-30/5a,b). The proximal end is a broad, triangular in shape in ulnar and medial aspect. The distal end is narrower in outline and triangular in transverse section.

Tibia:

This is a fragmentary bone 16 cm in length. Proximal end (Fig-30/4) is rounded, distal end tapering, triangular in sectional view (transverse section).

PLATE - I

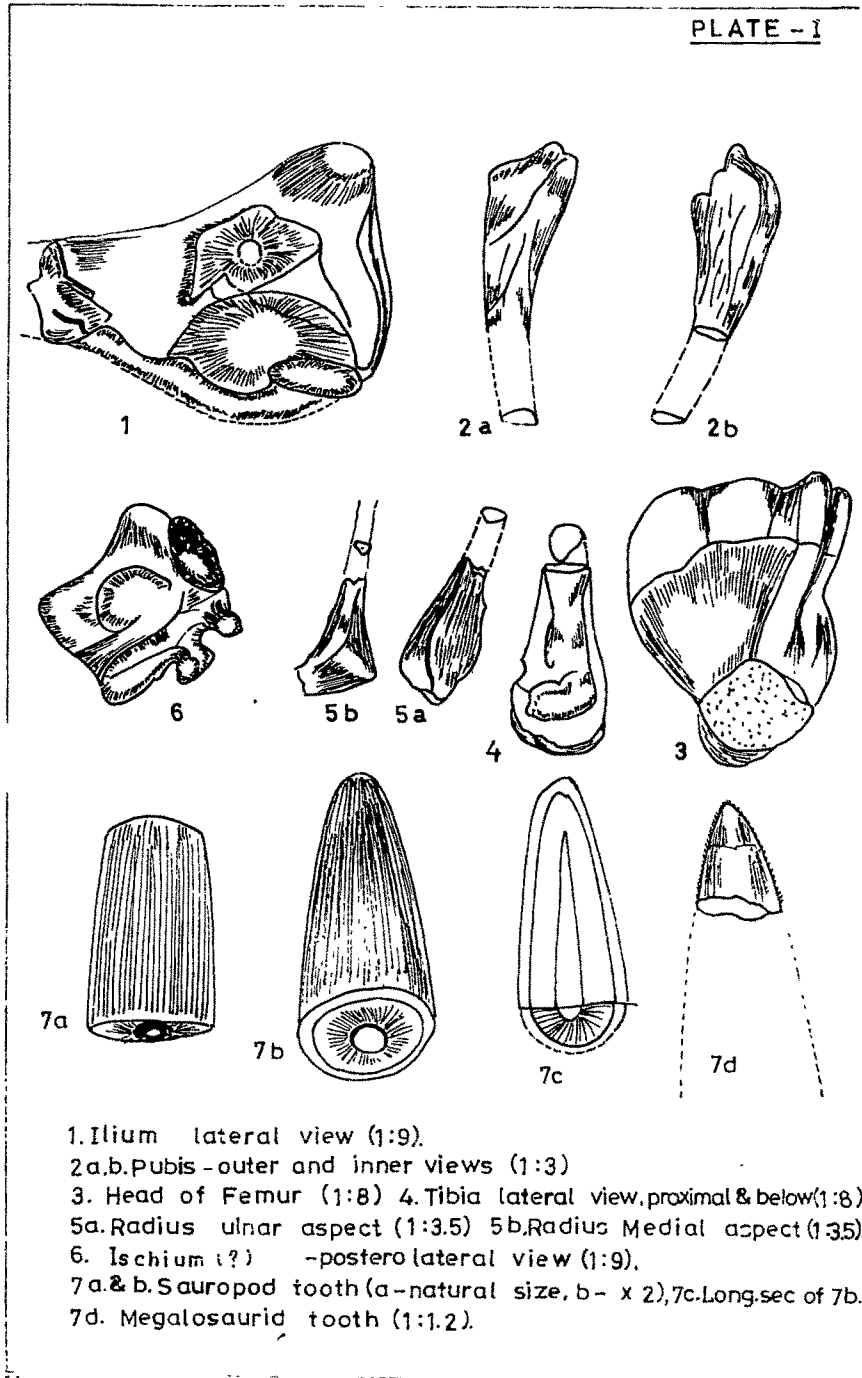


Fig. 50 Specimens of dinosaurs and other fossils of second and third intertropical beds of Anjar



Plate XIX/A/1 Microsection of a dinosaur egg shell from II Intertappean bed, Anjar.



Plate XIX/A/3 Microsection of Avian egg with broad spongy layer from III intertappean bed at Anjar.

Plate XIX/A

Microsection of Dinosaurian/Avian eggs from Anjar Intertappean beds

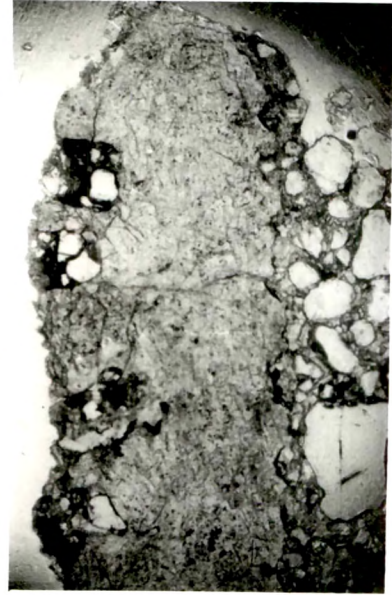


Plate XIX/A/2 Microsection of a dinosaurian egg shell from Intertappean bed.

### Claws and Digits:

The claws are silicified, 4 cm long, sharp, pointed, apical end broader (about 1.5 cm) in middle part, and rounded at the proximal end. Longitudinal extending wrinkles forming grooved ridges are seen on surface. The claw is slightly convex on outer surface and flat to concave flat in central part. Longitudinal striations seen on surface (Plate-XVIII/2). The claw comparable to allosaurus claw (Matley and Von Heune, 1932) from Central India.

The digital bones (metatarsal) of manus are 3 to 4 cm long, triangular at proximal end, tapering, flattening triangular in out line at the distal end. Slightly curved, concave on dorsal side and convex round proximal end on ventral side (Plate-XVIII/2). The metatarsal digital bones are similar to carnivorous groups.

### Skin and Coprolites:

The *Dinosaurian* skin is nodous burros in appearance on surface. The individual tubercles are 0.25 to 0.5 sq cm in out line, and are about 0.5 to 0.75 cm thick (Plate-XXX/1,2). The bulbous tubercles in microsections comprise of central zone of cell layer and a distinct layer of pyroerector muscles, with micro openings to surface which probably regulate the body temperature and perspiration in a crude way. The outer zone lying between central cell layer and dermal (outer most) layer contains profusely stained melanocyte pigments along with pylierector muscles (Plate-XXX/3). These pigments protect the animals from ultraviolet solar radiation and give dark brown to reddish colour to the skin. Such melanocyte pigment layer is very poorly seen in the skin of *Dinosaurs* of third Intertrappean bed.

### Egg shells and eggs:

During the course of excavation at Anjar, small fragments of egg shells were recovered from the material along with sieve material. The egg shell fragments are thin (less than 3 mm thick) and show smooth outer surface with few domal knobs (Plate-XIX/A/4) with distinct openings. The inner side of the shell is smooth. The microstructure of these shells show very thin knobs, very short prismatic layer with broader spherulith layer (Plate-XIX/A/2) at the top, which are at times either fused with each other or at separate but in close contact. The canalicules are distinct and continue in case of normal eggs (Plate-XXVIII/2,4). Some times development of pathological condition is also seen, where, the spherulith (prismatic layer) shows more than one layers. The canalicule is blocked and some times such shells show excessive thickening (Plate-XXVIII/3). The *Dinosaurian* egg shells (Plate I/2 and XIX/A/1, XXVIII/3) recorded from the second Intertrappean bed also shows similar structures with pathological condition. This suggests a stress during life of animal.

Apart from the *Dinosaurian* egg shell, other very thin egg shells with plain surface are also noted. Their microstructure shows an excessive development of spongy layer

above the prismatic layer (Plate-XXVIII/3,4). In this case, the prismatic layer is excessively thin and prisms are thin, long and slender, almost rectangular in out line. The mammillary zone and mammillary knobs layer is very short. The microstructure of such egg shells are very much similar to avian egg shells. Thus the egg shells show mixed assemblage of *Dinosaurian* and avian.

#### **IX.8.2.2. Bone Histological Studies:**

The bone historical studies were carried out by preparing micro section of selected dinosaurian bone fossil samples from time and space. For this purpose, the samples covered a range from Upper Jurassic (from Patcham Island Fig-29) and from Intertrappean beds II and III from Anjar area. The micro sections of these bones (Plate XXVII and Plate XXVIII/1) were studied for comparison of internal structures and also for studies of possible change in structures in time and space.

The dinosaurian bone sections and studies have been dealt in detail by Regules, (1970), Reid (1987). The bone microstructure of the dinosaurian bones from patcham Island show normal well developed haversian canal system, which is partly filled by calcareous material. The individual canals are fully grown and at times slightly oblong to elongated nature. The peripheral part (plate XXVII/1) shows thin Calcareous rim. The central part is filled by calcitic matter. The canal diameter is varnishable and is in different stages of growth. The annular circular rims of growth can be seen under high magnification.

In case of the section of the dinosaurian bone from second Intertrappean bed, the haversian canal units are circular in outlines and show different stages of growths in concentric annular growth rings and zones are clearly visible under higher magnification (Plate XXVII/2). The outermost rim of individual canal consists of a thin white calcareous material. The central opening is circular in outline and is occupied by growth bluish material comprising calcareous and partly (?) 'magmatic' material as a later replacement. The central part of the canal shows micro-radial fractures under high magnification. The rims surrounding central parts of the canal comprising of from central to peripheral part of light greyish white part dark brownish to yellow part and finally a rim of white calcareous material. The radial fracture system in majority of the cases has traversed up to the mid way of haversian units and in some other cases up to the peripheral areas. This anomaly is seen in all the stages of development of haversian units. Such a condition racial of fracturing and rupturing is termed as the pathological condition in the dinosaurian bone.

The micro sections of the dinosaurian bones from III Intertrappean bed (Plate XXVII/3) shows a circular pattern of haversian units with concentric growth lines, zone and a prominent radial fractures system evenly in early stage, matured & lately second generation of haversian system. In case of the dinosaurian bones in third Intertrappean bed, this radial fractures in later stage rupturing is more pronounced and severely evident in all the stages of the development of bones. The overall structure of the dinosaurian bone suggest endothermic characters as suggested by Ricaulse (1970) and a pathological

Plate XXVII Microsections of dinosaurian bones - palaeopathology.

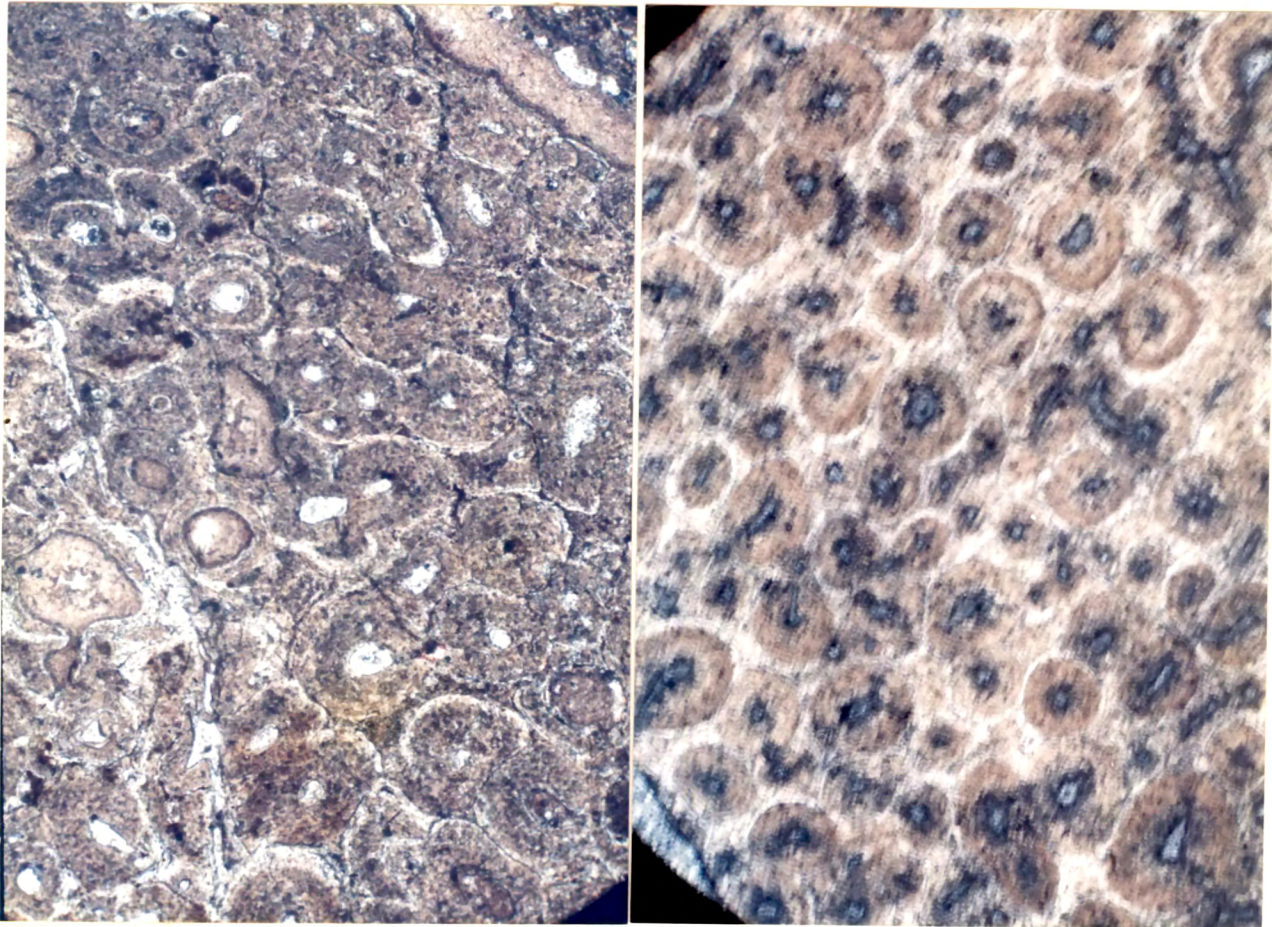


Plate XXVII/1 Microsection of a normal healthy dinosaurian bone from upper

Plate -XXVII. partly diseased bone from Sec. I Int. bed  
with initiation of rupturing of Haversian  
canals.

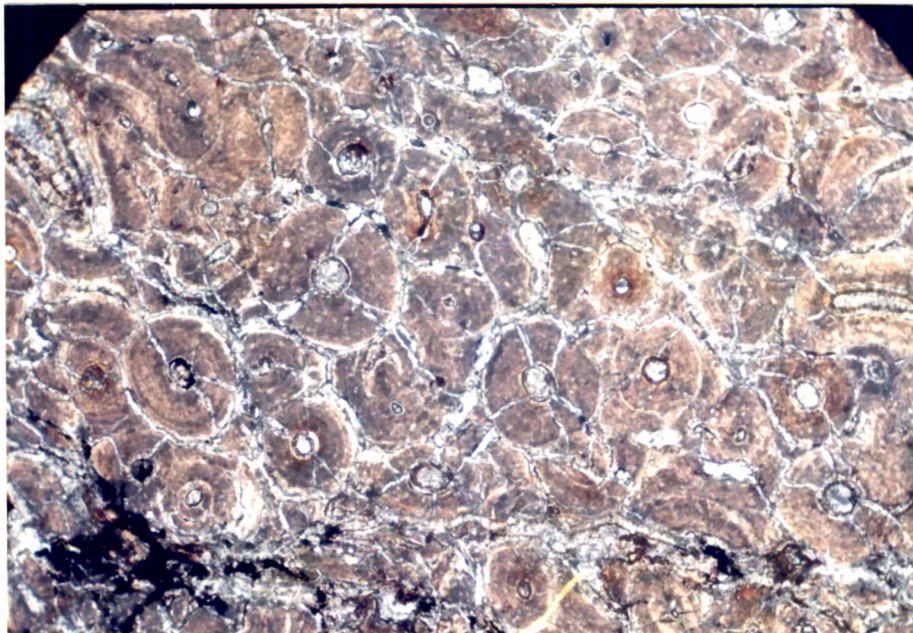


Plate XXVII/3 Pathological dinosaurian bone from III intertrappean bed at  
dinosaur pit locality.

(diseased) condition in the lasts of the dinosaurs.

The longitudinal section (Plate-XXVIII/1) of same dinosaur bone from Intertrappean bed No 3 (Plate XXVII/3), suggests system of multiple fractures in the bone which was partially healed during life time of the animal. It is seen that the bones are very fragile and probably lacked sufficient strength and compactness required to support the metabolic physiological and physical activities of the animal. These fractures are joined by calcareous matter.

### **IX.8.2.3. Dinosaurian Eggs:**

The study of the shell structures of the dinosaurian & related egg suggest the following important facts:

(1) There are more than one species of the dinosaurs (Plate XXVIII/2,3,4 XXIX/1,4,2).

(2) Two distinct types of conditions prevailed.

A. The Normal development of eggs, which was comparatively less (Plate-XXVIII/2, XXIX/1, 3).

B. Anomalous growth of the eggs, which included either the excessive thickening or thinning as well as multi-layered pathological conditions (Plate XXVIII/3,4, XXIX/2,4).

(3) Besides dinosaurs Avian geokoid and crocodilian eggs are recorded from third Intertrappean bed.

The Normal dinosaurian egg from II and III Intertrappean bed is generally less than 2 mm thick and comprises of basal mammillary knob layer, prismatic spherulith layer in form of broad conical, long slender biotic calcite layers with a domal outline at the top. In some cases there is a thin layer at the top as in case of (plate XXIX/1 XXIX/2 and XXIX/3) some egg shells. The intervening canalicule opening maintains a thin opening between atmosphere and the embryo for exchange of oxygen for survival. In some cases it is seen that canalicule is partly filled with calcite. The spheruliths shows longitudinal radial lines emerging from the basal mammaliary lines. Horizontal growth hinge (also known as the incremental lines are concentric and show little doming up in the central parts of the spheruliths (Plate XXVIII/2, and XXVIII/4). At time the spheruliths are fused together and joined at base (as in case of XXIX/2).

#### **IX.8.2.3.1. Pathological Eggs:**

In some eggs shells from second Intertrappean bed as well as in case of eggs from Third Intertrappean beds, (Plate-XXVIII/3 and XXVIII/4 and XXIX/2) more than one layer of prismatic spheruliths are seen. These multilayer egg shells show growth of the layer in such a way that the successive spheruliths cause blockade of the canalicule opening which disrupts the atmospheric oxygen supply to the embryo.

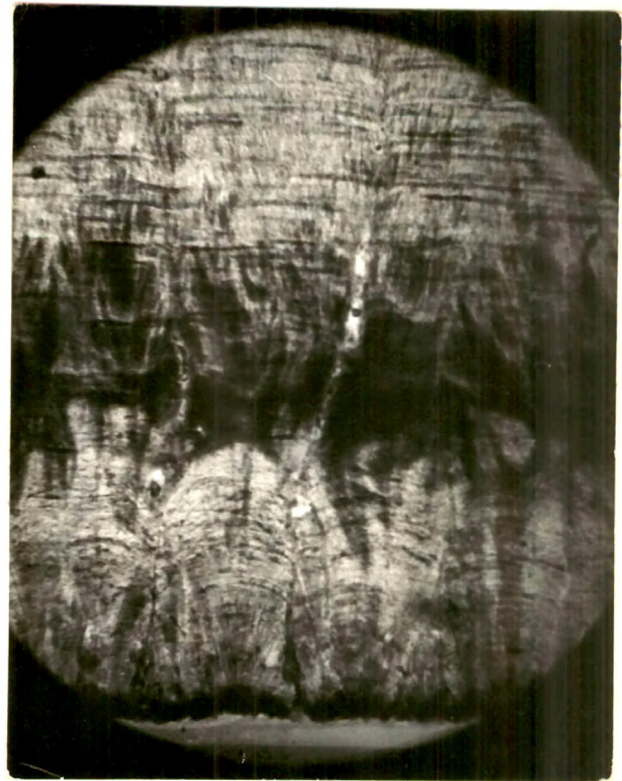
In case of some other egg shells from third Intertrappean bed, a comparatively thicker spongy layer is developed over the domal outlines of the spheruliths

Plate XXVIII microstructure of dinosaurian bone and egg shells with pathological conditions.

X XVI



1

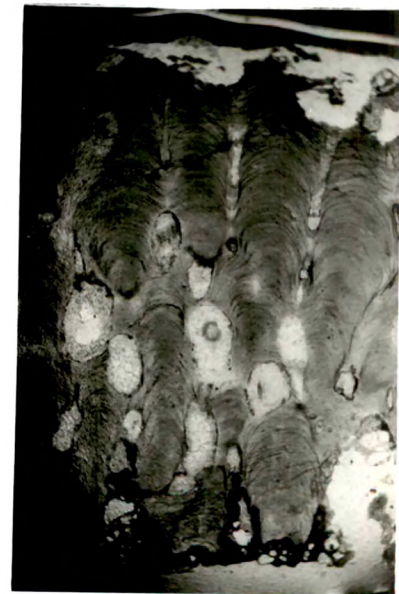


3

Plate XXVIII/1 Longitudinal section of pathological bone showing partly healed multiple fractures suffered by animal during life period.



2



4

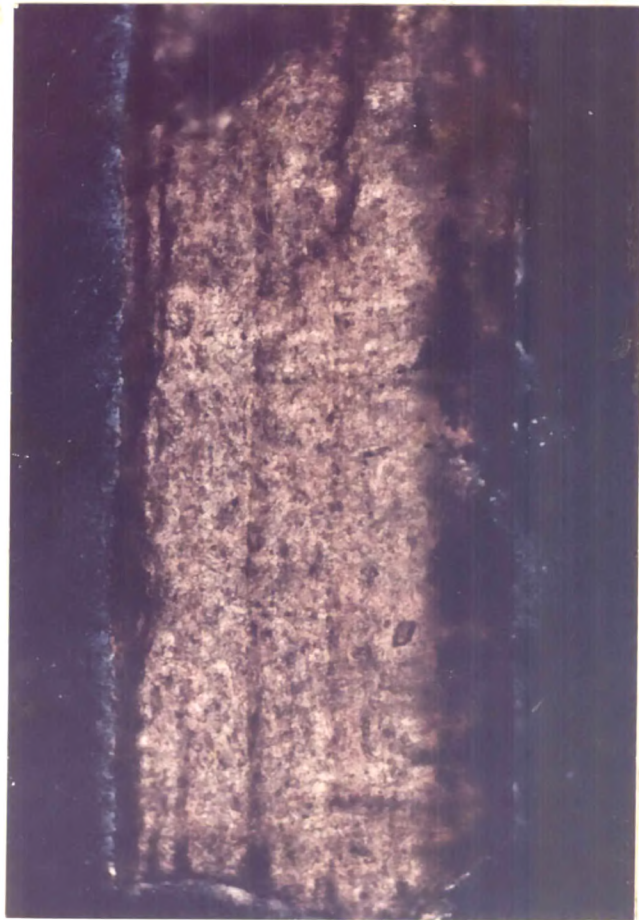
Plate XXVIII/2 Microsection of a normal healthy dinosaurian egg shell.

Plate XXVIII/4 Microsection of a pathological dinosaurian egg due to multilayer growth.

Plate XXVIII/3 Micro section of an excessively thick shell from III Intertappean bed. The Canalicules are blocked causing pathological condition due to multilayered structure.



XXIX/1 Microsection of dinosaur egg shell. II Intertrappean bed, Anjar. Plate XXIX/2 Microsection of dinosaur egg shell from Intertrappean bed, Anjar



XXIX/3 Microsection of Avian egg with broad spongy layer from III Intertrappean bed, Anjar.

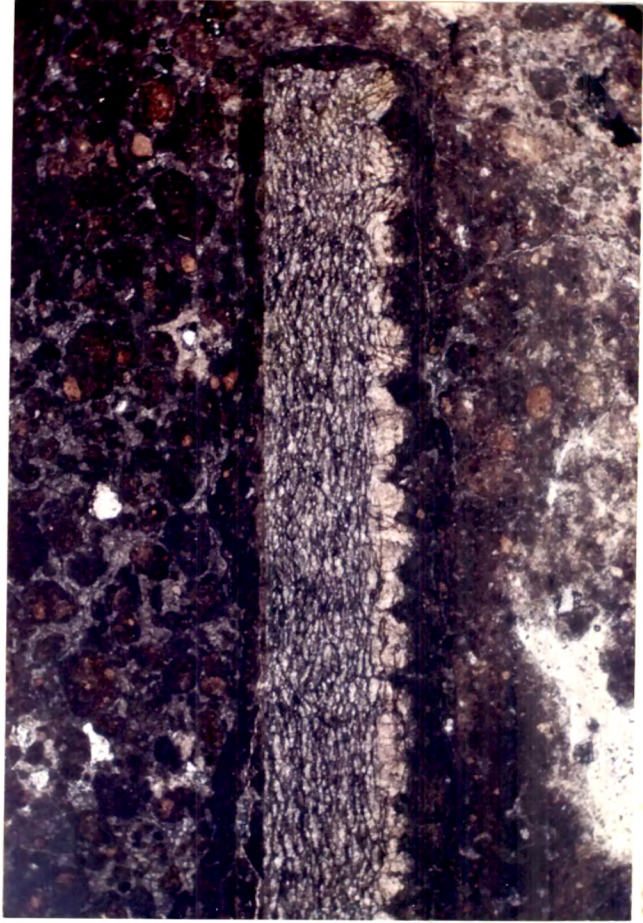


Plate XXIX/4 Avian egg shell with excessive thick spongy layer

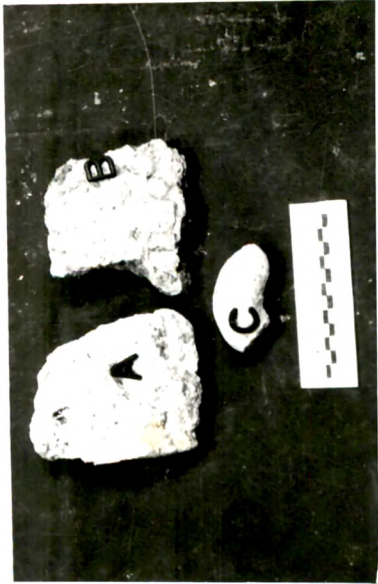
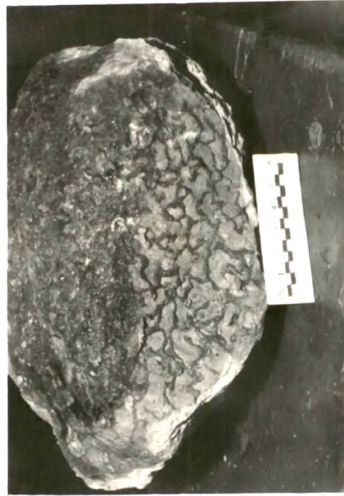


Plate XXX/2 a Ossified dinosaurian skin from Anjar dinosaur pit locality, Anjar Plate XXX/2 b Ossified skin of dinosaur- Titanosauridae.



Plate XXX/3 Microphotograph showing structure of the dinosaurian skin. All magnifications, except where mentioned are X400.

Plate XXX/1 Ossified dinosaurian skin from Rahioli, (Titanosauridae skin)



(Plate XXIX/1). In case of the Avian egg shells, from the second Intertrappean bed. This spongy layer is excessively thick and highly fractured. The canalicules and their passage through this layer is not very clear (plate XXIX/1) and show excessively thick nature.

#### **IX.8.2.3.2. Dinosaurian Skin and Pathological Condition:**

The dinosaurian skin (Plate XXX/1 and XXX/2) show replacement by silica in case of Rhioli and is partly replaced by calcareous matter. The skin shows bulbous nodous appearance with wrinkles forming about 1/2 to 1 cm thick dermal Scutes. The microsection of the dinosaurian skin show epiderm layer in form of parallel lammellar growth of five to six layers with central bulbous cavities in the central part of the dermal scutes comprise cellular growth centres, and surrounding cavities on either sides, which shows a homogeneous fine uniform white zone with openings of thin narrow capillary openings (Plate XXX/3). There is an innermost (basal) distinct layer on at the base of epidermal epithelial zone on either sides and above the central cavities. The cavities may have been filled with some liquid and must be helping in regulating the body temperature of the animals. The innermost basal layer zone support the growth of the skin layers as in case of the modern reptiles. The epidermis show layered structures of grey white and black coloured. There is a profuse staining by the black (dark) coloured pigments, in the epidermal zone. These pigments are melanocyte pigments, which absorbs the U.V. radiations and other fatal cosmic radiation, which have adverse effects on the body of the animals.

In case of the dinosaurian skin from the third Intertrappean beds, the melanocyte pigments are not well defined and well developed as compared to the dinosaurian skin from Rhioli area. This suggests a pathological condition of fossil skin in case of the dinosaurian skin from third Intertrappean bed. The pathological conditions of eggshells, skin and bone structures are discussed separately under palaeobiology and palaeoecology and under implications of data modelling and synthesis.

#### **IX.8.2.3.3. Dinosaurian Bone Structure (Palaeohistology):**

The *Dinosaurian* bones from Patcham Island show a crude haversian canal system parallel to length of spongy bones on weathered surface (Fig-29/b,c,d,e,f,g). The microsections of such bones when examined under microscope show circular out lines with primary type of haversian canal system (Plate-XXVII/1,2,3; XXVIII/1). The canaticules (central part) are filled with stained grey matter.

The dinosaurian bones from second Intertrappean bed (Plate-XXVII/2) show oval to oblong complex outlines of haversian canal system. The canalicules are at various stages of growths. In case of *Dinosaurian* bones from third Intertrappean bed, the microsection shows circular type of out line of the haversian system in various stages of growth. Radial cracks are seen at in almost all the haversian canals. The longitudinal sections of same *Dinosaurian* bones (Plate-XXVIII/1) show lensoid growth of individual system unit, with numerous transverse and angular microfractures. The lensoid nature of units indicated

different stages of growth and at the same time invariable voidous fractured nature suggest a definite pathological condition in bone development, which could be related to the deficiency in essential material, i.e. calcium and phosphate during the life span of the animal. Such pathological systems start appearing in the bones from Second Intertrappean bed and hence very common in the Third Intertrappean bed. Such diseased condition can be tied up with the factors responsible for extinction of *Dinosaurian* fossils during uppermost Cretaceous and later period in the *Dinosaurian* history.

#### **IX.8.2.3.4. Associated Fauna of Anjar and Dayapar Intertrappean Beds:**

The dinosaurian fossils at Dayapar are highly replaced, at times this completely replaced beyond recognition and are highly fragmentary in nature.

The white and grey limestone at Anjar contain mainly other invertebrates, mostly bivalves and gasteropods. The gasteropods are dominated by *Physa Sultinus* and *Physa Broncepil*. Apart from this, tiny small forams are found in abundance in the black chert and white cherty siliceous limestone. However, it is very difficult to separate these fossils from the chert and cherty limestone, hence the study was done on the microsection and with the help of magnifying lens wherever possible. Crocodilian teeth and other thin fragile bones (possibly chelonian and avian) are occasionally seen at Dayapar. These bones are very light, hollow and have developed abundant air cavities, so it is believed that these would be of some birds or of swimming reptiles like chelonia. At Dayapar, the fragmentary highly replaced bones of *Dinosaurs* are found within the pink and chocolate coloured clay horizon (Fig-8) of Dayapar section. The bony layer is found above the marly horizon. The fauna of Dayapar comprise of *Dinosaurian* limb bones, teeth, egg shell fragments and other reptilian bones. Definite identification of these bones is not possible, it mainly comprise mixed fauna of *Dinosaur*, *chilonia*, *boidean vertebrae* and limb bones and eggs.

#### **IX.8.3. Flora:**

The Intertrappean bed at Anjar contains abundant chertified wood and cycadean element (Plate-XXIII, XXIV). The other important fossils include microsporangia of cycades, fern spikes (Plate-XXVI/1/2), crown (Plate-XXV/2, 3) and sporangi (Plate-XXV/1) and sporomorphs. The study of wood tissue structure indicate angiosperm - monocotyledonus (Plate-XXIII/1) and dicotyledonous wood (Plate-XXIII/2) and creepers (Plate-XXII/1,2,3 and XXIII/2). However, in absence of major leaves or floral elements (Plate-XXVI/2,3), it is not possible to identify the complete floral composition.

#### **IX.8.3.1. Microflora of Anjar Section:**

The Anjar section has shown some dinoflagellates from the grey and black shale which contains *Dinosaurian* bone fossils. These dinoflagellate (Plate-XXI/1) show mixed characters of both Tertiary and uppermost Cretaceous indicating that this may be very close to the Cretaceous-Tertiary boundary. The flora is dominated by macrosporangia of cycades and dicotyledons wood. The presence of angiospermous wood and cycade elements

XXI

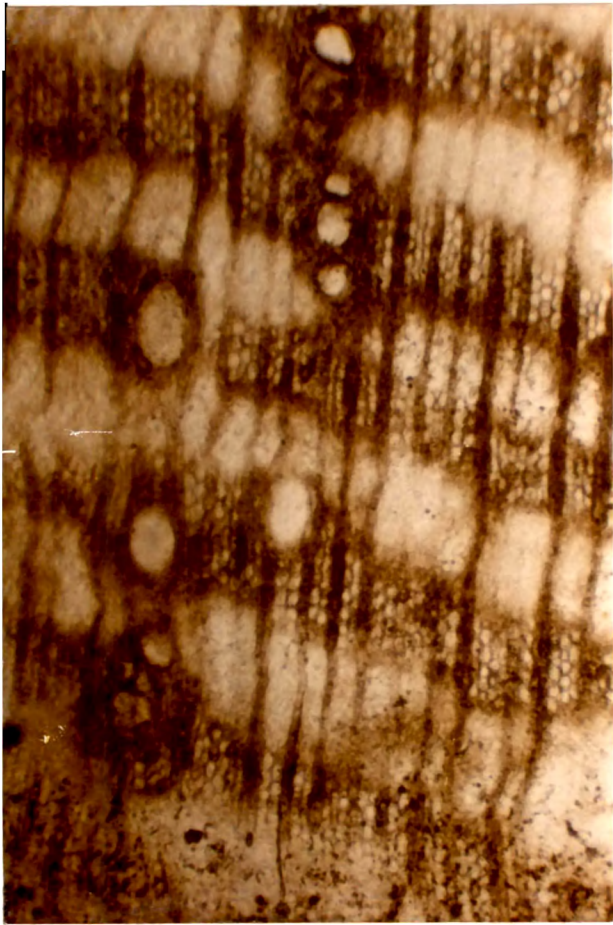


Plate XXII/1  
 Microsections of fossil wood from Third Intertrappean bed showing well developed vascular tissues Xylems, phloems (Dicotyledonous wood).

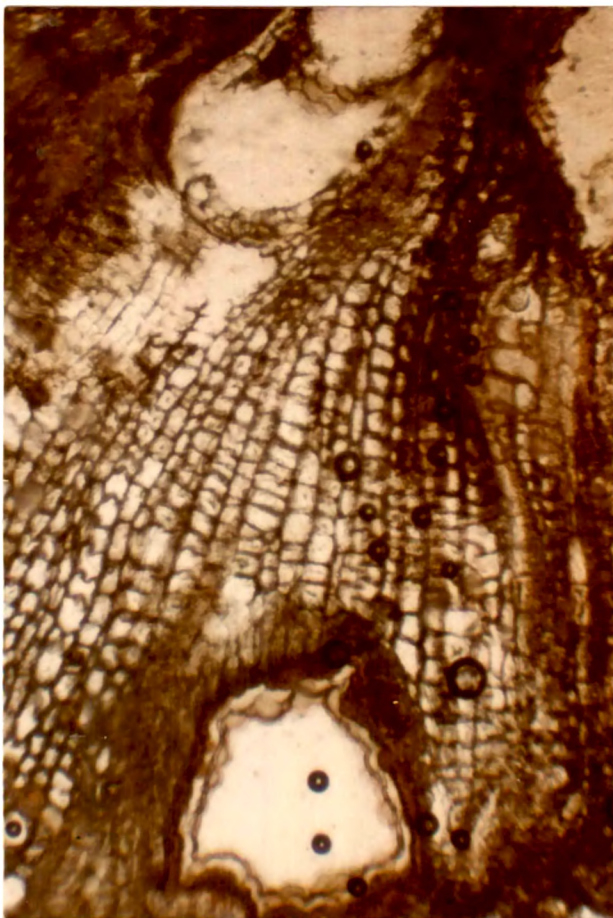


Plate XXII/2  
 Microsection of creeper/climber fossil wood from III Itn. showing well developed ring structures and arily lignified darker bands of constricted growth. The humid period growth is represented by broader rings.

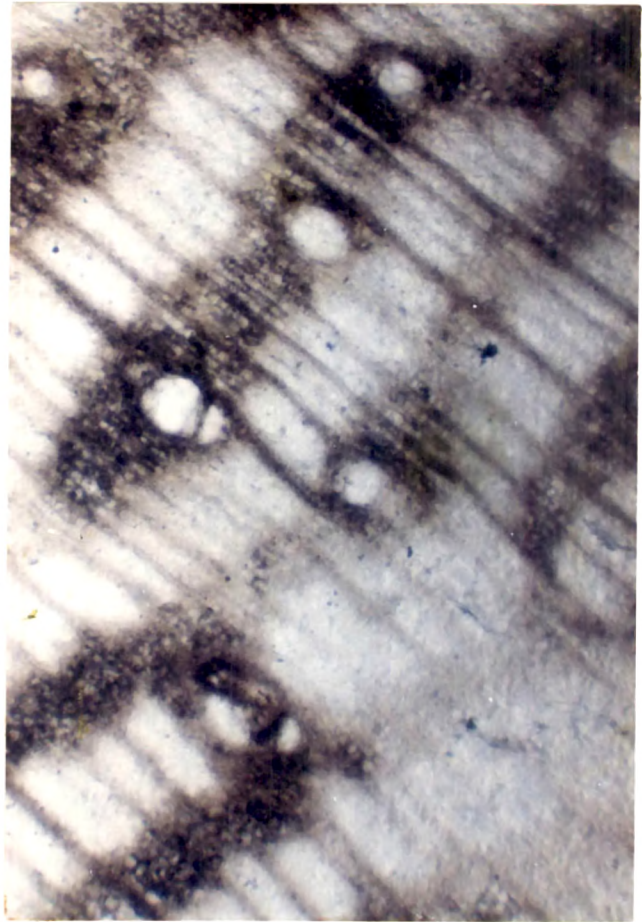


Plate XXII/3  
 Microsection of Creeper/toiner fossil wood from III intertrappean bed showing similar structure.



Plate XXIII/2 Photograph of Dicot fossil wood showing annular growth rings on weathered surface, III Int. bed, Anjar.



Plate XXIII/1 Photograph showing basal part of fossil palm wood from Third Intertrappean bed, Anjar.



Plate XXIII/3 Microsection of a fossil wood from Jurassic showing almost broadly uniform structure.

XXIV

Plate XXIV Microsections of fossil wood from Cretaceous rocks of Kutch.



Plate XXIV/2 Microsection of fossil wood from Lower Cretaceous showing quick alternate narrow and wide growth cycles.



Plate XXIV/3 Microsections of fossil wood from Upper Cretaceous with well differentiated growth. The cycles with constrained lignified growth are wider. The summer growth cycles are gradually initiating and ending with a peak in the centre. The humid cooler growth cycles are nearly three times larger.



(Plate-XXI/3) and mixed characters of dinoflagellates along with forams indicate closeness to K/T boundary. The absence of *Dinosaurian* elements within the above limestone and chert except a few fragments of bones, which are thought to be due to transportation, indicates that the assemblage definitely belongs to the Tertiary. This fact is supported by the radiometric dating of lava flows above (F4) and below (F3) the third Intertrappean bed, at Anjar, which have shown  $^{40}\text{Ar}/^{39}\text{Ar}$  age as  $65.2 \pm$  my and  $65.4 \pm 0.4$  my respectively. This indicates nearness to the K/T event.

The magnetostratigraphic measurements also indicate NR-N-R-N-R sequence, which also points to frequent change over of polarity.

#### **IX.8.3.2. Dendrological Studies and Mega Plant Fossils:**

##### **Mega Sporophylls:**

Mega sporophylls range in size from 3 to 8 cm and consist of upper broad leafy pinnates, tapering portion with a stalk like portion. A lower portion has serially arranged depressions of ovules (Plate-XXV/1, XXVI/1). They occupy lower part in the pinnate stalk. The fossil mega sporophylles of cycades have been recorded by Florins (reference in Gymnosperms by Vashishtha, 1985, p. 155-167). In the present one, only the scars of the seeds were seen as depressions. It was supposed by Florin that the scars were seeds and he reconstructed the whole plant from imagination. The reconstructions were supported by similar cuticular stomatal and epidermal structures. Cycades fossils were known from early Tertiary of Japan.

##### **Fossil Cones:**

The specimen is about 15 cm in size, ellipsoidal in shape. The cone scales are helically arranged, which are seen as traces on the surface (Plate-XXVI/2). The anatomical features of the basal part suggest that the seeds consist of 0.5 to 0.6 cm wide and about 1.3 cm long. Each ovuliferous scale bears one seed, partially embedded on the surface. The seeds are seen as domed spherulitic projections. In section, each mega sporophyll contain biserial embryo shoot. These are comparable to the araucarite fossil cones (Plate-XXVI/2), which appeared in Cretaceous and continued till recent with reduced numbers.

#### **IX.8.4. Micro Fossils:**

The micro fossils studies of the samples from the Anjar and Dayapar section were carried out on the basis of their microsections as they occur in the cherty limestone and in the treatment of the silica and carbonates, as the enclosed fossils get damaged and dissolved. The micro section studies have shown that the following important groups are present:

1. Foraminifera : The studies of microsections and their comparison with the available literature and similar findings elsewhere. The following forms could be identified: Globigerina fossil shells (based on comparison of micro sections (from Horwitz, Plate XX/1).

229.

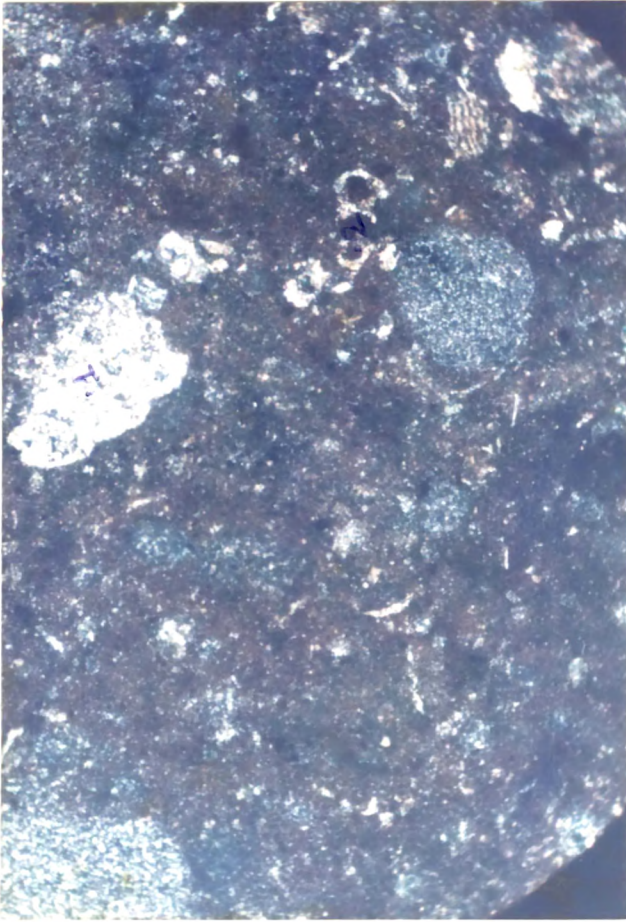


Plate XX/1/2 *Globoguembelerialanica* (Hopper) and *G. eugubina* from cherty limestone bed (Biserial form).

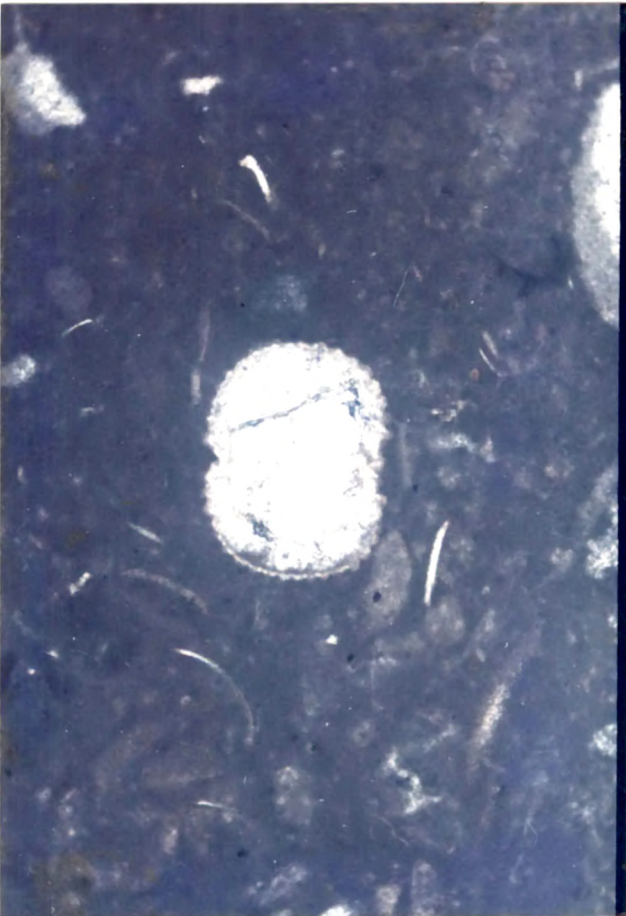


Plate XX/1/1 Microsection of globigerinid fossils (foraminifera) and associated broken shell of ostracodes, from third Intertrappean bed, Anjar.



Plate XX/1/3 Microsection showing *Palmaepollenite* sp. and *fraxinipollenite* resembling one Tertiary form described by Nichols and Fleming (1990).

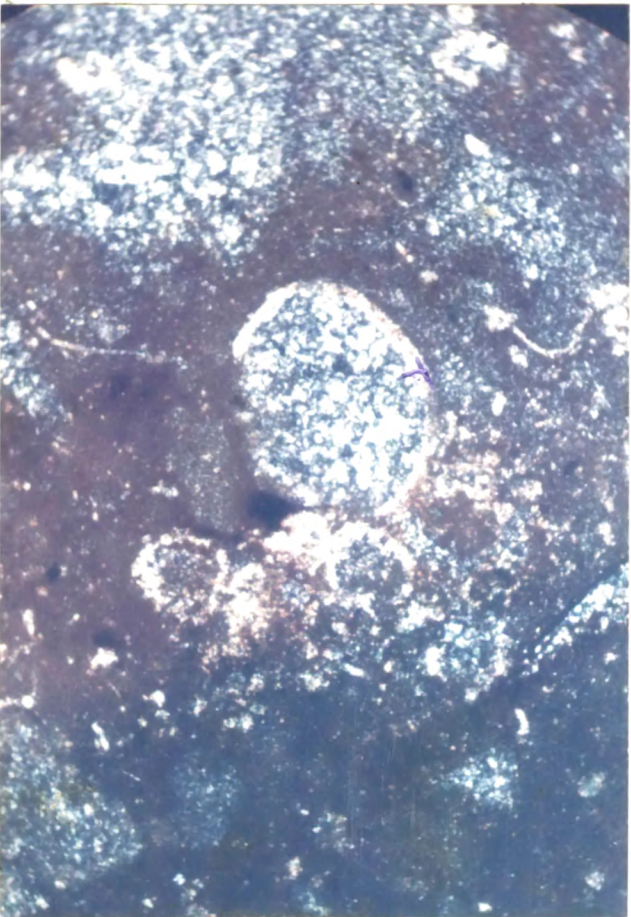


Plate XX/2/1 Palaeotaxtularia Brasier.

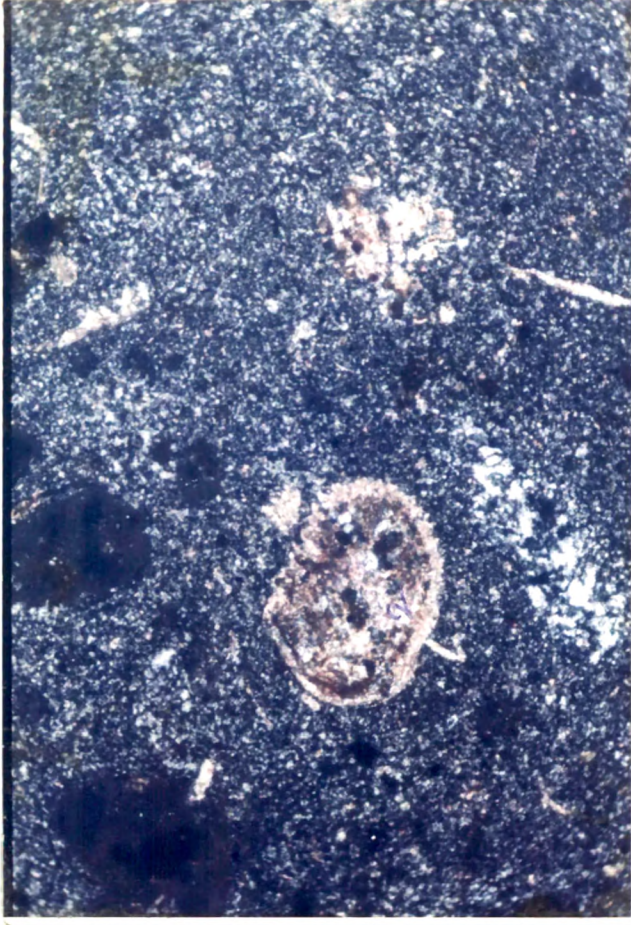


Plate XX/2/3 Spore of unknown affinity. Inset scdis, cup encloses spores.



Plate XX/2/2 Microvertebrate tooth of unknown affinity.

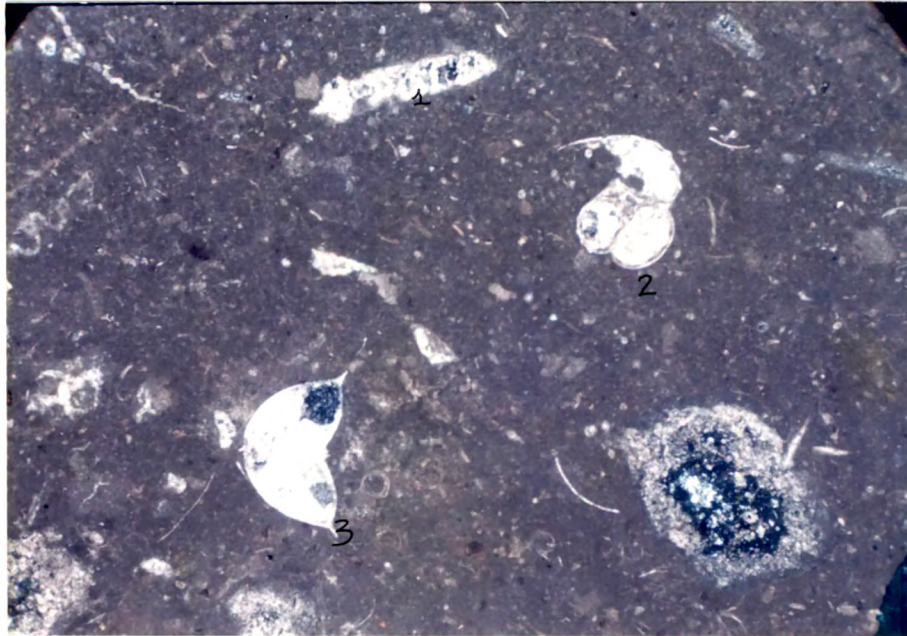


Plate XIV/1 1 *Nodosauria*, sp. 2 *G. bulloids* 3 *Manicorpus*.

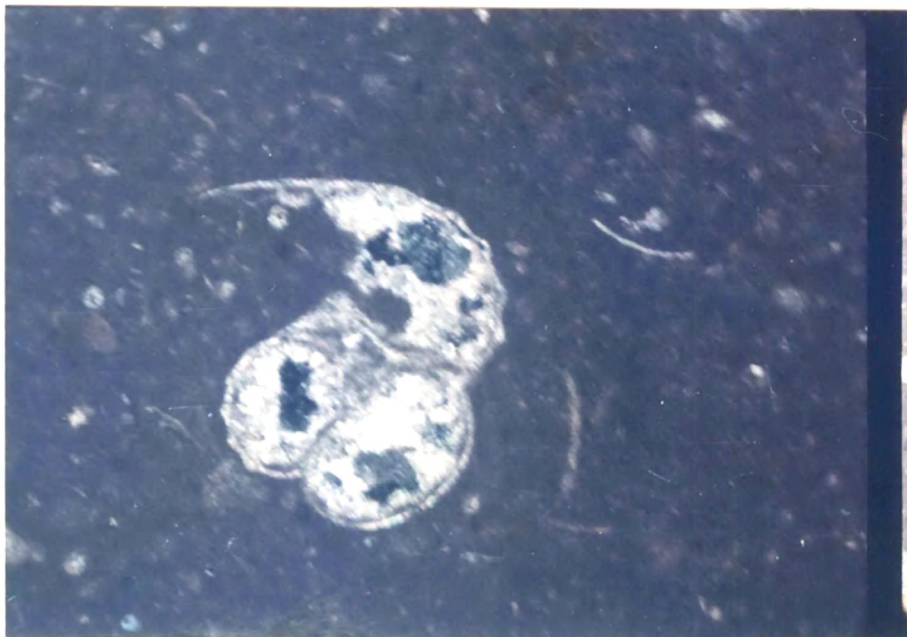


Plate XIV/2 Enlarged view of *Globigerina bulloids*.

2. Triserial form in microsection, comparable to Trochospiral (Triserial) form Vernerilina, Discoidal cerolute (?) Trochommina (Plate XX/1). Globoguembelirradanica Hoffner Geuqubina with matted chambers open bilious (Plate XX/2).
3. Suborder : *Nummulites*, larger forams, Parathuramminaces, Palaeotaxularia Brasier (Plate XX/2/1).
4. Larger Foram: Further identification is not possible, but it resembles section of Nummulite.
5. Suborder : Rotalina superfamily, Cassidulinaceae Virgulinella (Brasier, 1980).

The megaspores have large massulae, or floats above spores. Proximal region consists of a tripartate prolongation of the perspore terminal acromella.

#### **IX.8.5. Micro Flora:**

The wall of the megaspore is two layerED (XX/3.1) with systematic ultra structure. Associated with these fossils are abundant massulate up to 500 #m, long. Some containing recognizable anchor shape glochidia. Aquatic heterosporous ferns salviniales are represented by two exiting genera. Azola and Sawnia). Plants are small free floating in lakes and ponds. Sporocarpus are borne on submerged leaves. The microsporangia and megasporangia are borne in separate corps on same leaf.

#### **Mancicorpus Sp:**

In micro section, this is comparable to the Mancicorpus sp., described by Nichols and Flemming, (1990), Plate XX/ 3, 2.

#### **Caytonia sp:**

(Plridospermatophyta), Todisposite Cf.I, Minor Couper, 1958. Morphologically represented multi ovalata stalked capsules in sub opposite pairs. Scars along the megasporophyll suggests that capsules were shed. Each capsules is oblong to circular in outline and up to 4.5 mm or less in diameter (Plate XX/3.3). They are borne along the axis in such a way that capsule is recurved within the lip like projection near the point of attachment. Each capsule contains 8 to 30 seeds depending on species. Each is basal on a delicate stalk in an orthotropoons position along the mid vein of cupola. The seeds are 2 mm or less long and radially symmetrical. The integument consists of an outer uniseriate epidermis that covers a raw of radially directed fibres the necellus is attached at base. The other important spore are Palmidites maximus Couper, 1953 Plate XX/3-3) Palmaepollentes sp. (Plate- XXI/1/3) and Fraoxino pollenis sp. (Pl. XX/1/1) are known.

#### **Dinoflagellates**

Lycopodium Scariosum

This shows a dinoflagellate lycopodium scariosum which closely resembles to Rgoshispora minor (Norton) Srivastaya, 1978, described by Arunkumar (1992) from Texas. Enlarged view of the above shows a close resemblance to the above mentioned Ghoshispora



Plate XX/3/2 Mancicarpus sp. spore.



Plate XX/3/1 Azolla prinneva - an aquatic fern spore (Larger one).



Plate XX/3/3 Capsule of caytonia sp. spore (in centre). The ostracod shells (broken) are seen in the ground mass.



Plate XXI/1  
 Lycopodium scariosum, a cyst (smaller form). The larger form is cyst of unknown Affinity.

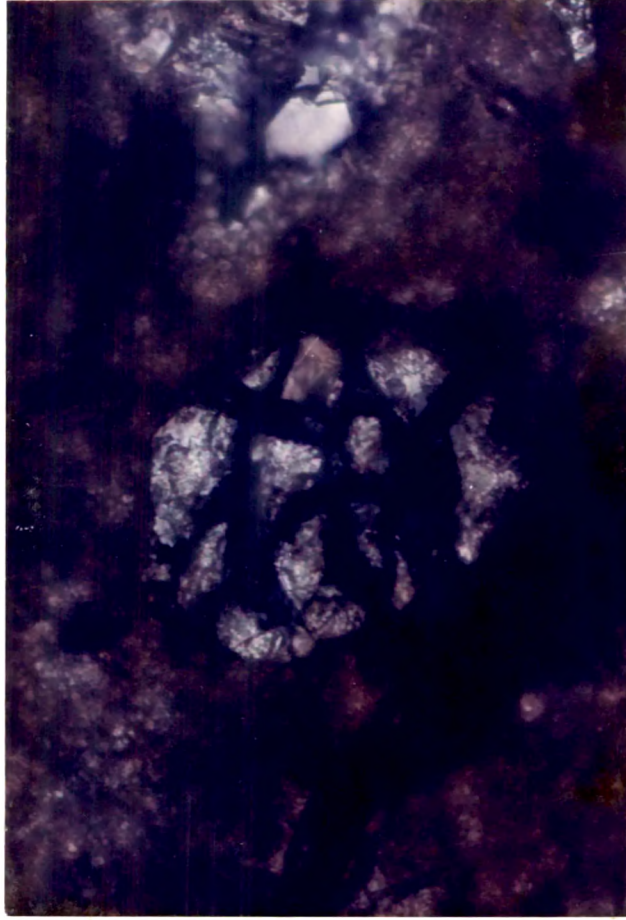


Plate XXI/2  
 Lycopodium scariosum (X750) showing detail structure. This shows close resemblance to Ghoshispora minor described by Arunkumar (1978).

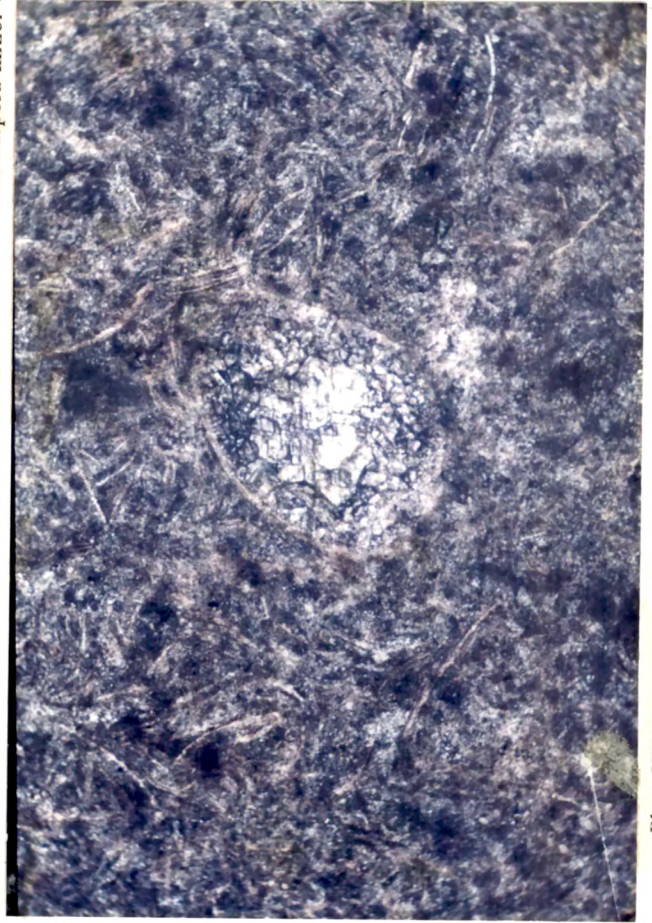


Plate XXI/3  
 Spore of cycadopytes (Scarbratus, Stanley 1965) similar to described by Arunkumar, 1992.)

Xxi/1

minor. (Pl. XXI/2). *Cycadopits scabratus* Stanley, 1965 (Pl. XXI/3). The other important spores of indeterminate affinity (Pl. XX/2/2) resembling a cup like structure, which is also found from the cherty limestone horizon. Micro vertebrate tooth of indeterminate affinity (Pl. XX/2/3) is also found from the cherty limestone horizon.

#### **Azolla:**

The fossils are identified by comparisons of microsections of samples from Anjar. The mega spores have large mesolite or the floats above the spore, that provide important criteria for comparison and identification. The proximal region of spore consists of tripartite prolongation of perispore termed acromella. Their fossil remains are described from Eocene sediments of southern British Columbia. In genus (*salrinia*), which dates back to Cretaceous, the mega spore lack floats.

The transverse sections of the fossil wood specimen from second and third Intertrappean beds were studied. These sections include different types of small herbaceous creeper and other types of fossil woods viz, Monocot as well suspected dicot types. The small herbaceous wood and creepers as well as the other types show a well developed systems of phloem, xylems and well marked ring structures (Plate XXII/1,2). A specimen of fossil palm wood (Plate XXIII/1) shows a developed xylem and flumes. The basal part of this stem (Plate XVII/1 enlarged view) shows serially arranged rows cells of different sizes. The micro sections of creepers and toiner type of plants show successive cycles (ring) of constricted smaller cell and comparatively larger, broader cells in annular growth ring structures. The width of constricted ring is slightly lesser than those of the broader, larger cells in both the cases. The narrow ring structures show deposition and profuse staining with darker material (lignin). The ring structure and contract in size and growth of the cells is well marked as compared to the micro sections from the Jurassic and Lower Cretaceous fossil woods (Plate XXIV/1). The fossil wood from upper member of Bhuj Formation (Plate XXIV/3) also show a well marked annular growth structures like the sections from Intertrappean beds II and III. In case of Upper Bhuj fossil woods, the ring structures with larger cells is wider as compared to some of the sections from lower Bhuj (Plate XXIV/1) and those from the Third Intertrappean bed. (Plate XXIII/2).

In case of micro sections of root zones of fossil specimen from the Intertrappean beds II and III, the conducting cell structures are highly organized. The micro sections of some of the fossil wood specimen from the Intertrappean beds from other plants also show similar structures, indicating a varied assemblage flora comprising creepers toiner, herbs (Plate XXV and XXVI). In case of the fossil wood of twisted and coiling type of flora the microsections show unequal constrictions of tissues at different places. The relative abundance of the fossil wood types was marked in the Anjar Intertrappean bed no. 3. It was found that the cycadean and fern woods (Plate XXVI I and II) were relatively abundant in the gray and chocolate coloured shale horizons below the cherty limestone bend. Their abundance continues with the dinosaurian bone fossil bed. The important

XXVI/1 Petrified fossils of (1) *C. revoluta*, (2) fern spikes, (3, 4) herbaceous stem and climber (5).

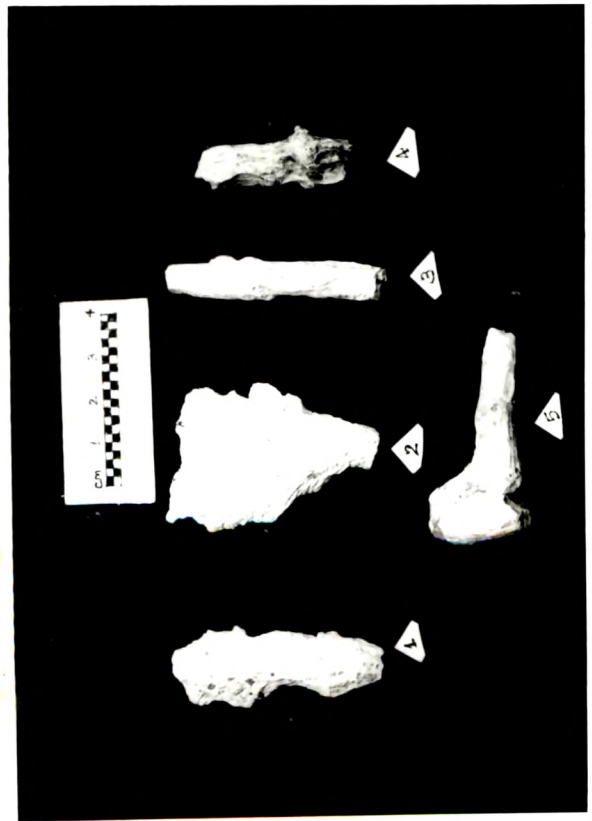


Plate XXVI/1 Petrified fossils of (1) *C. revoluta*, (2) fern spikes, (3, 4) herbaceous stem and climber (5).

Plate XXVI Megaplant fossils from III Intertrappean bed at Dinosaur pit locality.



Plate XXVI/2 Petrified araucariaceae fossil fruit.



Plate XXVI/3 Silicified fossil fruit of unknown affinity.

cycadean varieties include cycadean *circinalis*, *C. thourasii* and *C. revolute* : based on the arrangement of the ovules on megasporophytes (Sporengia Plate XXV/1) first three specimen from left side respectively). The cycadean megasporophyls the fossilised ovules and their depressions are well marked, which form the basis for details identification.

The ferns (Plate XXV/1 extreme right specimen, and XXV/2 and 3) are abundant in the chocolate coloured shale horizon which from the topmost unit of the dinosaurian bone bed at Intertrappean III in Anjar area. A fern spike (spores plate XXVI/1-2 No specimen) abundance is relatively, in the chocolate coloured shale horizon in upper part, which has yielded the last dinosaurian fossils. The gray and black shale and chocolate coloured shale horizon also contains petrified (siliceous) fragments of herbaceous wood (Plate XXVI/1/3) and creeper and oiner type of fossil woods (plate XXVI/1 - 5 No). The micro section suggest that these are dicotyledonous woods (of angiosperm plants). Precise identification is not possible in absence of further well preserved fossils. It has been observed that the partly burnt and oxidized organic matter is very abundant in the basal part of the Third Intertrappean bed.

The cherty limestone and banded chart above the dinosaur bone bed horizon and other higher cherty intercalation marls have yielded well preserved petrified fossil fruits (plate XXVI/2&3) and large petrified logs of angiosperm wood in abundance from Third Intertrappean bed at Anjar Dinosaurian locality as well as from the Intertrappean bed sequence of Roha in Western Kutch. The fossil ferns are in relatively more abundance in Reha section than in Anjar section. The fossil fruit (Plate XXVI/2) shows a close resemblance to Araucaraceae fruits. The external ornamentation in this case shows a close network of tubercles of spherical (conical) shape uniformly spread on the entire surface. These show a variation in size in central part as well as in the ends. At times, these are partly removed due to weathering (and leaching) have left depressions. The fruits are flattened and compressed reconstruction of their shape suggest an oblong to oval shape with maximum length of about 15 to 18 cms, and shorter diameter of about 10 to 12 cms. The araucariceae fruit is very closely comparable the modern jack fruits , both in the external surface ornamentations and structure.

The other important forms including *Brevicolparites*, *Colpella*, *Lavigatosporite* sp. *Cytheidites* sp., are also suspected in the Anjar dinosaur pit section and Intertrappean bed. The other micro plant fossils belonging to phylloid algae, Charophytes fossil cone, spores etc. are already dealt separately earlier, hence these are not repeated here.

#### **IX.9. TRACE FOSSILS:**

Important trace fossils that are found in the intertrappean bed, which mainly comprises of *ophiomorpha* burrows and some sub vertical / inclined burrows. Boring type of burrowing marks are not commonly found within the sandstone and clays/shale from second intertrappean bed. These are mainly suspension feeder burrows. The burraow pattern is aligned sub-horizontally to slightly inclined in position to the palaeocurrent laminae of the sandstones in second intertrappean bed (in the area towards west of Viri village).

In case of the third intertrappean bed the grey and black shale forming the basal part of the sequence at Anjar dinosaurian fossil locality are burrowed. This burrowing activity is more pronounced in the black and chocolate colour shale forming horizon below the cherty limestone bed. The burrows are mainly sub-vertical to slightly inclined and in some cases the burrowed chambers/holes are filled by the medium to fine grained loose ferruginous sand or clay shale, which is generally different from the host rock. The nodular and false bedded/stratified marl and laminated cherty limestones are not frequently burrowed. The intervening shale/clays and the gypsum and siliceous parting horizons are associated with vertical to sub-vertical burrows above the limestones bed. Thus it is seen that:

- (1) The sub-horizontal to inclined *ophiomorpha* type of burrows are common in the second intertrappean sandstone bed. These mostly suspension feeder type of trace fossils.
- (2) The basal part of the third intertrappean has a mixed burrowing community, which thrived on suspension feeder as well as the deposit feeder, but the later being dominant.
- (3) The trace fossils above the cherty limestone horizon are dominantly vertical and deposit feeder types. Hansen et. al., (1987), have established chronological events across such a boundary in Texas. The suspension feeders are replaced by the deposit feeder/carnivore type of animals and deposit feeder are commonly seen. This chronological event is recorded above the Iridium layer. The vertebrates - dinosaurs, fishes are found below cherty limestone and they do not occur in higher section at Anjar locality.

#### **IX.10. Trace fossils vis-a-vis Dinosaur foot prints/tracks:**

The dinosaur foot prints and tracks in the Tharauda area contain burrow marks in the siltstones and sandstone beds. The siltstone contains horizontal to sub-horizontal marks of trails, tracks of different groups of worms. Fish burrows and nests occur at the site of dinosaur foot tracks. These suggest a very shallow near shore (beach) set up for the Tharauda tracks site.

The dinosaur tracks at Fatehgarh are found on the current bedded, burrowed sandstone of upper member of Bhuj formation. The sandstone contains sub-vertical to sub-inclined burrows, which are generally not filled by sand or clay (or this has been removed subsequently). The foot tracks and foot print marks have caused slight flattening or widening of the burrows, due to the weight of the animal. This indicates possibly a lake or lagoon margin/strand line which was, where the burrowing animals thrived abundantly. The dinosaur herd event had happened subsequently and after that there was some thermal event, which has converted friable sandstone into compact quartzitic sandstone. The similar events are also recorded in case of Pakhera of Lower Member of Bhuj Formation) foot track site.

#### **IX.11. Geochemical Studies:**

Geochemical sampling was carried out collectively in 1993. Analysis for siderophile,

Why here? There have already been seen  
at Desai's place

chalcophile, lithophile elements and rare earth elements was carried out at the Physical Research Laboratory, Ahmedabad. The analytical results are summarised in table IX, X, XI and XII respectively. The plot of rare earth in different samples at different depths and variation in their concentrations are shown in figure 31.

The samples data 27A & B show exceptionally high values of Ir (723) and (1271), Pg/g (1123+155) and (1414+125) Pg/g, which is comparable to some continental sections of KTB. These values are about 20 times higher than the adjacent samples either immediately above or below in the section profiles and are about 127 times higher than the basalts. The other siderophiles elements which show higher enhancements include Co, Fe, Ni. In the lithophile and the chalcophile elements, the third Intertrappean bed shows enhancement in the values of Ba (56), Sb (795), Zn (1.88), Se (145), Ag (594), Cu (1) and A\_(5). The Se, Sb, Ag, and Cu show higher enhancement values for samples 27A and 27B as compared to the back ground values. The values for the same elements in the adjacent lithological horizons are different either above or below in the section, which indicates anomaly related to chocolate brownish red ochreous layer. Such layers were considered as the one representing the geochemical KTB layer. Two such layers 24A, 27A and 27B were encountered in the pit I. Subsequent digging, sampling and analysis indicated one more layer at the top indicating three layers with Ir anomaly. The position of *dinosaurian* bone fossils excavated earlier lies between Ir layer II (centre) and III (top). No insitu *dinosaur* bone fossils were found in the horizon above Ir layer III in pit I at Anjar except some isolated vertebrae fragments. Analytical results are as table-9, 10, 11 and 12.

#### **IX.12. Palaeomagnetic Studies:**

Palaeomagnetic studies were carried out at PRL. The samples were re-oriented to their original position, in field set up and were fixed in their original field set up in the R.C.C. base. Triplicate samples of size 1"x2.5" cylindrical cores were obtained with the help of coring machine from each sample. After various treatments the remnant magnetism was studied with the help of Spindle Magnetometers. The F1 to F3 flows of Anjar section shows normal magnetic polarity, whereas, the F4 to F7 flows show reverse magnetic polarity. The polarity inversion is suspected to have occurred during the sedimentation of third intertrappean bed. These indicates that there is a change, a reversal of magnetic polarity between F-III and F-IV in the Anjar section, and indicates that the determination of magnetic polarity of the third intertrappean bed at Anjar is very crucial. Similarly, for the sake of comparison, the palaeomagnetic measurements are essential at Bhachau, Matanomadh and Dayapar sections. The Ukra/Atda section is not physically continuous with the Dayapar section. Therefore, palaeomagnetic and geochronological measurements for these sections are important. Ukra is the only section where the volcanosedimentary sequence rests over the distinctly marine unit and is interstratified with Bhuj sediments. Therefore, there may be a possibility of getting some precise control either in Ukra or in Pranpur area.

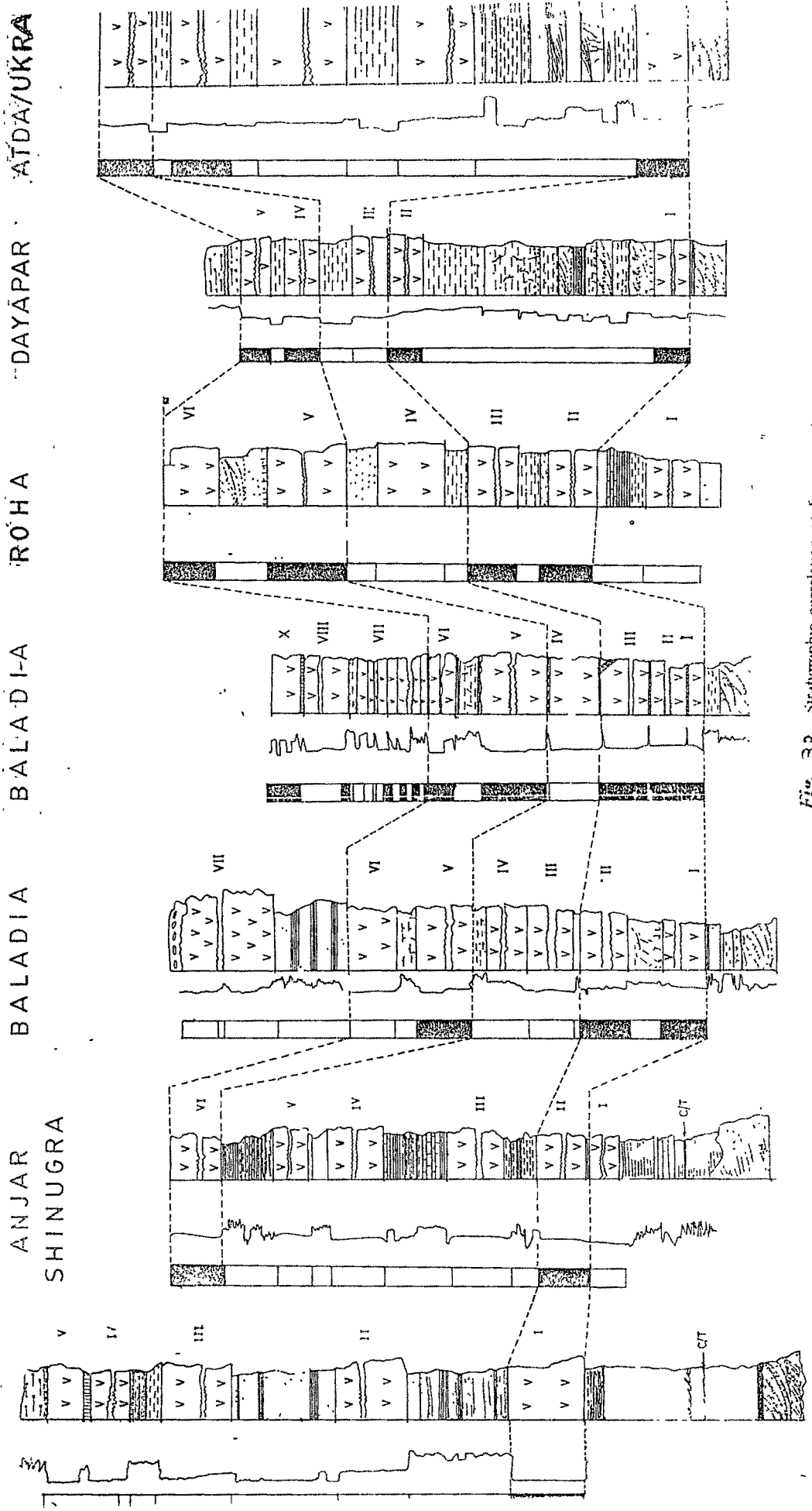


Fig. 32 Stratigraphic correlation of Deccan volcanics in relation to K/T boundary by geochronology, Palaeomagnetic and Palaeontology constraints. The minimum age span of Deccan volcanism may range from 68 Ma to 61 Ma (revised based on data from Yandananic and Courtillot, 1992; Hartland *et al.*, 1993; Gauger *et al.* 1989; Sittba Rao *et al.*, 1988; Sahu and Bajpai 1988; Chatterjee 1992; Venkatesan *et al.*, 1996 and Hoffman 1997).

LEGEND

SCALE

The sections are not correlated as:

- (1) some of them are widely spaced apart and the intervening areas are mapped by several workers, where the degree of detail information varies.
- (2) no physical continuity is established between different sections.
- (3) the intervening sedimentary beds are highly variable and lensoid in nature and there is no lateral persistence in the intervening areas.
- (4) the volcanosedimentary unit overlies different units of Bhuj Formation at different places. This is also clear from the fact that the basal most flows have different nature at Anjar, Baladia, Matanomadh and Ukra areas.

#### **IX.12.1. Field Measurements of Magnetic Polarity:**

The palaeomagnetostratigraphic measurements of flows were carried out by taking fresh oriented samples in the field. The oriented samples were cut in proper 4"-6"X3"X2.5" size blocks. Measurements were carried out with the help of flux gate magnetometer as per the standard methods. The results of the palaeomagnetic polarity of samples is measured and given in figure-32.

Oriented samples were collected at the time of geochronostratigraphic studies.

#### **IX.13. Geochronological Studies:**

The collective sampling for geochronological studies were carried out during 1993. The analysis were carried out by Dr. T.R. Venkateshan and Dr. K. Pandey of PRL, Ahmedabad. The two samples from the lava flows overlying (F4) and underlying (F3) the *dinosaurian* fossil bearing intertrappean bed no 3 were collected and dated by  $^{40}\text{Ar}/^{39}\text{Ar}$  indicated  $65.7 \pm 0.7$  Ma and  $64.9 \pm 0.8$  Ma. Subsequent measurements of the samples from all the flows have shown the following integrated and plateau ages.

Table - II

Sr.No.	Sample	Integrated age Ma	Isochron age Ma	$^{40}\text{Ar}/^{36}\text{Ar}$	Plateau age Ma	$^{39}\text{Ar}$ %
1.	F-VII	$60.0 \pm 2.0$	$58.61 \pm 6.0$	$323 \pm 17$	$61.0 \pm 1.6^*$	96
2.	F-VI	$65.0 \pm 1.2$	-	-	-	-
3.	F-V	$65.9 \pm 1.6$	-	-	-	-
4.	F-IV	$65.1 \pm 1.5$	-	-	-	-
5.	F-III	$64.3 \pm 1.5$	$65.4 \pm 6.8$	$291 \pm 20$	$65.3 \pm 0.6$	80
6.	F-II	$67.1 \pm 1.6$	$67.0 \pm 6.7$	$284 \pm 22$	$66.7 \pm 0.6$	95
7.	F-I	$68.9 \pm 1.7$	$68.7 \pm 10.4$	$302 \pm 35$	$68.7 \pm 0.8$	83

\*Plateau like age

Thus from the above it is clear that the absolute age of  $65.2 \pm 0.6$  and  $64.9 \pm 0.8$  Ma of the F-III underlying the dinosaur horizons are in excellent agreement with the KTB ages of the microtektites determined elsewhere.

#### **IX.14. Microprobe Studies:**

The microprobe studies of the samples collected from the Ir rich layers Ir-I of Anjar were carried out by Prof. Castogroli Cini G. of Institute di Geocosmofisica, Torino, Italy (Prof. N.Bhandari, 1996, personal comm.) have indicated presence of spinels in the Ir rich layer. The spinels are considered as indicators of impact origin by extraterrestrial bodies during their collision with earth.

#### **IX.15. Synthesis of Data:**

##### **IX.15.1. Geochemical Studies:**

The geochemical profiles of siderophile elements at Anjar dinosaur pit (Fig.31a,b,c,d) suggest that various elements show abnormally high value in the section with uniform lithological assemblage. These values for similar lithological association do not show that high concentration as in the case of 75 cm thick zone of chocolate coloured shale, gray and black clay, shale, mud and marly bands at dinosaur pit locality. The siderophile Ir and Os show enhancement to the factor of 127 times to the normal. Other elements Co (2.65), Fe (89) show 3 to 127 times higher values than the adjacent unit of the section. The lithophiles and chalcophiles show Be (3 times), Sb (795 time), Zn (22.5 time), Se (14.5 times), Ag (59.4 time), Cu (3 to 4 times) and Sb (495 to 750). Different workers have studied and estimated loading of the atmosphere by volcanism, impact (meteoritic) and bolide (asteroidal) as given by Shukla and Bhandari (1997) and others. According to these estimates  $\text{CO}_2$  total discharge in the atmosphere would be  $2.65 \times 10^{19}$  tons or 5.2 grams/sq.cm.,  $\text{SO}_4$  would be  $4.25 \times 10^{19}$  tons or 8.3 grams/sq.cm., Hcl  $2.7 \times 10^{17}$  tons or .05 grams/sq.cm.  $\text{NO}$   $3.15 \times 10^{19}$  tons or .62 gram sq.cm. Carbon soot  $\times 10^{17}$  or 0.14 gram/sq.cm. ejecta  $10^{19}$  or 2gram/sq.cm. The studies were carried out on Ir concentration, carbon isotopes and oxygen isotopes by different workers (Bhandari 1991, Rompino and Haggerty, 1996) suggest that Ir range from 5 to 18 ng/g with one peak or several peaks and the isotopic carbon and isotopic oxygen show a sudden drop at the K.T. boundary level. These isotopic analysis of  $\delta^{13}\text{C}$  and  $\delta^{18}\text{O}$  was not done in case of Anjar section, and those of the Lameta rocks of Rahioli area suggest that there was a sharp drop in their values, which is in conformity to other KTB sections in the world.

##### **IX.15.2. Geochronological Studies:**

The geochronological studies suggested a total span of volcanism spreading from  $68.7 \pm .8$  m.y. to  $61.0 \pm 1.6$  m.y. The age of the last dinosaur fossil bearing horizon i.e., the third intertrappean bed range between  $65.2 \pm .6$  m.y. to  $65.1 \pm 1.5$  m.y. covering a period of about 0.2 m.y for the sedimentational history of about 6.75 m thickness. The rate of

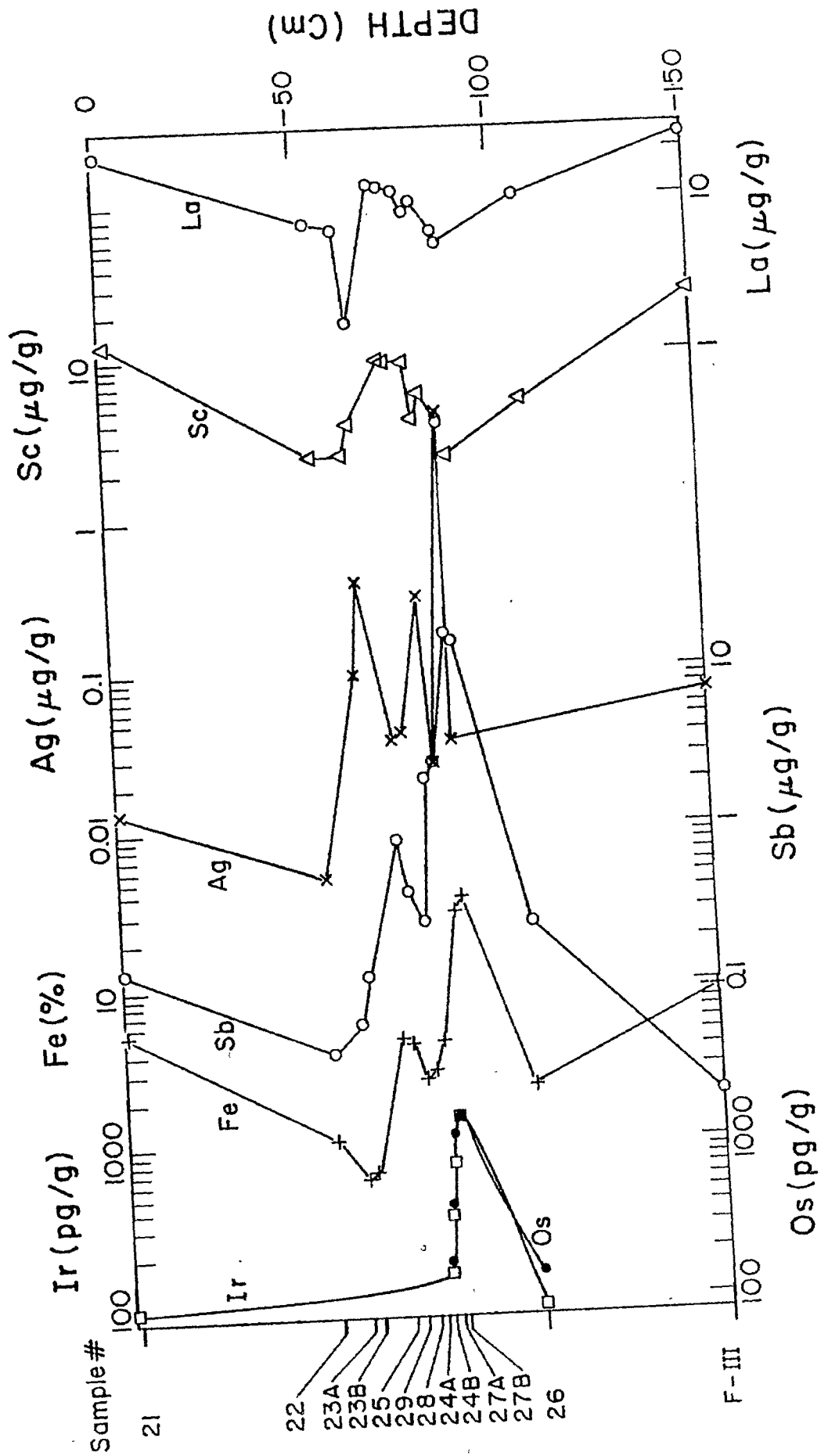


Fig. 31. Chemical profiles of various elements in the deep-sea pit Z locality at Aqta.

21 27

107

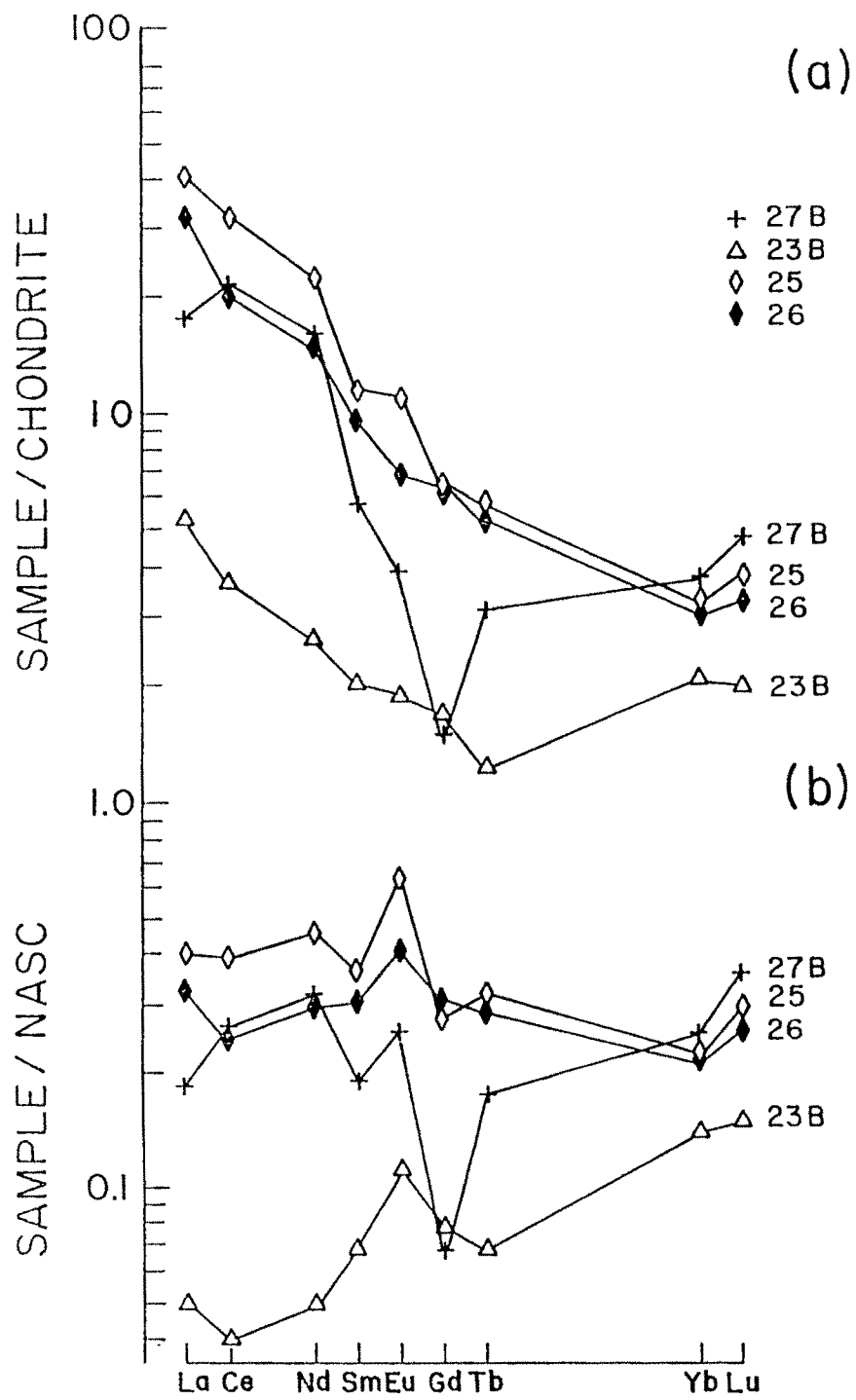


Fig 34 Chemical profiles of various elements in the dinosaur pit 2 locality at Anjar.

sedimentation, though was not uniform throughout the deposition of the section, but some broad generalisations can be visualised and applied on the basis of the vertical compositional variations of the section.

### **IX.15.3. Sedimentological Consideration :**

The section comprises 7.5 cyclotherms of cyclically repeating alternations of black mud, clay, shale with fragmentary, at times crudely current bedded, mottled limestone and marl with thin partings and lenses of cherty bed. The cherty partings are comparatively more pronounced in the third cycle and sixth cycle. The third cycle is comparatively shorter covering about 90 cm to 1 m thickness. The rate sedimentation was comparatively faster in the lower argillaceous part as compared to the calcareous (Upper) part of the section. The complete time span of 0.2 m.y. with 7.5 cyclotherms averages out the sedimentation rate per cycle roughly 26,660 years for thickness of about 95 cm to 1 m. (Average thickness of each cycle) the marl fraction and cherty intercalation fraction for nearly 30 to 35 cm thick package of each cycle. The deposition of carbonate is controlled by salinity factor, sediment influx composition and Eh-pH conditions of the lagoon/ponds. These sub basins were mostly evaporating playa type with limited extent. The sediment composition of each cycle suggest a quick alternation of periods with high precipitation, followed by comparatively dry, warm to temperate conditions with sporadic showers during which the salinity and the pH of lagoon and pools were considerably increased favouring the carbonate precipitation (during temperate condition). The warm temperate conditions at times fluctuated to nearly semi-arid to arid, during which the gypsum and cherty lenses (1 to 3 cm thick) were deposited. The dryer spells also comprised of intervening alternations of very short humid spells within a larger dry circle, where the thin muddy lenses were deposited. The humid spells were short, but with high precipitation, which diluted the Eh-pH condition and salinity of pools. These changed the climate to cool, pleasant for shorter spells during which the deposition of marl and gypsum were replaced by shale clay and mud. Thus, a palaeoclimatic scenario existing during the sedimentation of Anjar intertrappean suggest a seasonal composition of humid warm to pleasant phase (monsoon), ill define but prominent mixed season of temperate to semi arid type with short spells of showers (dominantly hot summer) and a short period of cool winter as suggested by palaeodendrological studies of fossil wood.

The sediment package of each cycle suggest a period of about 26,660 years for each cycle, nearly half of which (about 13,000 to 14,000 years) may be considered for active sedimentation of argillaceous fraction, which gives about 4.5-5 cm per thousand year as sedimentation rate for Anjar section. Average rate for one cycle comes to about 5 cm/1000 yr. The sedimentation rate for marine sections range around 5 cm per thousand years and maximum rate for continental sections may range up to 20 cm per thousand years. The sedimentation rate for marl and chemically precipitated limestone may be lesser than this rate. The composition of second and third cycle of Anjar section suggest slightly higher rate. These cycles comprises loose, silty debries, concretion and pebbles with them

which are aligned along the lamina and suggest deposition by comparatively faster torrential type of streams. The marl shows a mixture of sandy and trappean sand in the concretion. These are mottled and aligned in broad laminae of larger palaeochannel.

#### **IX.15.4. Relation of Sedimentation to Iridium anomalies and spaciations of events :**

The successive three anomalous layers occurring within the basal part of second top part of 185 cycle cyclothem. They cover a span of 80 cm thickness between basal most (1st event) to top most event (third event) and form topmost part of first cyclothem to lower part of second cyclothem. These are located in at a distance of 1 m above the top of third flow. The prevailing sedimentation rate of Anjar pit section suggest that the first meteorite strike took place at a time of about 30,000 years after the eruption of third flow. The second strike was after another 18,000 years, which was follow by another minor incident within next 300-400 years. The third major meteoritic strike occurred after a another period of 6000-7000 years of the second meteorite strike. These strikes were within a period of 54,000 to 55,000 years after eruption of third flow in Anjar area.

#### **IX.15.5. Palaeomagnetic Implication :**

The palaeomagnetic polarity of the Anjar sequence is very typical and field measurements suggest a first normal, followed by a reversed and again by normal sequence of polarity. The interfering factors were not eliminated during field measurements. The laboratory measurements of polarity suggest a normal and a reverse sequence of polarity. The first three basal flows (F1 to F3) are normal and the upper flows (F4 to F7) show reverse polarity. The actual point of change of polarity may be in the intervening intertrappean sequence, which is not yet known. The reversal may coincide with the multiple meteoritic strikes and it may be possible that the palaeomagnetic reversal may exactly start with the last iridium level (Ir 3) in this section.

#### **IX.15.6. Palaeontological data and their Implications :**

The important palaeontological characters and events of Anjar sections suggest :

- (1) Disappearance of dinosaurs in the basal part of the section exactly below the third Ir anomaly. No dinosaurian record of body fossils has so far been found above this last Ir anomaly.
- (2) The drastic reduction in the ferns, bivalves and gymnosperms in the upper part of this section above the last Ir anomaly. Similarly, planktonic forams also suffered heavy casualty and are limited to cherty bed only above the last anomaly.
- (3) Continuance of angiosperms and larger forams and charophytes with relatively lesser dominance.
- (4) The fish also were reduced greatly, and confined to the basal most part of the section below the last Ir event. The dinoflagellates, spore pollens planktonic forams and charophytes suggest Maestrichtian age for basal most part of Anjar sections. The dinosaur bone bed is also Maestrichtian in age.

The horizon above dinosaur suggest a basal most Tertiary (Palaeocene-Danian-P1) for the Anjar section. The palaeontological studies of eggs, bones, skin suggest a very unfavourable conditions for survival and stress on the biota. These facts in light of the speciations of meteoritic events, suggests devastating amount of pollution generated by the volcanoes and meteoritic strike, greatly restricting the favourable conditions of survival. The process of reduction of dinosaurs and associated biota had actually stated after the first eruption of Deccan volcanic flows around 70 million years before. For a period of nearly 3.9 million years the severity of ecological degradation greatly increased and were further aggrieved by multiple strike of meteorite, which put a final dot on the process of extinction.

#### **IX.15.7. Petrological Studies and their Implications :**

The Petrographic studies and analytical results of Anjar Volcanics suggest that volcanism started with alkaline olivine phase. The detail plotting of discriminant functions (Pearce, 1976) fall in the L.K.T. and W.P.B. fields. The detail plotting on Pearce diagram shows that the major part of basalts falls near Fe-Al portion of enlarged field, - in an environment of actively spreading centres and volcanism near the plate margins. The petrographic studies of basal show effects of spilitisation. The feldspar show effect of spilitisation near the outer marine in Anjar, Bhachau and Baladia areas. In the Anjar area pillow lava have been recorded at few places. The above facts point to a sub-aqueous phase of eruption, though the central type of shield volcanoes where also active in the circum Mesozoic belt. The studies of associated intertrappean beds suggests that the Iridium was spread as dust particles along with ash in the pools and ponds immediately after the strike. Some of the Iridium particles along with ash are entrapped in the limonitic matter, which now occur as widely distributed spherules in association with 1 cm thick layer of Ir. This spherules are coated with a layer of calcite. The paragenetic sequence of minerals in cherty beds suggests replacement of gypsum followed by calcite and finally followed by length slow chert This indicates a presence of original evaporite sequence within Intertrappeans which is now replaced by silica.

The palaeoposition of India during the upper Cretaceous (Maestrichtian) when this event happened, was to the south of equator in the low latitude zone. The volcanism, palaeoclimatic indicators, palaeontological data (Fig-17) and continuance of geological horizon in parts of western India Madagascar Seychelles and eastern African countries (Fig-28) suggests attachment of India Madagascar and Seychelles (Fig-33). In the early Palaeocene Indian plate was moving at a faster rate towards north and northeast words for a collision with Eurasian plate.

Ref.

#### **IX.16. Palaeoecological, Palaeobiological Considerations and Palaeoenvironmental Scenario:**

Geological conditions of foot tracks of Tharanda area suggest a shallow marine to estuarine set up, very close to the shore. The associated flora and fauna suggest a very

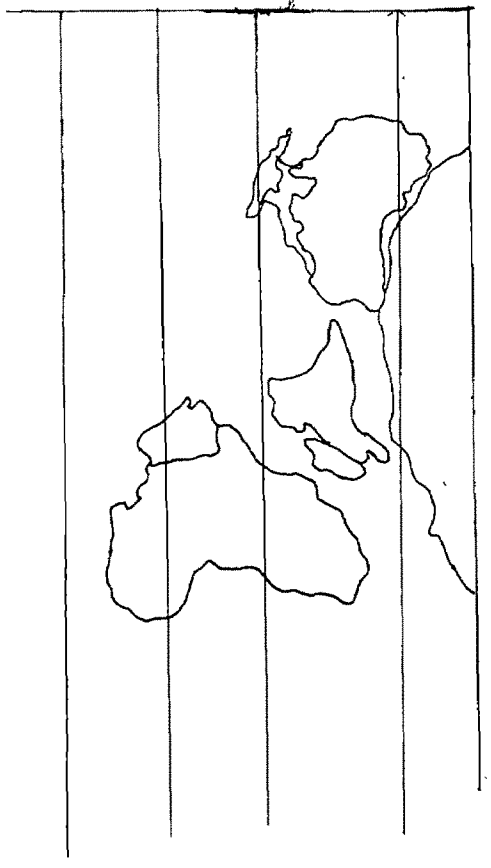


Fig. 28B2

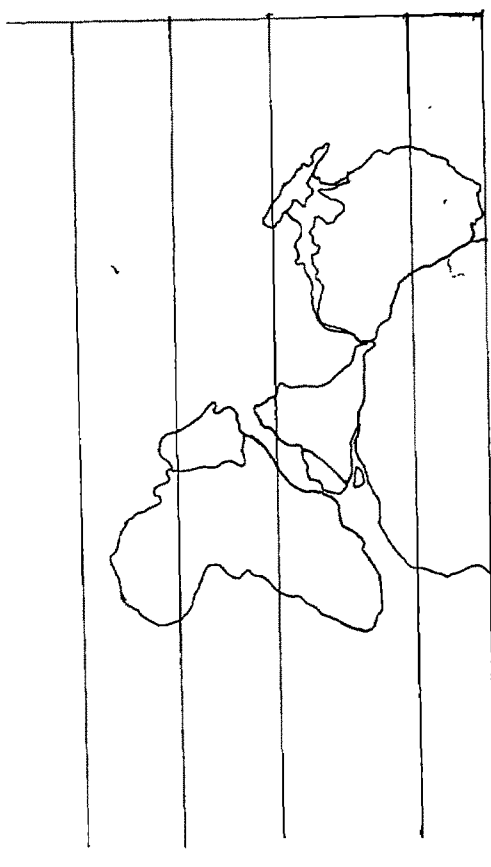


Fig. 28B1

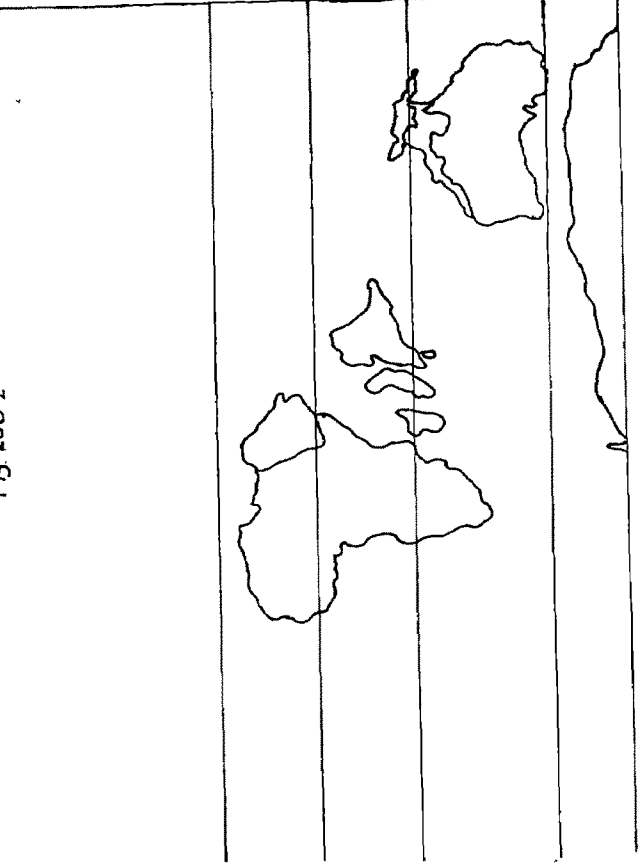


Fig. 28B4

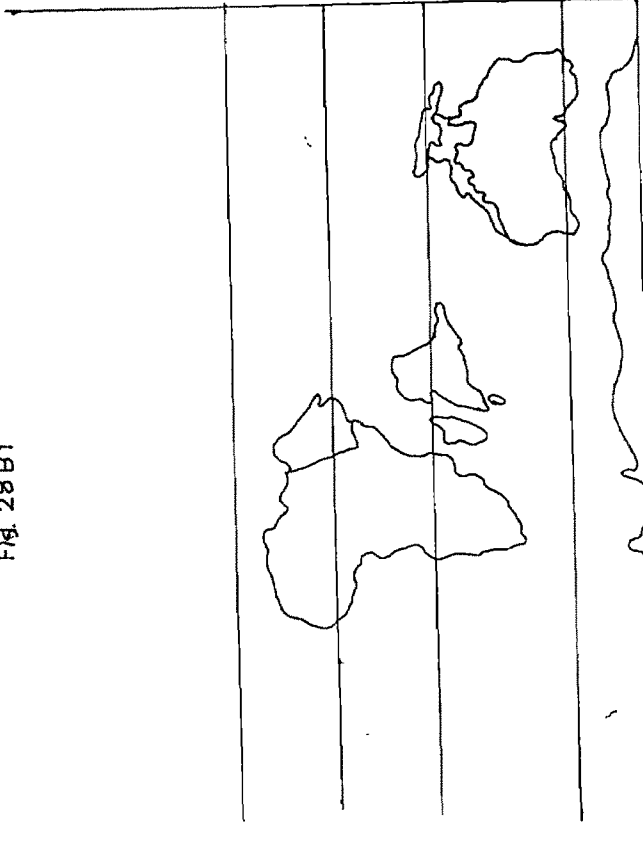


Fig. 28B3

Fig. 28 Palaeogeographical reconstruction showing palaeoposition of India during Maastrihtian and Palaeocene ( modified after Scot's et al., 1988 , Chatterjee 1996 and Barrera and Nishi, 1994).

GARWARE

shallow periodically drying environmental setup. The dinosaur preferred loose, wet ground as habitat. The dinosaur foot tracks at Fatehgarh also point to the similar setup. The stable isotopic studies carried out by Sarkar et. al., (1991) and the associated plant fossils suggest small shallow marshy water pool (like the one at Anjar Intertrappean-III dominated by shrubs, dense grass, calcareous/sandy or muddy shore/lake margins which were used as the nesting sites by the dinosaurs. The oxygen isotope values indicate that perhaps the dinosaur were consuming water from the same excessively evaporating ponds / pools. The  $\delta^{13}\text{C}$  isotope carbon values and study of coprolite indicate that dinosaurs were eating the C-3 and C-4 plants like grasses, succulents, small herbs, fibrous vegetations like ferns, conifers, cycades, araucarites etc. The dinosaurs were gregarious in nature and they roamed in groups for grazing hunting and in search of predestined seasonal breeding nesting sites. Evidences of regular seasonal mass migrations to certain places in search of food and drought induced conditions are widely recorded from many places in North America. The dinosaur had selectivity of choices on the soft sediments in flood plane areas, shore lines, strand lines, or margins of pools of water in dry ponds. The flood plain setup was covered by small water pools and back swamps with shrubs, herbs and grass / ferns. The dinosaurs dug their nests, laid eggs and covered them with sediments. The eggs were incubated by the solar heat. Dinosaur had site fidelity and visited same sites over years. They had colonial habit and cared for the young ones. The foot prints and foot tracks from many parts of the world suggests that the dinosaur moved in structured herds while grazing/hunting. The micro sections of the dinosaurian eggs suggests that certain eggs, bones and skin of these animals were pathological and they indicate tremendous amount of constraints and pressure on the ecology and environments. The last of the dinosaur were roaming amidst the active volcanism. The volcanic eruption of Daccan Traps and their contemporary volcanism were widespread. These had global effects on atmosphere and on the ecology. It raised huge dust clouds and millions of tones of halogens, Sulphur, nitrogen, carbon in form of soots, forest fires and ejecta from volcanoes, were discharged in the atmosphere. The net effect of this was immediately sharp drop of temperature and complete masking of solar and cosmic radiation eliminating the photosynthesis and the food chain of the ecosystem was hampered. After some time, there was a steep rise in the temperature due to green house effect. Thus, a sharp contrast in temperatures were created within comparatively shorter span of time. The larger land dwelling animals - dinosaurs had to struggle hard for existence. In the new setup, small lagoons, ponds drying marshy lakes were available to these animals, which, then were forced to migrate to such places. The forest fires completely destroyed the well established floral regime. The degradation of ecosystem was further accelerated by successive meteoritic impacts of large bodies, which struck the earth around 65 my at Chixulub and at off the western coast of India. (Chetterjee and Rudra, 1996). These impacts also triggered a series of devastating episodes. The three Iridium anomalies in the III Intertrappean bed at Anjar has recorded these three separate events within a thickness of 75 cm of section.

The sedimentation rates of these landlocked lagoon were comparatively faster. The

Anjar section reveals effect of brackish water incursion at the K/T event around 65 m.y. wherein the small streams drained the newly formed trappean terrain and accumulated debris in the lakes. There is a resolution of about 24,000-25,000 years between these three events. The rate sedimentation was faster enough since except the cherty limestone bed above chocolate coloured shale and ash layer, the other units show current dominated fluvial regime. Hence, each of these events of meteorite strikes were 18000 and 6000-7000 years apart. All these events are indicating probable timings within 54000-55000 years after 65.2 Ma, i.e., the pre- cherty limestone deposition.

The higher part of Anjar sequence is devoid of important plant and dinosaurian fossils. The lakes were shallow, rich in calcareous ooze and mud at margin and had swampy, muddy bottom depth must be very shallow. Numerous streams drained down the palaeoslopes of the flows. Numerous sub regimes of channel bars, small alluvial fans/colluvial fans, small island with insitu soil formation and a small zone of numerous distributaries near margins existed. Frequent subaerial exposure and isolation of sub lagoon into drying pools were common as testified by frequent intercalated gypseous and cherty layers within the marl and grey shales. Seasonal differentiation existed with short spells of humid periods. Initial part of Tertiary and latest Cretaceous represented longer humid, cooler periods with interventions of shorter warm periods in a cyclic manner.

The above scenario caused tremendous amount of stress on the life style and palaeobiological activity of dinosaurs and contemporary biota. The palaeopathological conditions of egg shell structures (multi layer ovum-in -Ova condition). Pathological conditions of bones and skin structures suggest that the effect of stress mounting on ecosystem was initiated during the upper most Cretaceous time around 68.9 M.a. before, and by 65 Ma, it was mounted on full fledged scale, where the malfunction of physiological processes and biological processes led to almost cancerous conditions in the bones, skin and reproductive system. The digestion also must have been badly affected, since deadly effects of volcanism and meteoritic impacts were wide ranging on the atmosphere. The plants and surface water resources were highly polluted. The invertebrates-pelecypods, gastropods and the forams form abundant shell hush suggesting the mass mortality, below the cherty limestone units. The gastropods are also affected, but still they continued up to the upper part of the sections in the third intertrappean bed. This fact is substantiated by spherules of Iridium rich matter coated with calcitic layers suggesting within the Ir3 layer and just above and below it, suggesting sedimentation event of ash (volcanic fine dust particles and aerosols of meteoritic dust charged with Iridium particles and ferruginous matter in the midst of continuous sedimentation process. There was a sudden influx of such sediments, recording a multiple event of impacts, which have completed the process of mortality initiated by volcanism about 2.5 - 3.0 m.y. before the K.T.B event. The various studies on reptiles and other groups and studies in physiological sciences have suggested that the imbalances in hormonal secretion are caused by conditions of stress due to ecological imbalances. These have caused various pathological conditions of eggs and bones.

\*\*\*\*\*